

©Copyright 2024

Heidi Weakly

Lipid membranes and the biophysics of protein-lipid interactions

Heidi Weakly

A dissertation
submitted in partial fulfillment of the
requirements for the degree of

Doctor of Philosophy

University of Washington

2024

Reading Committee:

Sarah L. Keller, Chair

Anne B. McCoy

Joshua Charles Vaughan

Program Authorized to Offer Degree:

Chemistry

University of Washington

Abstract

Lipid membranes and the biophysics of protein-lipid interactions

Heidi Weakly

Chair of the Supervisory Committee:
Sarah L. Keller
Chemistry

Lipid membranes are a fundamental structure of cells. In addition to compartmentalizing biological components and forming a physical barrier to protect against unwanted interactions. Membranes are a platform for protein signaling. This thesis investigates mechanisms of protein-lipid interactions based on the membrane's biophysical properties. First, we examine relationships between phase-separable membranes and 3D protein condensates, and we describe how thermodynamically coupling these systems can alter the details of their phase separation. We summarize key challenges in obtaining quantitative measurements of these coupled systems, and we present solutions to circumvent some of these challenges. Second, we use lipidomics to discover how common methods of making vesicles alter lipid compositions (or not) with respect to a stock solution. Third, we investigate the mechanisms of an enzyme in cholesterol synthesis, squalene monooxygenase. Specifically, we develop an approach to measure the effects of cholesterol levels and membrane curvature on the interaction of squalene monooxygenase's degron with the membrane surface. Fourth, we develop a template for implementing Wikipedia edits with undergraduates to increase students' appreciation and understanding of biophysics and biophysicists.

TABLE OF CONTENTS

	Page
List of Figures	iii
List of Tables	v
Chapter 1: Introduction	1
1.1 Overview	1
1.2 Phospholipids: Structure and Properties	1
1.3 Lipid vesicles	3
1.4 Liquid - liquid phase separation	4
1.5 Protein-Lipid Interactions	6
1.6 Thesis Outline	7
Chapter 2: Coupling liquid phases in 3D condensates and 2D membranes: Successes, challenges, and tools	9
2.1 Abstract	9
2.2 Introduction	9
2.3 Terminology and theoretical concepts of liquids on surfaces	11
2.4 Recent progress in experiment, theory, and simulation	11
2.5 Experimental challenges of characterizing phase-separation of membranes in contact with protein solutions	16
2.6 Tools and Methods	20
2.7 Conclusion	27
Chapter 3: Common methods of making giant vesicles (except emulsion techniques) capture intended lipid ratios	29
3.1 Abstract	29
3.2 Introduction	30
3.3 Materials and methods	33

3.4	Results and discussion	38
3.5	Caveats	45
3.6	Conclusions	46
Chapter 4:	Membrane-sensing properties of the Squalene Monooxygenase Degron	47
4.1	Introduction	47
4.2	Aims and hypothesis	51
4.3	Materials and Methods	53
4.4	Results and Discussion	58
4.5	Conclusions and Future Work	62
Chapter 5:	STEP-UP: Students write biophysics content for Wikipedia	66
5.1	What is STEP-UP?	66
5.2	Inspiration: Why ask students to edit Wikipedia?	67
5.3	Project Design	67
5.4	Challenges and recommendations	71
5.5	Final thoughts and conclusions	74
Chapter 6:	Conclusions and Future Directions	76
Bibliography	78
Appendix A:	Supporting Materials: Common methods of making giant vesicles (except emulsion techniques) capture intended lipid ratios	106
Appendix B:	Supporting Materials: Membrane-sensing properties of Squalene Monooxygenase Degron	120
Appendix C:	Supporting Materials: Step-Up Wikipedia Assignment	122

LIST OF FIGURES

Figure Number	Page
2.1 Schematic of dewetting, partial wetting, and complete wetting.	12
2.2 Surface condensates form at lower protein concentrations than bulk condensates.	13
2.3 Protein condensates can shift the mixing temperature, T_{mix} , of lipid membranes to higher values.	15
2.4 Schematics of four membrane configurations.	16
2.5 Lipid vesicles can aggregate in buffer.	17
2.6 Membrane tubules can form at vesicle surfaces.	19
2.7 Coexisting Lo and Ld phases can be imaged in black lipid membranes. . . .	22
2.8 Condensates can destabilize as temperature increases.	28
3.1 Structures of several lipids frequently found in GUVs.	31
3.2 Methods of producing vesicles, showing reservoirs of unincorporated lipids. .	32
3.3 Lipid percentages in 5-component vesicles produced by different methods. . .	40
3.4 Emulsion phase transfer incorporates more saturated and long-chain lipids into vesicles.	43
3.5 Extrusion of giant vesicles decreases their cholesterol content.	44
4.1 HMG-CoA reductase and squalene monooxygenase control rate-limiting steps in cholesterol synthesis.	48
4.2 Structure and membrane binding mechanisms of the regulatory domain of squalene monooxygenase.	50
4.3 SEC analysis of MBP-SM50-100 and SM50-100.	60
4.4 MBP-SM50-100 binding to lipid vesicles.	61
4.5 Fluorescence emission spectra of Bimane-labeled MBP-SM50-100 with lipid vesicles.	62
A.1 Sedimenting vesicles removes some lipid aggregates.	106
A.2 Representative fluorescence micrographs of vesicles made by electroformation on ITO-coated slides.	107

A.3	Representative fluorescence micrographs of vesicles made by electroformation on platinum wires.	108
A.4	Representative fluorescence micrographs of vesicles made by gentle hydration for 24 hrs.	109
A.5	Representative fluorescence micrographs of vesicles made by emulsion phase transfer.	110
A.6	Vesicles after extrusion.	111
A.7	Lipid percentages in 5-component vesicles produced by different methods. . .	112
B.1	Optimization of MBP-SM50-100 cleavage by TEV protease.	120
B.2	Fluorescent sensitivity of bimane-C3-maleimide by cysteine conjugation. . . .	121

LIST OF TABLES

Table Number	Page
A.1 Lipid compositions of five-component vesicles analyzed by mass spectrometry, expressed as percentages of total lipid	113
A.2 Percentages of lipids in GUVs made by emulsion transfer from a binary mixture of an unsaturated lipid and a saturated lipid	113
A.3 Percentages of lipids in GUVs made by emulsion transfer from a binary mixture of lipids with different chain lengths	114
A.4 Lipid compositions analyzed by mass spectrometry and expressed as percentages of total lipid for vesicles produced by gentle hydration (“before extrusion”) and then extruded (“after extrusion”). For example, “Experiment 1 – After” was made from an aliquot of the solution from “Experiment 1 – Before”.	114
A.5 Phospholipid abundances of five-component vesicles analyzed by mass spectrometry.	115
A.6 Cholesterol abundances of five-component vesicles analyzed by mass spectrometry.	116
A.7 Phospholipid abundances in GUVs made by emulsion transfer from a binary mixture of an unsaturated lipid and a saturated lipid	117
A.8 Phospholipid abundances in GUVs made by emulsion transfer from a binary mixture of lipids with different chain lengths.	117
A.9 Phospholipid abundances in GUVs produced by gentle hydration (“before extrusion”) and then extruded (“after extrusion”). For example, “After extrusion 1” was made from an aliquot of the solution from “Before extrusion 1”.	118
A.10 Cholesterol abundances in GUVs produced by gentle hydration (“before extrusion”) and then extruded (“after extrusion”). For example, “After extrusion 1” was made from an aliquot of the solution from “Before extrusion 1”.	119

ACKNOWLEDGMENTS

I want to express my gratitude to my advisor, Sarah L. Keller, for her unparalleled mentorship and support. Since my first day in her group, her encouragement and optimism have been true constants, helping me overcome many scientific hurdles and achieve many personal goals. Thank you for believing in me and helping me discover my strengths. I hope to be as inspiring a mentor as you one day.

I am also grateful to the other UW faculty members who have supported me, especially Sharona Gordon, Bill Zagotta, Anne McCoy, Andrea Carroll, and Ben Wiggins. Sharona opened her lab and shared her scientific expertise with me, marking a turning point for my research. She is not only a brilliant scientist but also a wonderful human being, and I look forward to our continued collaboration. Much of this work would not have been possible without access to Bill's lab. Anne McCoy served on each of my committees and provided invaluable guidance. Beyond my research mentors, Andrea Carroll and Ben Wiggins were fantastic supporters of my interests in scientific education and shaped the teacher I am today. They are both forces in STEM education, I and look forward to following their achievements.

Thank you to the Keller Lab, both past and present, for the teaching moments and the camaraderie. Your support through exams and experimental woes, as well as the joy you brought to this experience, were invaluable. Thank you to all of the members of the Gordon and Zagotta labs, for your patience and teaching me the ins and outs of proteins.

A special thanks to my undergraduate advisor, Amber Krummel. Your encouragement and lessons on hard work have had a lasting impact on my life. I also want to thank the many other graduate students I learned from in Colorado, Germany, and Utah. It took completing my Ph.D. to fully appreciate all you taught me, and I would not be the scientist I am today without your influence.

Thank you to all of the friends outside the walls of Bagley and graduate school. You all have kept me sane. Good conversation, dinner parties, coffee and wine dates, and hikes through the PNW with you helped me maintain a good work/life balance with the demands of graduate school.

Finally, I extend my heartfelt gratitude to my family. My parents, Mariann and Nile, made all of this possible and have supported me wholeheartedly from one day. You guys are my biggest fans and have always encouraged me to follow my dreams, no matter how far away my dreams take me. Your wisdom has guided me here, and I stand on your shoulders every day. Thank you to my sister, Maggie for always being there. You are my cheerleader in life, and I couldn't have achieved this without your encouragement and love.

To Dr. Rob Weakly, I am deeply grateful for your partnership, compassion, and humor day in and day out. I am also grateful that I completed my master's and chose Washington, and you, and UW. Truly, our whole life awaited us here and I can't wait to live the rest of it. In the past few months, you have made it possible for me to meet all of the tough deadlines, and I will always be grateful for that. I'll take the torch now.

DEDICATION

To my dad, Nile J. Spears, whose wisdom sparked the curiosity that set me on this path.

Only with your unwavering love and support have I arrived here.

And to my daughter, Maya E. Weakly, whose boundless joy and energy fueled my spirit
and carried me across the finish line.

Chapter 1

INTRODUCTION

1.1 Overview

Cell membranes are composed of lipids and proteins. The lipids play a large role the membrane's structural integrity, and the proteins play a large role in its function. These roles are connected. The composition of lipid membranes influences the activity of various membrane proteins and ion channels. Similarly, proteins can act to change the lipid compositions of membranes.

1.2 Phospholipids: Structure and Properties

Phospholipids self-assemble into membranes because they are amphiphilic. Amphiphilic molecules are molecules that contain both hydrophilic (water-attracting) and hydrophobic (water-repelling) components. A single phospholipid contains a polar, phosphate “head” and two, fatty acid “tails” linked together via a glycerol backbone. This structure enables phospholipids to self-assemble into a lipid bilayer when they are dispersed in aqueous solution. The bilayer structure orients the hydrophobic, oily tails inward, shielding them from the water. At the same time, the hydrophilic, polar head groups face the aqueous interior and exterior, allowing favorable interactions with water.

The chemistry of the head and tail groups determines the physical properties of the lipid and their organization within the membrane. For example, some phospholipids are zwitterionic (neutrally-charged) at physiological pH (e.g., phosphatidylcholine; PC and phosphatidylethanolamine; PE); their positively-charged headgroups balance with the negatively-charged phosphate group. In contrast, some phospholipids have an overall negative charge (e.g. phosphatidylglycerol; PG, phosphatidylinositol; PI, and phosphatidylserine; PS) and

some have an overall positive charge (e.g., dioleoyl-3-trimethylammonium propane, DOTAP). In the plasma membranes of cells, phospholipids are asymmetrically distributed between the inner and outer faces of the bilayers (the leaflets). Zwitterionic lipids are enriched in the outer leaflet, whereas anionic lipids reside within the inner leaflet. The anionic lipids enhance binding of specific proteins such as synaptotagmins [1, 2]. Disruption of lipid asymmetry within the plasma membrane has dire biological consequences. For example, if distribution of PS on the outer leaflet changes by a little as 1 - 2 mol%, it activates an irreversible signal to initiate clearing mechanisms such as cell death (apoptosis) [3].

The hydrophobic tails of phospholipids are made up of carbon chains of various lengths and degrees of saturation. Each chain can be completely *saturated*, indicating all carbons are connected by single bonds, or *unsaturated*, indicating the chains contain one or more double bonds. The term *unsaturated* refers to the reduced number of hydrogen atoms. The chains can also be methylated (-CH₃), as in the lipid DiPhyPC. The chain length and degree of saturation of the tails are the predominant contributors to the melting temperature of the lipid.

In its broadest definition, the term “lipids” includes fats, oils, fatty acids, phospholipids, and sterols. The melting temperature of lipids is easily conceptualized when considering household fats and oils. For example, butter, a solid at room temperature, contains long, saturated chains, whereas cooking oils that are liquid at room temperature contain unsaturated lipid chains. The degree of saturation also influences the melting temperature. Adding methylation of lipid chains generally decreases melting temperatures further. For example, the melting temperature of lipids DPPC (di(16:0)PC), DOPC (di(18:1)PC), and DiPhyPC (4ME(16:0)PC) are 41 °C, -17 °C, and < -120 °C, respectively [4]. Importantly, just as butter can exist as a solid or liquid depending on the temperature, lipid bilayers can exist in a liquid or solid-like (i.e., gel) state that is temperature-dependent.

The area ratio of the lipid head to the lipid tails determines the shape of the space occupied by the lipid. For example, phospholipids with a large head group, such as phosphatidylcholine (PC), have cylindrical shapes. When cylindrical lipids self-assemble, they

tend to form planar layers. Conversely, phospholipids with a small head group and bulky tails, such as phosphatidylethanolamine (PE) form a cone-like shape, and therefore, tend to form highly-curved structures such as micelles or tubes. These irregular shapes can facilitate biological functions like membrane fusion [5].

Cholesterol is another vital lipid for the normal functioning of mammalian cells. It contains a flat, rigid ring structure and a small, polar hydroxyl group (-OH). Structurally, cholesterol influences both the permeability and fluidity of the plasma membrane [6], creating a strong barrier between the cytosol and the extracellular milieu. Membranes containing cholesterol are typically less permeable, yet permit membrane bending, which is important in processes such as endocytosis. Chemically, cholesterol is a precursor for the biosynthesis of many molecules including bile acids, vitamin D, and several steroid hormones. When cholesterol levels are low, synthesis is upregulated by increasing the activity of various enzymes, such as HMG-Co reductase and squalene monooxygenase (see chapter 4). At the same time, excess cholesterol can be toxic to cells. Therefore the cell must also be able to rapidly initiate or cease cholesterol synthesis to maintain appropriate cholesterol levels. This process is part of cell homeostasis. Dysregulation of cholesterol regulation networks is associated with diseases including atherosclerosis, hypercholesterolemia, and cancer [7, 8]. A molecular understanding of the enzymes that regulate cholesterol levels is critical to understanding these networks and to developing the next generation of therapeutic targets to treat and prevent cholesterol-related diseases.

1.3 Lipid vesicles

Cellular membranes contain hundreds to thousands of different lipid molecules and proteins. Furthermore, the specific composition varies between cell types and cellular organelles. The lipid composition determines membrane biophysical properties such as charge, curvature, lipid packing, melting temperature, bending rigidity, and liquid-liquid phase separation. In light of the complexity of biological membranes, simple vesicles (also known as liposomes) are used as models to isolate and test the influence of specific lipids on membrane behavior.

Numerous techniques have been developed to produce vesicles exhibiting a range of sizes and physical characteristics (refer to chapter 3 for detailed methods). For instance, electroformation methods predominantly yield very large vesicles ($> 10 - 100 \mu\text{m}$ in diameter) with single bilayers, called Giant Unilamellar Vesicles (GUVs). Other methods such as sonication and extrusion are best for generating small vesicles (10 -100 nm) characterized by high curvature. Because GUVs are at least as big as most human cells, they enable the visualization of membrane behaviors that would otherwise be too small to resolve with regular light microscopy.

1.4 Liquid - liquid phase separation

Liquid-liquid phase separation (LLPS) is familiar from everyday experiences with immiscible liquids like water and oil, which spontaneously separate into distinct phases. Biomolecules such as RNA and proteins, and, separately, lipids can undergo similar demixing transitions.

1.4.1 Lipid Phase Separation

In membranes, liquid-liquid phase separation is a two-dimensional (2D) phenomenon. Lipids separate laterally within the planes of the membranes into co-existing phases, call the “liquid-ordered” (Lo) and “liquid-disordered” phases. These phases are distinguished by different ratios of lipids and by the degree of order in the acyl chains. Reversible liquid-liquid phase separation within membranes has been observed in synthetic lipid membranes, giant plasma membranes vesicles (GMPVs) derived from cells, and the vacuole membrane in living yeast cells [9–11]. Our lab and others typically observe co-existing phases in GUVs composed of as few as three lipid types: high chain-melting temperature lipids, low chain-melting temperature lipids, and cholesterol [12–14]. Recently, our lab discovered that liquid-liquid phase separation is also possible with two components when the high chain-melting lipid is replaced with a saturated sterol-lipid [15].

Phase separation is an energy-driven process. At low temperatures, the free energy is lowest, when the membrane is demixed into co-existing liquid phases. Phase separation

enhances favorable enthalpic interactions between similar lipid tails. At high temperatures, entropic forces overcome interactions between individual lipids causing the membrane to mix into a single, liquid phase. The temperature at which the membrane transitions from a mixed to demixed state is called the miscibility transition temperature (T_{mix}). T_{mix} is dependent on the membrane's lipid composition and pressure. Researchers can identify liquid phases and quantify T_{mix} using a variety of experimental techniques. These include imaging methods such as fluorescence microscopy [16], cryo-electron microscopy (cryoEM) tomography [17], and atomic force microscopy [18, 19] and indirect structure-probing measurements such as small-angle-x-ray scattering (SAXS) [20], nuclear magnetic spectroscopy (NMR) [21], and electron paramagnetic resonance spectroscopy (EPR) [22].

1.4.2 Protein Phase Separation: Protein Condensates

Solutions of protein and RNA molecules have the potential to demix forming three-dimensional (3D) liquid droplets. In a biological context, these droplets are commonly referred to as membrane-less organelles, whereas in a physical context, they are commonly referred to as condensate. Scientists first discovered the physical processes that drive condensate formation over 100 hundred years ago. However, the work of pioneering work of Cliff Brangwynne and Anthony Hyman of liquid-liquid phase separation in P granules in the germ cells of *C. elegans* revitalized the search for LLPS in biological systems [23]. Due to the relatively large size (2–4 μm in diameter) of the P granules, they were able to directly observe these membrane-less organelles deforming and fusing with one another around the germ nucleus, and they found rapid molecular exchange with the surrounding cytoplasm [23]. Both processes are indicative of liquid-liquid demixing. Since then, researchers have discovered similar structures, including nucleoli, Cajal bodies, and stress granules, all exhibiting liquid-like properties [24]. These structures form via spontaneous phase transitions that occur during molecular supersaturation, which can be caused by amplified gene expression and post-translation modifications. Above a concentration threshold, two distinct phases form: one is enriched in a specific set of proteins and/or RNA, and the other phase is dilute.

While the distinct driving forces for condensate formation are dependent on the protein/RNA system, multivalency and intrinsically disordered regions are common features in phase-separable proteins. For example, many proteins contain repeats of the SRC-homology 3 (SH3) domain, which bind to proline-rich motifs (PRMs) to enable signaling complexes. Multivalent peptides SH3_n and PRM_n (based on the sequences of SH3 and PRM) were demonstrated to phase-separate when the valency of each sequence was $n \geq 3$ [25]. Moreover, the SH3 and PRM domains have been shown to facilitate phase separation in several full-length proteins including the adaptor protein Nck and N-WASP [26].

Other protein condensates are highly enriched in intrinsically disordered regions that contain high densities of polar and charged amino acids. These residues can enable charge-charge, charge- π , and $\pi - \pi$ stacking interactions, depending on their pattern and frequency. [27–29]. The germ granule protein DDX4 phase-separates into 3D condensates due to intrinsically disordered regions at its N and C terminus [28]. Conversely, if DDX4 becomes arginine-methylated, the saturation concentration required for condensate formation increases 10-fold. DDX4 liquid droplets are an example of how cells use post-translational modifications to control the composition and stability of 3D condensates. Liquid droplets provide the cell with a powerful mechanism to concentrate or sequester various biomolecules and have been implicated in critical biological processes including T-cell signaling [30] and gene silencing [31, 32].

1.5 Protein-Lipid Interactions

Membrane proteins can be membrane-spanning (transmembrane proteins) such as G-coupled receptors and ion transport channels or peripheral such antimicrobial peptides and peripheral enzymes. This thesis will focus on protein-lipid interactions of the latter. Despite the often transient and weaker interaction (of peripheral proteins with membranes compared transmembrane proteins), peripheral proteins are critical to many cellular processes from signaling and recognition to membrane trafficking and cell division. Recruitment of proteins to membranes can be tuned through electrostatic interactions, hydrophobic interactions, and

fatty-acid modifications.

An excellent example of different types of membrane interactions is the secretory pathway. The secretory pathway synthesizes proteins in the endoplasmic reticulum (ER) and folds and delivers the proteins to various organelles throughout the cell. The pathway proceeds from the ER membrane to various organelles, and eventually ends at the plasma membrane. At the beginning of the secretory pathway, membranes exhibit less ordered packing of lipids, allowing cytosolic proteins to bury large hydrophobic groups within the membrane at spaces in the membrane surface (defect sites) [33]. Towards the end of the secretory pathway, membrane electrostatics plays a larger role in promoting the binding of charged proteins. Again, these physicochemical parameters are a result of membrane composition. Membrane electrostatics depend on the fraction of negatively charged lipids such as phosphatidylserine and phosphoinositides, whereas packing defects are promoted by lipids with noncylindrical shapes such as phosphatidylethanolamines and lipids with unsaturated chains [34, 35].

1.6 Thesis Outline

The research in this thesis employs model membranes to investigate two mechanisms that drive interactions between proteins and membrane bilayers. Chapter 2 describes mechanisms by which protein condensates interact with membranes and examines the effects of thermodynamic coupling of membranes and condensates on their miscibility phase behavior. We summarize foundational experiments coupling 2D and 3D phase-separable components, outline experimental challenges of coupling these systems, and present tools to overcome some of these challenges. In Chapter 3, we present lipidomics data for vesicle populations produced by five common techniques: gentle hydration, electroformation (on both ITO slides and Pt wires), emulsion phase transfer, and extrusion. We find that the ratios of the lipids in the vesicles closely match the intended ratios from a master stock, except for vesicles prepared by emulsion phase transfer, which contained lower ratios of cholesterol and unsaturated PC lipids. Chapter 4 investigates how the degranulation of squalene monooxygenase - a rate-limiting enzyme in cholesterol synthesis, senses various properties of lipid membranes.

Specifically, we develop a method to test the effects of lipid composition and membrane curvature on binding and interactions of the squalene monooxygenase's degron with lipids vesicles. Chapter 5 presents biophysics curricula developed for an undergraduate course. The curricula guide students through creating Wikipedia articles, with the goal of increasing of biophysical concepts among the students as well as the public.

Chapter 2

COUPLING LIQUID PHASES IN 3D CONDENSATES AND 2D MEMBRANES: SUCCESSES, CHALLENGES, AND TOOLS

This chapter was first published in *Biophysical Journal* in 2023, and was written in collaboration with Sarah L. Keller [36].

Heidi M. J. Weakly and Sarah L. Keller. “Coupling liquid phases in 3D condensates and 2D membranes: Successes, challenges, and tools”, *Biophysical Journal*, 2023; **123**: 1329-1341. <https://doi.org/10.1016/j.bpj.2023.12.023>.

2.1 Abstract

This review describes the major experimental challenges researchers meet when attempting to couple phase separation between membranes and condensates. Although it is well known that phase separation in a 2D membrane could affect molecules capable of forming a 3D condensate (and vice versa), few researchers have quantified the effects to date. The scarcity of these measurements is not due to a lack of intense interest or effort in the field. Rather, it reflects significant experimental challenges in manipulating coupled membranes and condensates to yield quantitative values. These challenges transcend many molecular details, which means they impact a wide range of systems. This review highlights recent exciting successes in the field and lays out a comprehensive list of tools that address potential pitfalls for researchers considering coupling membranes with condensates.

2.2 Introduction

Organelles in cells are either bounded by a two-dimensional (2D) membrane or are membraneless, three-dimensional (3D) condensates. Membranes and condensates can both or-

ganize through liquid-liquid phase separation, which can be crucial for cell viability. For example, during periods of nutrient stress, lipid membranes of yeast vacuoles phase separate into 2D domains [37–39], corresponding to liquid-ordered and liquid-disordered (Lo and Ld) phases in model membranes [38]. These membrane transitions are reversible, and the domains can merge quickly, like liquids [11, 40]. Likewise, stress granules, which are condensates enriched in RNA-binding proteins and mRNA, arise when cells experience stressors, including heat and pH [41, 42]. When 3D condensates touch, they can merge quickly, like liquids rather than solids [43].

In some cases, membranes and condensates interact. Wetting of membranes by molecules found in condensates has been implicated in crucial biological functions such as signal transduction pathways in T cells [31], tight junctions in endothelial cells [44], endocytic vesicle formation [45], and other processes [46–50]. The biological importance of these phenomena has prompted researchers to investigate thermodynamically coupled systems of phase-separating membranes and phase-separating solutions.

Liquid-liquid phase separation has been widely reviewed for both 2D membranes [16, 51–54] and 3D condensates [27, 55–60]. Given the rich literature about the conditions needed to achieve phase separation in both systems, it may seem surprising that few measurements quantifying the effects of coupling between membranes and condensates have been reported to date. This paucity is not due to researchers’ lack of interest. Rather, it reflects significant experimental challenges that researchers have faced. Our goal in this review is to help new researchers in the field quickly surmount challenges in coupling membranes to condensates. We will briefly introduce relevant terminology and theoretical concepts, and then highlight recent groundbreaking measurements. We will then describe experimental challenges that researchers have faced and conclude with a list of techniques and molecular tools to mitigate the challenges.

2.3 Terminology and theoretical concepts of liquids on surfaces

Dewetting, partial wetting, and complete wetting reflect the strength of interactions between molecules in liquid droplets and surfaces (Fig. 2.1A). As an example, dewetting occurs when water beads on a hydrophobic surface. At the other extreme, wetting occurs when water completely covers a hydrophilic surface. Partial wetting is characterized by a contact angle between 0° (wetting) and 180° (dewetting); the “critical wetting point” occurs at the first nonzero contact angle [61]. In the absence of a macroscopic droplet, interactions may be sufficient to create a molecularly thin, 2D surface phase of the same molecules found in liquid droplets, a phenomenon called “prewetting” [62–66]. These concepts apply equally well when the droplet is a phase-separated fluid condensate and the surface is a membrane (Fig. 2.1B-C) [67, 68].

2.4 Recent progress in experiment, theory, and simulation

To date, investigators have focused on two observables that can provide insight into coupling between liquid phases of membranes and condensates: (1) changes in morphology and (2) shifts in phase boundaries, whether in concentration or miscibility transition temperature, T_{mix} .

Membranes bend easily

When vesicle membranes are in contact with phase-separated 3D fluids, they adopt a range of shapes (Fig. 2.1B–C and reviewed elsewhere [69–72]). When the membrane is also phase-separated, coupled phase separation can occur. Coupling can be facilitated by incorporating molecular tethers (discussed in detail in Tool 4) that link condensates to membranes (Fig. 2.1D). For example, when a phase-separating solution of polyethylene glycol (PEG) and dextran is encapsulated in a vesicle containing a small fraction of PEG-lipids [67], membrane domains enriched in PEG-lipids coat the solution phase enriched in PEG molecules. Subsequent fission of the vesicles results in two populations: one of which is enriched in PEG-lipids and encapsulates PEG molecules [67].

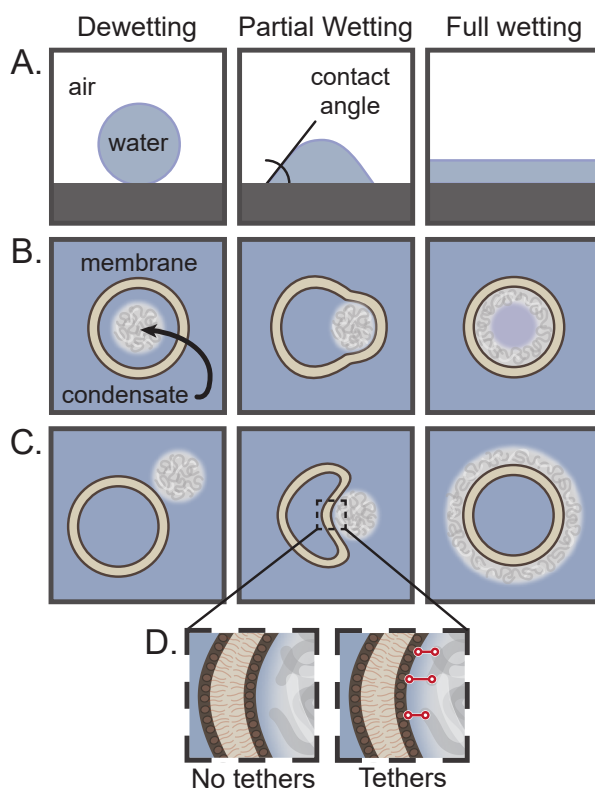


Figure 2.1: **Schematic of dewetting, partial wetting, and complete wetting.** **A)** Liquid drops on solid surfaces. Liquid condensates **B)** inside or **C)** outside vesicle membranes, both **D)** with and without tethers between lipid headgroups and molecules in the condensate.

New concentration thresholds for proteins coupled to membranes

Condensates are dense clusters of biomolecules with reversible, multivalent interactions. Protein solutions demix into condensed and dilute phases when the protein concentration surpasses a threshold, sometimes called the “saturation concentration” (Fig. 2.2). When at least one protein in a condensate binds to a membrane, the concentration of condensate locally increases, so that condensate proteins prewet the membrane at lower concentrations than required for bulk condensates (Fig. 2.2) [26, 73, 74]. For example, when Whi3 proteins, which are involved in RNA transcript regulation at the endoplasmic reticulum, are tethered to membranes, they form surface condensates at concentrations orders of magnitude lower than

in solution [50]. Similarly, the protein FtsZ, which is involved in cell division in *E. coli*, forms small condensates with the DNA-binding protein SlmA at a lipid interface [75]. FtZ:SlmA surface condensates coalesce on short timescales, characteristic of liquid phases [75]. Future work will undoubtedly demonstrate this concept with other proteins, where the importance of each system will lie in its cellular role.

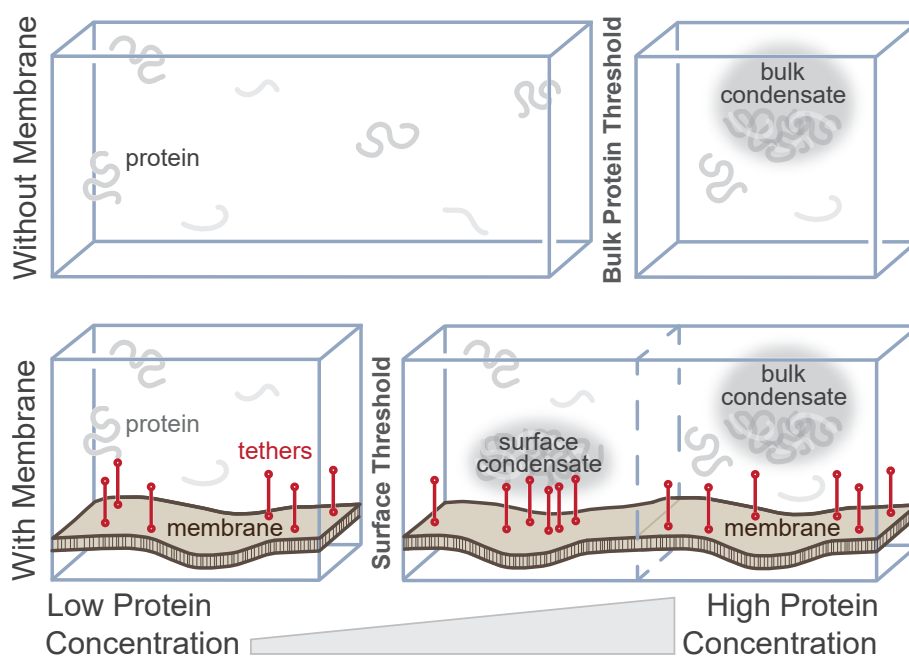


Figure 2.2: **Surface condensates form at lower protein concentrations than bulk condensates.** Top: At low concentrations, soluble proteins are in a uniform, dilute phase. When the protein concentration exceeds bulk condensate threshold, a droplet of condensed protein phase coexists with the dilute protein solution. Bottom: If the protein binds to a membrane, whether via a tether or not, a molecularly-thin, 2D condensate can prewet the surface at a lower concentration than the bulk threshold. The surface condensate alters the local distribution of tethers, but not their number. The bulk condensate threshold is unchanged by the presence of the membrane.

If condensate proteins are tethered to only one of the membrane phases, domain formation can further concentrate the proteins [76]. Wang et al. found that low concentrations of a particular protein (pLAT, the phosphorylated intracellular domain of linker for the activa-

tion of T cells) condense on phase-separated membranes, whereas no condensates formed on mixed membranes [76]. Similarly, charged lipids that are highly enriched in one membrane phase can enable surface phases [77,78]. One example is the Noc condensate (a bacterial nucleoid occlusion protein complex), which is enhanced by high surface densities of negatively charged lipids [79].

Protein condensates shift membrane T_{mix}

Above a characteristic temperature, T_{mix} , membranes are uniform, whereas below T_{mix} , membrane lipids demix into coexisting liquid ordered (Lo) and liquid disordered (Ld) phases (Fig. 2.3). Given that T_{mix} increases when membrane components are crosslinked or accumulate in one phase [80–84], and that lipid packing can increase in membranes that are wet by condensates [85], T_{mix} should increase when 3D condensates couple to one membrane phase.

Indeed, Lee et al. found that more membranes phase separated when proteins were coupled to the membrane’s Ld phase [86]. Chung et al. achieved a breakthrough by quantifying a shift in T_{mix} [87]. They found that coupling a condensate of the proteins LAT, Grb2 and SOS with model membranes increased T_{mix} (by 6°C for their specific membrane and solution conditions) [87]. Wang et al. also quantified T_{mix} for a similar model system [76].

Tether density is a key parameter

In model membranes, increasing the coupling between condensates and membranes generally increases phase separation [88,89]. In simulations and theory [65,66], coupling or tethering a dilute solution of phase-separable molecules to a membrane expands the prewetting regime. Rouches et al. found the prewetting regime increases further when the membrane is near a miscibility critical point [65]. Integral membrane proteins may act as obstacles, further modulating condensate-molecule interactions and reducing effective tether densities [90].

One way to tune the coupling strength is to vary densities of molecules that tether the membrane to the condensate. Unfortunately, limited ranges of tether densities for measurements of T_{mix} are experimentally accessible. Condensate molecules attached to a membrane

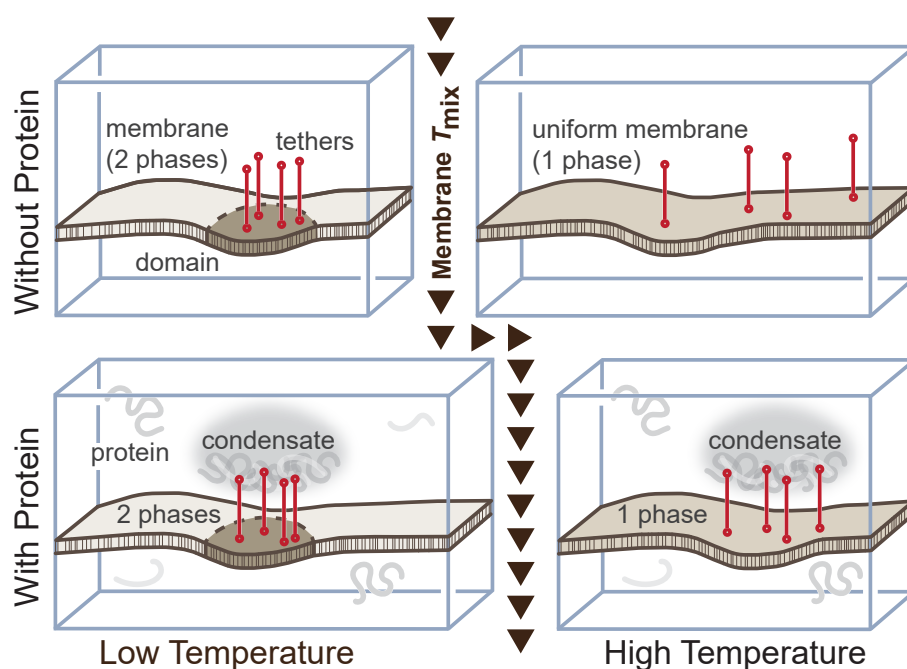


Figure 2.3: **Protein condensates can shift the mixing temperature, T_{mix} , of lipid membranes to higher values.** Top Row: At low temperatures, two liquid phases coexist in the membrane: the liquid ordered phase (Lo) and the liquid disordered phase (Ld). At high temperatures, the lipids mix in a single liquid phase. Bottom Row: Interactions between a protein condensate and lipids in only one membrane phase (either the Lo or the Ld phase) are predicted to increase the membrane's T_{mix} , independent of molecular details [65].

surface experience lateral steric pressure above a surface density that is a function of the molecule's molar mass [91,92]. Large molecules like PEG5000-DOPE can experience steric pressure at membrane concentrations of only 1-2 mol% [92].

In cells, interfering with molecular linkers between condensates and membranes can disrupt downstream signaling pathways. For example, decoupling LAT protein from membrane domains by mutating the transmembrane domain of LAT prevents LAT condensate formation and curtails downstream signaling events in T cells [76]. Mutating LAT's transmembrane domain changes the partitioning of the condensate within the membrane, effectively lowering the local tether density. However, the specific molecular mechanisms by which de-coupling condensates from membrane domains interferes with signaling is not yet known.

2.5 Experimental challenges of characterizing phase-separation of membranes in contact with protein solutions

Four challenges that researchers encounter when attempting to measure T_{mix} of membranes in contact with protein and/or RNA solutions include: 1) aggregation of free-floating vesicles, 2) membrane tubulation, 3) difficulties in exchanging aqueous solutions, and 4) slow collective motion of lipids in membranes deposited on solid surfaces. Liquid-liquid phase separation in membranes is commonly imaged in $\geq 10 \mu\text{m}$ single-walled vesicles, in membranes on solid or polymer substrates, or in membranes spanning holes in supports (Fig. 2.4). These systems are called “giant unilamellar vesicles” (GUVs) [93], “supported lipid membranes” (SLBs) [94,95], and “black lipid membranes” (BLMs) [96,97], respectively. While experiments may be possible in all these systems, each has advantages and disadvantages.

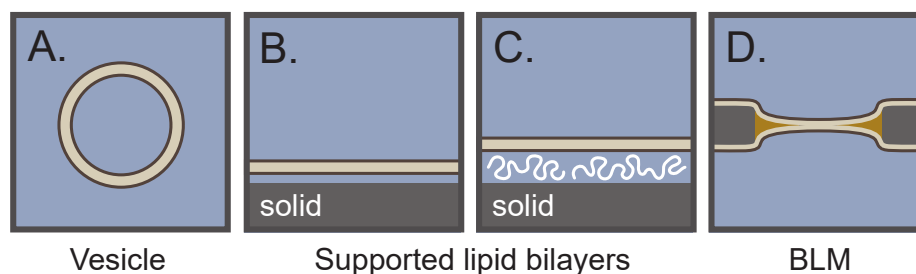


Figure 2.4: **Schematics of four membrane configurations.** **A)** a giant unilamellar vesicle (GUV), **B)** a supported lipid membrane (SLB) on a solid support, **C)** a supported lipid membrane on a polymer support, and **D)** a black lipid membrane (BLM) spanning solid supports coated with oil (orange wedges). In all panels, hydrophobic regions of the bilayer are light tan and lipid headgroups are dark brown.

For example, one feature of taut giant vesicles is that micron-sized domains can be imaged by standard fluorescence microscopy. Moreover, when phase-separable solutions are enclosed within vesicles, condensates are easily formed through changes in osmotic pressure [98] or pH [99]. Challenges of free-floating vesicles include aggregation and shape changes, especially under conditions optimized for proteins.

2.5.1 Challenge 1: Aggregation of free-floating vesicles

Mixing vesicle solutions with condensate solutions can cause aggregation. Even simple salt-containing buffers can cause aggregation of lipid vesicles as shown in Fig. 2.5. Furthermore, when protein condensates bind to free-floating vesicles, condensates can bridge the gap between adjacent vesicles to create aggregates. Aggregation presents three disadvantages. First, imaging membrane domains on aggregated vesicles is difficult, especially when domains are small. The best method for imaging aggregated vesicles is confocal microscopy; however, these microscopes typically lack the temperature control systems required to measure T_{mix} . Second, proteins' access to some membranes in the aggregate is hindered, leading to large variation in protein concentration across membrane surfaces. Third, when membranes adhere, ordered domains localize to the interfaces and can appear at temperatures above T_{mix} of unadhered membranes [100, 101].

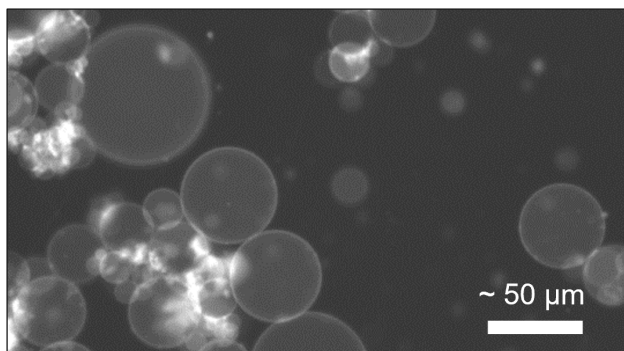


Figure 2.5: **Lipid vesicles can aggregate in buffer.** Here, vesicles are composed of 98 mol% di(18:1)PC and 2 mol% 18:1 DGS-NTA(Ni) (Avanti Polar Lipids) were produced by a standard electroformation technique [102] and then introduced to an osmotically-matched buffer of 25 mM HEPES and 150 mM NaCl. The image was collected by H.M.J.W. with a Nikon Eclipse ME600L upright epifluorescence microscope and a Hamamatsu C13440 camera.

Aggregation of vesicles is frequently mitigated by adding charged lipids or surfactants [103]. However, at high salt concentrations the Debye length is shorter, reducing electrostatic repulsion between charged lipids. Adding a hydrophilic polymer such as PEG to lipid

headgroups confers some steric repulsion, albeit at molecular length scales [104]. If experiments can be completed quickly, it may be sufficient for vesicles to aggregate slowly, as when they are dilute in solution. Tactics to avoid membrane aggregation include immobilizing vesicles or directly assembling membranes on supports; the advantages and caveats of which are discussed in Sec. 2.6.

2.5.2 Challenge 2: Membrane bending and tubulation

Tubules are common in membranes (Fig. 2.6), especially in vesicles with excess area (more membrane than necessary to enclose their volume) [105, 106], in supported membranes with area changes [107, 108], and in membranes that bind proteins [88, 109, 110]. Tubules can also form in vesicles during gentle hydration [111] and electroformation [102, 111]. In experiments that couple membranes to condensates, tubules complicate quantitative measurements. First, membrane phase separation is difficult to identify when domains nucleate in thin, undulating tubules. Second, tubulation can cause nonuniform lipid compositions [112]. Third, confounding variables arise. For example, Ld phases appear in highly curved membranes of vesicles [113] and supported bilayers [114]. Similarly, some proteins (e.g., the I-BAR protein IRSp53 [115] preferentially partition onto tubules. Therefore, if condensate proteins interact with tubules of only one membrane phase, it is unclear if the interaction arises from the membrane's lipid composition or its shape.

Membrane tubulation can be mitigated by membrane tension, typically applied through osmotic pressure gradients. However, tension can shift the membrane's miscibility temperature [116–119]. Unfortunately, membrane tubulation can be increased by factors as benign as making membranes with different types of molecules (e.g., noncylindrical lipids [109, 120], charged lipids [121], or block copolymers [122], applying gradients in temperature [123] or pH [124], introducing a plastic microbead [125], or establishing asymmetry in aqueous salt or sugar concentrations [126, 127]. When vesicles encapsulate immiscible solutions, inward tubules can coat the interface between the two solutions, whether the solutions have few components (e.g., dextran and PEG [128]) or many (e.g., tonoplasts of *A. thaliana*) [70].

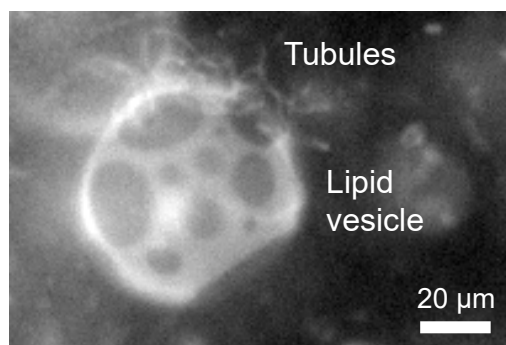


Figure 2.6: **Membrane tubules can form at vesicle surfaces, complicating quantitative measurements of coupling between protein condensates and membranes.** Fluorescence micrograph of thin, white, Ld-phase tubules protruding from a broad area at the top of the vesicle. The vesicle contains 31:31:35 mol% di(18:1)PC: di(16:0)PC:cholesterol with 2.2 mol% 18:0-PEG5000 PE (Avanti Polar Lipids) and 0.8% Texas Red PE (Thermo Fisher Scientific), in a hypertonic solution of sucrose at 33°C. The image was collected by H.M.J.W. on instrumentation described elsewhere [17]. Contrast was enhanced to make dim tubules visible.

Tubulation is also driven by membrane asymmetry [105] in lipids (e.g., GM1 [129], DHA [130], cholesterol, or DOPC [107]), fatty acids [131], DNA origami [132,133], peptides [134,135], or proteins [109,110,136]. Polypeptides with attractive domains, like FUSLC, generate inward tubules in vesicles, whereas repulsive protein domains generate outward tubules [137]. Some proteins interact directly with membranes (e.g., N-BAR domains [110,136]). Others may be tethered to the membrane and interact via steric crowding; smaller proteins produce membrane tubes more frequently [109]. Some tethered condensate proteins (the RGG domain of LAF-1, the low-complexity domain of FUS, and the low complexity domain of hnRNPA2) form molecularly thin, liquid domains on membranes and cause tubulation [88]. Higher densities of tethers cause more tubules [88,109]. Testing prewetting theories [65] by varying tether densities becomes challenging when broad ranges of tether densities become inaccessible due to tubulation.

2.5.3 Challenge 3: Difficulties in exchanging solutions

Condensate proteins are typically added to phase-separated membranes by solution exchange. However, fluid flow can push free-floating giant ($>10\ \mu\text{m}$) vesicles out of the field of view, even when they have sunk in lower density solutions. To address this problem, membranes can be tethered to surfaces, discussed further in Tool 3. Vesicles can also be deposited in flow cells, captured in microfluidic wells, or trapped behind partitions [84,106,138,139]. One caveat is that trapped vesicles often touch a solid surface, which can cause phase-separated domains to reorganize, even when the surface is passivated with BSA proteins or when the membrane's temperature is above its miscibility transition [100,140,141]. An alternative trapping method places neutrally buoyant vesicles in a dead-end microfluidic channel while a solution flows past the channel's entrance [142].

2.5.4 Challenge 4: Slow collective motion of lipids in membranes on solid surfaces

Depositing lipid membranes on surfaces solves many challenges, especially if the surface fits inside a low-volume flow cell. However, hydrodynamic theory suggests that if the aqueous layer between the membrane and surface is too thin, then lipid domains cannot form (or grow by colliding and coalescing [143]) on experimental timescales [144]. As a result, the domains are typically noncircular and can be too small to resolve by fluorescence microscopy [145,146]. Although circular, micron-scale liquid domains sometimes form in membranes deposited directly on clean glass, they are immobile, and their thermal history may be important [146,147].

2.6 Tools and Methods

2.6.1 Tool 1: Black Lipid Membranes

Black lipid membranes (BLMs, Fig. 2.4D), which span holes in supports, have several advantages for coupling condensates to membranes. Because both sides of the membrane are in contact with thick water layers, round, micron-scale liquid domains form on experimental

timescales. BLMs are compatible with fluid exchange. When proteins are introduced to both sides of the membrane, transmembrane coupling of proteins is possible [73]. Even when proteins are introduced to only one side, membrane tension prevents tubulation [73]. BLMs that span large (micron-scale) distances are typically formed by one of four methods:

1) An oil droplet containing lipids is “painted” over a hole in a plastic sheet or microfluidic device [148,149]. A lipid bilayer forms as oil drains to the hole’s perimeter, where oil bridges the molecular thickness of the membrane and the macroscopic thickness of the plastic.

2) A Transmission Electron Microscopy (TEM) grid with an array of holes is coated with an oil layer containing lipids by moving the grid from an oily solution into an aqueous solution [97]. Bilayers form as oil drains to the perimeters of the holes. A challenge is that the volume of oil must be optimized for each lipid composition [97].

3) In the Montal-Mueller technique [96], lipid monolayers at air-water interfaces are passed over a hole in a hydrophobic, plastic sheet pre-coated with long-chain oils. The oil at the perimeter of the bilayer and any oil molecules that persist within the bilayer do not alter its miscibility transition temperature or the areas of the two phases [150]. An advantage of Montal-Mueller membranes is that each monolayer leaflet can contain a different ratio of lipids: these asymmetric bilayers have opened new avenues for probing transbilayer coupling of liquid phases [150]. Disadvantages are that the method is challenging and that volumes are large (≈ 1 mL), so temperature changes slowly.

4) In modified Montal-Mueller techniques, lipid monolayers at two oil-water interfaces assemble into a bilayer. These bilayers are called various names (including contacting monolayers [151] and droplet interface bilayers [152]), and they may contain nm-scale decane inclusions [153]. In one technique [154], phase-separating membranes can span very large areas (≈ 1 mm², Fig. 2.7).

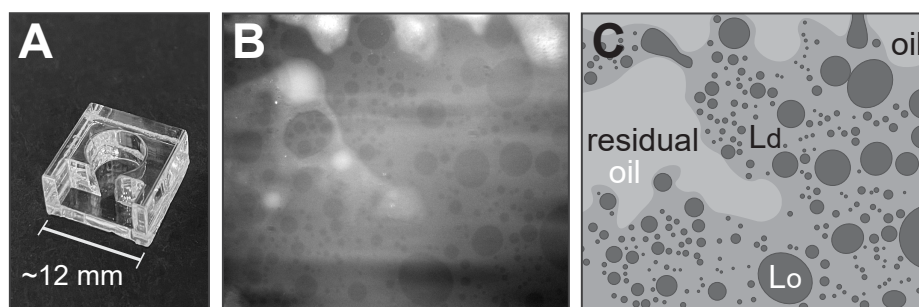


Figure 2.7: **Coexisting Lo and Ld phases can be imaged in black lipid membranes.** **A)** Custom chamber of laser-cut acrylic by Dave Richmond and Dan Fletcher [155]. Vertical black lipid membranes form across the gap between the rectangular and circular wells. **B)** Fluorescence micrograph of a membrane spanning ≈ 1 mm (the image width). The membrane contains the lipids di(18:1)PC, di(16:0)PC, and cholesterol, and was imaged by Dave Richmond and S.L.K. **C)** Schematic of Panel B, identifying Lo/Ld membrane phases. In the micrograph, excess oil has not entirely drained to the hole's perimeter.

2.6.2 Tool 2: Stacked and cushioned membranes

Membranes can be offset from solid supports by stacking membranes or assembling them on polymer cushions. Controls may be needed to account for higher transition temperatures in SLBs [156], especially on inhomogeneous surfaces [157], with respect to vesicles.

1) Stacked membranes

Membranes can be stacked by bursting a GUV on a membrane supported on a solid substrate. The upper membrane may be separated from the lower membrane by a uniformly thin layer of water or by a thick water pocket [145]; both present advantages and disadvantages. If the upper membrane lies flat, binding of proteins can cause it to roll and delaminate; similar changes in spontaneous curvature cause tubulation [158]. Affixing the upper membrane to the lower membrane (e.g., via DNA binding) leads to other problems: the upper membrane can disintegrate within hours unless it contains high ratios of saturated lipids [159,160]. If there is a water pocket, domains in the upper membrane may diffuse or may be immobilized by membrane deformations, which are enhanced by protein binding [161]. An alternative method of generating membrane stacks is to spin-coat lipids on a substrate such as mica [94]

and erode the resulting multilayer with a jet of water [162]. In regions where only two stacked membranes remain, domains in the upper membrane have some attributes of GUV domains: liquid domains deform due to fluid flow, become round in tens of seconds, grow to be tens of microns by Ostwald ripening, and occasionally coalesce [162]. Stacks of phase-separating membranes are also made by hydrating dry lipids on a silicon substrate [163].

2) Membranes cushioned by polymer headgroups and/or substrates

Lipopolymers (lipids with polymer head groups) can offset membranes in which they reside from solid substrates. Because polymer lengths can be varied, the distance and interaction between the membrane and support can be tuned. Membranes separated from glass supports by PEGylated fatty acids can grow to be micron-scale but are thereafter stationary and/or noncircular on experimental timescales [164]. Other headgroup modifications include poly(2-oxazoline) polymers [165] and oligopeptides [166]. Another strategy is to coat supports with polymers before depositing membranes. For example, polydimethylsiloxane (PDMS) is easily patterned with microstructures to test the impact of curvature on domain formation [114, 167]. The PDMS surface must be hydrophilic; otherwise, cholesterol can leach into it from the membrane [168]. Membrane domains on PDMS or other stiff cushions (e.g., cellulose) can be stationary on experimental timescales [169]. When the two strategies are combined (membranes contain lipopolymer headgroups and rest on PDMS surfaces), micron-scale, circular, liquid domains form in membranes cooled very slowly through T_{mix} , at ≈ 0.04 °C/min [170]. A challenge is that these domains are also stationary on experimental timescales [170].

2.6.3 Tool 3: Membrane-substrate tethers

To mitigate aggregation of free-floating vesicles and their displacement by fluid flow, vesicles can be attached to substrates via molecular tethers. A typical approach is to coat the substrate with a functionalized polymer such as PEG-biotin, followed by the addition of an avidin, which binds biotinylated lipids anchored in the membrane [171–173]. Optimizing the tether concentration is important: giant vesicles with high tether densities deform such that

large areas are in contact with the substrate, leading to domain reorganization [140]. This adhesion can be reduced by incorporating a co-polymer like PEG-silane or PLL-g-PEG at the interface [174, 175]. Alternative tethers use DNA-lipids [176], which are well suited for ≈ 100 nm vesicles. However, as with other tethers, high concentrations of DNA-lipids cause giant vesicles to rupture, forming patches on glass and SLB supports [160]. However, when too few tethers are deployed, lipid anchors pull out of giant vesicles when flow is introduced. Another alternative is to use electroformed vesicles that are still tethered to their conductive substrates by tubules that withstand slow exchange of solutions [177]. However, these vesicles often touch, and quantification of the total membrane area is difficult.

2.6.4 Tool 4: Tethers to couple condensates to membranes

To couple phase separation in condensates and membranes, the two systems must be in contact. One option is to link condensates to membranes via tethers (Fig. 2.1D), which include histidine-binding lipids, phosphoinositide lipids, polymer-based linkers, lipid-DNA linkers, and biotinylated lipids. In the literature, “tethers” include molecules that bind membranes to substrates (see Tool 3). Some molecules can be used for both purposes, although membrane-substrate tethers are often designed to bind irreversibly under experimental conditions, whereas membrane-condensate interactions should be reversible. One clever approach is to tether only one protein of a multi-component condensate to the membrane and then introduce remaining proteins in solution [86, 87]. Tethers enable strong controls that distinguish effects of localizing a protein on a membrane and adding more proteins to form a condensate [86, 87] or that distinguish effects of attaching condensate molecules to immobile versus mobile tethers [50]. In turn, new controls are warranted. For example, Cans et al. [98] attribute increases in membrane T_{mix} to the addition of PEG-lipid tethers and to encapsulation of a solution of PEG and dextran in vesicles. Similarly, membrane T_{mix} can shift when tethers bind multiple lipids (as streptavidin with biotinylated lipids, or cholera toxin with GM1-lipids) [80]. Most tethers strongly partition into either the Lo or Ld membrane phase, which likely also shifts T_{mix} .

Histidine-binding lipids Polyhistidine tags (His-tags) are sequences of 2-6 histidines attached to proteins, commonly used to purify them via affinity chromatography [178]. The tags can also link proteins to membranes via phospholipids with nickel- or copper-chelating headgroups (e.g., NTA(Ni) or IDA(Cu)). Metal-chelating tethers have two advantages. First, binding of his-tagged proteins to lipids is reversible upon addition of EDTA at low concentrations [179]. Second, the tethers can preferentially partition to the Lo or Ld phase of membranes, depending on the length and saturation of their lipid tails [17].

A disadvantage of metal-chelating lipid tethers is their high melting temperatures. For instance, lipids with IDA (iminodiacetic acid) headgroups and 16:0 carbon chains melt at 55 °C (73 °C in the presence of Cu^{2+}). As a result, binary membranes of this lipid and a low melting lipid (e.g., POPC) demix into gel and liquid phases at room temperature [109,179]. Also, metal-chelating tethers are incompatible with thiol compounds, which disrupt links between His-tagged proteins and NTA(Ni) lipids [180]. This impedes super-resolution imaging techniques, which frequently use thiols to enable fluorophore photoswitching. Similarly, if aqueous solutions require oxygen scavenging systems with glucose, it is important to run controls that measure how glucose affects phase separation of condensates [180].

Phosphoinositides

Negatively charged phosphoinositide (PI) lipids are found in membranes of eukaryotic cells, including the endoplasmic reticulum, endosomes, and plasma membranes. Although PI-lipids are low abundance, they are important because of the specificity with which several proteins bind to them [181], making PIs a convenient tether to protein condensates. One such protein, N-WASP, has been used to anchor actin networks to membranes containing a fluorescently labeled PIP2-lipid (di(16:0)-TMR-PIP2) that preferentially partitioned to the Ld phase [84]. Challenges of PI-lipids are that they may cluster if buffers contain divalent cations [182,183], they are difficult to incorporate in model membranes at concentrations above a few mole percent [182], and they can leach from membranes to form micelles in solution [184].

PEG-lipids

Pegylated lipids (PEG-lipids) can directly couple membranes to phase-separating solutions of PEG and dextran [67, 98, 185] or can behave as a tether when modified with functional groups like biotin. At low concentrations of PEG-lipids, their partitioning between membrane phases is influenced by the lipid tails, the length of the polymer, and the hydrophobicity of the functional group [186]. At higher concentrations set by the PEG-lipids' molar mass, steric interactions can drive PEG-lipids from domains [92]. At membrane concentrations of PEG(2000)-lipid above ≈ 10 mol%, vesicles break up into membrane discs [187].

DNA-lipids

Liquid-liquid phase separation has been implicated in organization [30, 188] and repair of DNA [189, 190]. DNA strands attached to lipid headgroups can interact with biocondensates by binding to complement strands, interacting with DNA-binding proteins, or folding into aptamers that bind other molecules. For short strands, hybridization can be reversed by increasing temperature. DNA strands are typically anchored to the membrane by one or more sterols. By modifying the number of sterols, replacing cholesterol with tocopherol, or replacing model membranes with giant plasma membrane vesicles, the partitioning of DNA-lipids can be tuned between the Lo and Ld phases [191–193].

Biotinylated lipids

Biotin and avidin proteins bind with high affinity ($K_d \approx 10$ -15 M) [194]. Biotin conjugated to the headgroup of phospholipids is frequently used to facilitate protein-membrane interactions. A caveat is that vesicles that contain biotinylated lipids can be crosslinked by avidin (which contains four binding sites for biotin) and form multi-vesicle aggregates. Vesicles can be redispersed by adding soluble biotin, which has a higher affinity than biotinylated lipids for avidin [195, 196]. Some researchers incorporate a third molecule that reversibly interacts with a membrane or condensate, such as a biotinylated DNA oligonucleotide [50]. If proximity between a lipid and its biotin label is a concern, polyethylene glycol can be inserted as a spacer, as in biotin-PEG-lipids. A caveat is that the spacer length (and the mole fraction of biotin-PEG-lipid in the membrane) affects the partitioning of biotin-PEG-lipids between membrane phases [197].

2.6.5 Tool 5: Compatible proteins

Tools 1-4 focused on membrane components. Which corresponding protein systems should researchers choose? The PhaSepBD database contains thousands of entries [198], but will any protein system that undergoes phase separation suffice? The phase behavior and molecular interactions of condensates are reviewed elsewhere [27, 71, 199]. In brief, condensate molecules that are primarily polar and charged are described by Flory-Huggins theory for enthalpically driven phase separation. Above an upper critical temperature or upon addition of salt, entropic forces overcome chain-chain interactions and the system ceases to phase separate. In contrast, condensate molecules that are primarily hydrophobic, such as elastin-like polypeptides, have lower critical temperatures above which interactions between the peptides and solvent are disfavored, and the system phase separates [199]. The ideal choice of proteins depends on the experimental design. For example, if salt will be added to affect protein phase separation, the proteins should be charged and potential effects of salt on membrane phase separation should also be considered [77, 78]. Similarly, if temperature will be varied to affect membrane phase separation, the potential effects of protein interactions and denaturation should be considered (Fig. 2.8). Molecules that may tolerate higher temperatures include engineered peptides [25] or a polymeric systems [200]. An alternative tactic is to choose membranes that demix at lower temperatures [76].

Several researchers have leveraged protein systems known to cluster on membranes. For example, condensates of the linker for the activation of T cells (LAT) and its binding partners (Grb2 and Sos1) have been employed to shift membrane miscibility temperatures [76, 87]. Another protein system in use is Nephren and its cytoplasmic binding partners (Nck and N-WASP) [25, 26].

2.7 Conclusion

In conclusion, quantitative experiments that couple lipid membranes and protein condensates require clever design choices. Here, we have reviewed several challenges that arise in the ex-

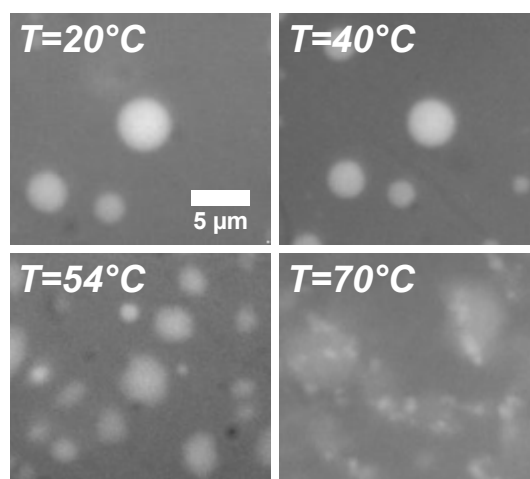


Figure 2.8: **Condensates can destabilize as temperature increases.** Representative fluorescence micrographs of solutions of 25 μM MBP-(SH₃)₅-His, 37.5 μM (PRM)₅, 25 mM HEPES, and 150 mM NaCl after mixing 2 hr at room temperature. At low temperatures, the condensates form spherical droplets with sharp edges, characteristic of liquid-liquid phase separation (20°C and 40°C). At higher temperatures, the edges of the condensates blur, their shapes become nonspherical, and bright puncta appear throughout the solution (54°C and 70°C). This behavior cannot be explained by shape fluctuations near a critical point and may reflect protein denaturation. The proteins were produced and purified by Michael Cotten and Michael Rosen; solutions were mixed and imaged by H.M.J.W.

periments, as well as several tools that mitigate the challenges. Using these tools, researchers have made recent, exciting successes in observing thermodynamic changes in coupled systems, including shifts in membrane transition temperatures and the formation of surface condensates. We expect to see additional advances in the future, especially in research that combines theory and modeling to support quantitative experiments that characterize surface phases under prewetting conditions.

Chapter 3

COMMON METHODS OF MAKING GIANT VESICLES (EXCEPT EMULSION TECHNIQUES) CAPTURE INTENDED LIPID RATIOS

This chapter was first published in *BioRxiv* in 2024, and was written in collaboration with Kent J. Wilson, Gunnar J. Goetz, Emily L. Pruitt, Amy Li, Libin Xu, and Sarah L. Keller [201].

Heidi M. J. Weakly, Kent J. Wilson, Gunnar J. Goetz, Emily L. Pruitt, Amy Li, Libin Xu, and Sarah L. Keller. 2024. “Common methods of making giant vesicles (except emulsion techniques) capture intended lipid ratios.” bioRxiv doi: 10.1101/2024.02.21.581444

3.1 Abstract

Researchers choose different methods of making giant unilamellar vesicles in order to satisfy different constraints of their experimental designs. A challenge of using a variety of methods is that each may produce vesicles of different lipid compositions, even if all vesicles are made from a common stock mixture. Here, we use mass spectrometry to investigate ratios of lipids in giant vesicles made by four common methods: electroformation on indium tin oxide slides, electroformation on platinum wires, gentle hydration, and emulsion transfer. The vesicles are made from a mixture of common lipid types: di(18:1)PC, di(16:0)PC, di(18:1)PG, di(12:0)PE, and cholesterol. We find that electroformation and hydration methods result in only minor shifts (≤ 5 mol%) in lipid ratio relative to the stock solution. It was previously known that the remaining method, emulsion transfer, severely reduces the amount of cholesterol in membranes. Here, we show that the emulsion transfer method also skews the ratios of lipids in a chain-dependent manner. For example, vesicles made by emulsion trans-

fer using only PC-lipids contain less unsaturated lipid (di(16:1)PC relative to di(16:0)PC) and less shorter-chain lipid (di(16:1)PC relative to di(18:1)PC). A separate technique, extrusion, is often used by researchers to convert giant vesicles into smaller vesicles. We find that extrusion decreases cholesterol fractions (by 5.0 ± 3.3 mol% in vesicles that originally contained ≈ 25 mol% cholesterol). Even if all researchers were to use the same method of making vesicles, a separate question arises about whether vesicle lipid compositions vary from experiment to experiment. For the most common methods of producing GUVs (electroformation and gentle hydration), sample-to-sample variations in average lipid ratios are roughly ± 2 mol%.

3.2 Introduction

Giant unilamellar vesicles (GUVs) come in many forms, from simple models of minimal membranes to complex mimics of living cells. Each application of GUVs requires that different constraints be met, such as controlling vesicle size [202–204], number of lamellae [205–207], compositional asymmetry [208–210], membrane charge [78, 211] and encapsulation of solutes [212, 213]. In response, many methods have been developed to produce GUVs [93], where each method prioritizes different constraints. However, when the community uses more than one method to make GUVs, an uncomfortable question arises: do the vesicles produced by each method contain the same ratio of lipids as the stock solution from which the vesicles were made? If not, do all methods alter the intended lipid ratio in the same way, or does each method yield different ratios? These straightforward questions have a huge impact: researchers who use different methods cannot compare their results unless they know that their vesicle compositions are comparable, or, at the least, unless they know how to estimate the magnitude of the offset in lipid composition they might observe.

Concerns that different vesicle-making methods may incorporate different ratios of lipids into membranes are well-founded, especially when one of the lipids is a sterol. The solubilities of sterols in membranes of giant vesicles are sensitive to experimental conditions and to the identities of the other lipids in the membrane [214–217]. Even when the mole fraction

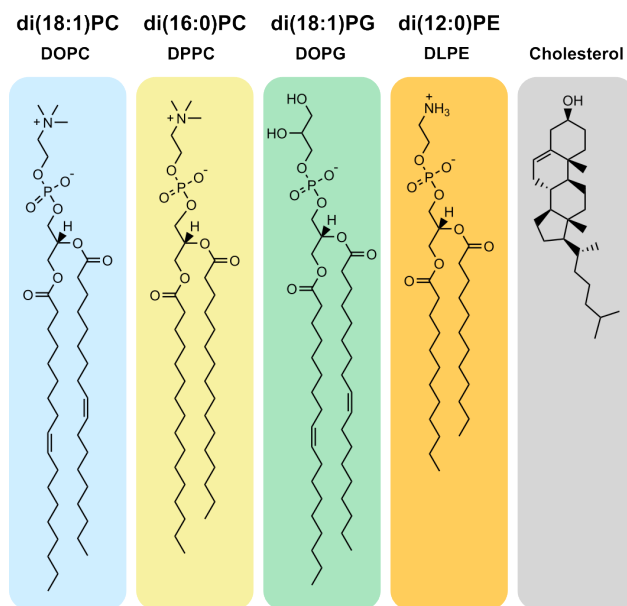


Figure 3.1: **Structures of several lipids frequently found in GUVs.** Formal names of lipids reflect the length and unsaturation of the acyl chains and the headgroup type, whereas common names reflect historical sources. For example, di(18:1)PC (commonly called DOPC) is a zwitterionic lipid with a phosphatidylcholine (PC) headgroup and two 18-carbon chains, each with one double bond, whereas di(16:0)PC is saturated, with 16 carbons in each chain. Di(18:1)PG is a charged and unsaturated lipid with a phosphatidylglycerol (PG) headgroup. Phosphatidylethanolamine (PE) headgroups, as in di(12:0)PE, are smaller than PC headgroups, so PE-lipids are typically cone-shaped. Cholesterol has a hydroxyl moiety as a headgroup and a fused, four-ring structure with an 8-carbon chain.

of cholesterol is below its membrane solubility limit, extrusion of vesicles may perturb the cholesterol fraction [218]. Cholesterol levels are known to be especially low in vesicles made by emulsion transfer techniques [219–221]. Challenges also exist in incorporating sufficient lipids with high melting temperatures [16], high charge [78,222] or high spontaneous curvature [205] into membranes of giant vesicles.

Here, we used mass spectrometry to directly measure average mole fractions of lipids in vesicles made by multiple methods. To minimize experimental error, we produced the vesicles from a common lipid stock solution. We chose the lipids in our stock to span a broad range of characteristics (Fig. 3.1). They include cylindrical, zwitterionic lipids with both low

and high melting temperatures (di(18:1)PC and di(16:0)PC), a charged lipid (di(18:1)PG), a cone-shaped lipid (di(12:0)PE), and a sterol (cholesterol). Each lipid is included for a different reason. PC-lipids produce stable membranes and are the most abundant lipid in mammalian cells [223–225]. PG-lipids are abundant in mycobacteria [226]. Their low pKa [227] and subsequent charge can increase the yield of vesicles made by gentle hydration, as does charged phosphatidylserine (PS) lipids [211]. PE-lipids facilitate membrane fusion and are abundant in the inner leaflet of red cell membranes [223, 225, 228]. Cholesterol, in addition to facilitating membrane fusion [229], enables large-scale, liquid-liquid phase separation in membranes [230] and constitutes a large fraction (up to ≈ 40 mol%) of lipids in mammalian membranes [225]. We mixed these lipids in a ratio likely to produce high yields of giant vesicles. Specifically, our stock solution contains high fractions of PC-lipids to stabilize GUVs and low fractions of PE-lipids to avoid inverted hexagonal phases and minimize tubule formation [223]. Similarly, we use low fractions of PG-lipids to enable electroformation and low fractions of cholesterol to avoid its membrane solubility limit [214–217].

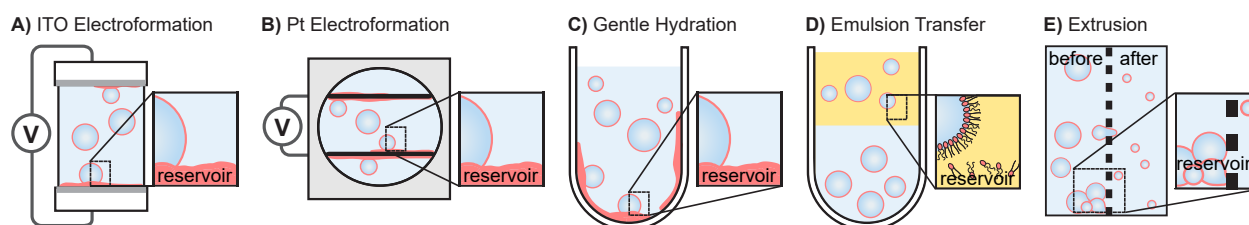


Figure 3.2: Methods of producing vesicles, showing reservoirs of unincorporated lipids. **A)** In “ITO electroformation”, an alternating field is applied across a hydrated lipid film on slides coated with indium tin oxide. Afterward, a residue of lipid remains on the slide. **B)** In “Pt electroformation”, an alternating field is applied across a hydrated film on platinum wires. Afterward, a residue of lipids remains on the wires. **C)** In gentle hydration, vesicles form spontaneously from a hydrated lipid film on a glass surface. Afterward, a residue of lipids remains on the glass. **D)** In emulsion transfer, lipids from an oil solution assemble at water/oil interfaces to form emulsion droplets, which then pass through a second interface to form vesicles. Afterward, a reservoir of lipids remains in the oil. **E)** In extrusion, smaller vesicles are made by passing giant vesicles through a porous filter. Afterward, a reservoir of lipids and vesicles remain on the filter. Figures are not to scale.

We chose four common techniques of producing GUVs: electroformation on slides coated with indium tin oxide (ITO), electroformation on platinum (Pt) wires, emulsion transfer, and gentle hydration (Fig. 3.2). We also included a common technique of converting giant vesicles into smaller vesicles: extrusion across a porous membrane filter. Each technique has advantages. Electroformation produces stable GUVs that span a wide range of sizes, frequently up to 100 μm [102]. Emulsion transfer is valued for high encapsulation efficiency [231]. Gentle hydration incorporates (and often requires) charged lipids in GUVs [211]. Extrusion converts GUVs into vesicles of smaller and more uniform sizes. Each technique leaves a reservoir of excess lipids that were not incorporated in the vesicles. These reservoirs may not contain the same ratio of lipids as the vesicles (Fig. 3.2, insets).

Our use of mass spectrometry to measure average vesicle compositions complements recent advances in using Time-of-Flight Secondary Ion Mass Spectrometry (ToF-SIMS) to directly measure vesicle-to-vesicle variations in lipid compositions [232]. The two techniques are synergistic. Whereas current ToF-SIMS analyses excel at measuring relative compositions in individual vesicles, the technique currently has low sample-to-sample reproducibility for vesicle populations [232]. Our mass spectrometry technique does the opposite. It excels in reproducibly evaluating lipid ratios in vesicle populations and does not evaluate compositions of individual vesicles.

3.3 Materials and methods

Chemicals

PC-lipids, PG-lipids, PE-lipids, and all lipid standards for mass spectrometry were obtained from Avanti Polar Lipids and used without further purification. Lipids are denoted for their headgroup (e.g., “PC”, “PG”, or “PE”), the number of carbon chains (e.g., “di” = 2), and each chain’s number of carbons and unsaturation (e.g., “18:1”). Specific lipids in our samples include dioleoyl-phosphocholine (di(18:1)PC or DOPC, $T_{melt} = -18.3 \pm 3.6^\circ\text{C}$ [4]), dipalmitoyl-phosphocholine (di(16:0)PC or DPPC, $T_{melt} = 41.3 \pm 1.8^\circ\text{C}$

[4], dioleoyl-phosphoglycerol (di(18:1)PG or DOPG, $T_{melt} = -18^{\circ}\text{C}$ [233]), and dilauroyl-phosphoethanolamine (di(12:0)PE or DLPE, $T_{melt} = 49.3 \pm 1.7^{\circ}\text{C}$ [234]). Lipid standards include di(15:0)PC, (16:0/18:1)PC, di(15:0)PE, di(15:0)PG, and d_7 -cholesterol. Cholesterol (Sigma-Aldrich) and a fluorescently labeled lipid (Texas Red DPPE, Life Technologies) were dissolved in chloroform at 10 mg/mL and 1 mg/mL, respectively. Mineral oil (light, bioreagent, 0.84 g/mL, 14.2-17.2 cSt at 40°C) was from Sigma Aldrich.

Master Stock

A master lipid stock solution was prepared for a 5-component mixture (DOPC/DPPC/DOPG/DLPE/Cholesterol with 0.8% Texas Red-DPPE) in chloroform and stored at -20°C in a vial sealed with Teflon tape and electrical tape.

Electroformation on ITO Slides

Electroformation followed standard procedures [102]. Briefly, for each sample, 0.25 mg of total lipid (29 μL of master stock solution) was heated to 60°C and spread across two ITO-coated glass slides using the side of a glass Pasteur pipette. The slides were placed under vacuum for ≈ 30 min to allow residual chloroform to evaporate. An electroformation chamber was made by sandwiching 0.3 mm thick Teflon spacers between the ITO-coated slides. The chamber was filled with 300 mM sucrose (≈ 300 μL) and sealed with vacuum grease. The chamber was then attached to metal electrodes using stainless steel binder clips. An AC voltage of 1.0 V was applied across the electrodes at 10 Hz for 2 hr at 60°C . The temperature of 60°C is roughly 20°C above the highest lipid T_{melt} in the system.

Electroformation on Platinum wires

A chamber was adapted from previous designs [235]. Briefly, a vertical hole of 15 mm diameter was cut in a 25 mm x 25 mm x 5 mm block of Teflon. Two holes of ≈ 0.25 -mm diameter were cut horizontally through the chamber, separated by 2.5 mm. Two 0.25-mm

platinum wires were inserted into the two holes. Before each use, the wires and chamber were cleaned with chloroform. The bottom of the Teflon chamber was sealed with a glass cover slip, and the chamber was placed on a 60°C hot plate. Next, 5.7 μL of master stock solution was deposited in evenly spaced 0.5- μL drops on both wires. The interior of the chamber was filled with 300 mM sucrose solution, and the top was sealed with a glass cover slip. An AC voltage of 2.5 V was applied at 10 Hz for 2 hr at 60°C.

Gentle Hydration

For each sample, 0.2 – 0.8 mg of total lipid from the master stock was transferred into a glass test tube. The test tube was placed in a water bath at $> 50^\circ\text{C}$ while chloroform was removed from the lipid solution by a steady stream of N_2 gas to form a lipid film. To remove residual chloroform from the film, the test tube was placed under vacuum for ≥ 1 hr. After drying, the lipid film was rehydrated by adding 0.2 - 0.8 mL of 300 mM sucrose, so that the test tube contained 1 mL of solution for every 1 mg of lipid. The test tube was sealed with parafilm and maintained in an oven at 50°C for 24 hr. while vesicles formed.

Emulsion Transfer

The procedure was adapted from standard protocols [220, 231, 236] and was conducted at room temperature (20-25°C). A lipid film was deposited inside a test tube by drying 45.8 μL of master stock solution (0.4 mg total lipid) under a gentle stream of nitrogen gas and placing the test tube in a vacuum chamber for ≥ 30 min. The test tube and a sealed container of mineral oil were quickly transferred to a glove box (Techni-Dome 360° Glove Box Chamber) which was then purged with N_2 gas until humidity reached $\leq 25\%$ (ThermPro Digital Indoor Thermometer). The container of mineral oil was opened only in the glove box, and 200 μL of mineral oil was added to the test tube. The test tube was sealed with Teflon, parafilm, and electrical tape, removed from the glove box, and sonicated in a water bath (CO-Z Digital Ultrasonic Cleaner Model 10A, 40 kHz) for ≥ 30 min at 50°C. The resulting lipid-in-oil solution was mixed with 20 μL of an aqueous, 300 mM sucrose solution by vigorous pipetting

or by mechanical agitation to create an emulsion. Approximately 200 μL of the emulsion was layered above 300 μL of an aqueous, 300 mM glucose solution in a 1.5 mL microcentrifuge tube and then centrifuged at 9000 g for 30 min to drive dense, sucrose emulsion droplets through the oil/water interface. The supernatant was removed without disturbing the vesicle pellet until minimal solution covered the pellet. The pellet was resuspended in 600-800 μL of 300 mM glucose by gentle pipetting, using tips that had been cut to larger diameters to minimize shearing.

Vesicle Sedimentation and Storage

For vesicles made by electroformation and gentle hydration, vesicles were separated from lipid aggregates by sedimenting vesicles in an osmotically matched glucose solution as in Fig. A.1. Briefly, 200 μL of vesicle solution was added on top of 800 μL of glucose solution in a 13x1000 glass test tube (Fisher Scientific). Vesicles sank to the bottom of the tube for 10 min. Then 150 μL of vesicle solution was transferred from the bottom of the tube to a microcentrifuge tube. For emulsion transfer, vesicles were sedimented after resuspension in 600-800 μL of a glucose solution. For all methods, separated vesicle samples were stored at -20°C in parafilm-sealed 1.5 mL microcentrifuge tubes.

Vesicle Imaging

To verify that the four methods above produced giant vesicles, vesicle solutions were imaged between glass slides on a Nikon Eclipse ME600L upright epifluorescence microscope using a Hamamatsu C13440 camera at room temperature (25°C).

Extrusion

Vesicle solutions were prepared by gentle hydration, and then sedimented to remove lipid aggregates. The sedimented vesicle solution was split into two samples of equal volume. The first sample was reserved for “Before” extrusion measurements and the second sample

was extruded to obtain an “After” measurement. To minimize the loss of solution due to dead volume of the miniextruder (Avanti Polar Lipids), the filter supports and 0.1 μm polycarbonate filter were prewet by passing 1 mL of a sucrose solution through them prior to loading the sample. The complete extruder assembly (the heat block, the syringe with the vesicle solution, and the empty syringe) was maintained at 50 °C for 30 min before extrusion. Finally, the vesicle solution was passed through the filter 9 times and collected for analysis.

HILIC-IM-MS Analysis of Phospholipids

Internal lipid standards were added to samples prior to lipid extraction to account for lipid loss during extraction and to aid in relative quantitation for each lipid class. Total lipids from aliquots of each sample were extracted by the method of Bligh and Dyer [237]. Extracts were dried in a vacuum concentrator and reconstituted in 2:1 acetonitrile-methanol. Lipid analysis was conducted using hydrophilic interaction liquid chromatography (HILIC) coupled with ion mobility-mass spectrometry (IM-MS) in positive electrospray ionization mode (Waters Synapt XS HDMS; Waters Corp., Milford, MA). Chromatographic separations were carried out using a Phenomenex Kinetex HILIC column (50 x 2.1 mm, 1.7 μm) with 95% acetonitrile/5% water/5 mM ammonium acetate as mobile phase A and 50% acetonitrile/50% water/5 mM ammonium acetate as mobile phase B (Waters Acquity FTN UPLC; Waters Corp.). Collisional cross-section calibration and IM-MS analysis were conducted as described previously [238–240]. Data alignment and peak detection were performed in Progenesis QI (Nonlinear Dynamics; Waters Corp.). Retention time calibration and lipid identification were calculated with the LiPydomics Python package [241]. Lipid abundances were normalized to their internal standards.

For the five methods tested, the lipid components were normalized to the following internal standards: di(16:0)PC and di(18:1)PC to di(15:0)PC, di(12:0)PE to di(15:0)PE, and di(18:1)PG to di(15:0)PG. For the two-component emulsion transfer measurements, the master stock solution included mass spectrometry standards for saturated and unsaturated lipids (di(15:0)PC and (16:0)(18:1)PC, respectively).

UHPLC-MS/MS Analysis of Cholesterol

An internal standard d₇-cholesterol was added with lipid standards to samples prior to extraction. The same extracts were used for analysis of phospholipids and cholesterol. Extracts were prepared as described in the previous section and analyzed through ultra-high performance liquid chromatography-tandem mass spectrometry (UHPLC-MS/MS) using atmospheric pressure chemical ionization (Sciex QTRAP 6500; SCIEX, Framingham, MA or Waters Xevo TQ-XS; Waters Corp.) [242]. Reversed-phase chromatography separations were carried out using a Phenomenex Kinetex C18 column (100 mm x 2.1 mm, 1.7 μm) with a 90% methanol/10% water/0.1% formic acid mobile phase. Quantitation methods and peak integration were performed using Analyst software (SCIEX Analyst 5.1; SCIEX) or MassLynx and TargetLynx software (Waters Corp.). Concentrations of cholesterol were obtained using peak ratios relative to d₇-cholesterol [242].

Analysis and Plotting

The lipid abundances are the raw values obtained from the mass spectrometry measurements. To calculate lipid composition as mole percentages, the abundance of each lipid (normalized to a lipid standard) was divided by the total lipid abundance for each sample (Tab. A.5). The mean percentage of each lipid type and the standard deviation were calculated for three independent samples. Ternary plots were generated using the open-source Python library, `python-ternary` (<https://github.com/marcharper/python-ternary>).

3.4 Results and discussion

Our experiments answer four types of questions: 1) Do all methods produce giant vesicles with sufficient yield? 2) How do the ratios of lipids in vesicles produced by each method differ from ratios in vesicles produced by the other methods, 3) How do those ratios differ from the stock solution, and 4) How reproducible is the lipid composition each method?

All methods produce giant unilamellar vesicles

As expected, electroformation on either ITO slides or platinum wires typically produces high yields of unilamellar vesicles (Fig. A.2 and Fig. A.3). Electroformation on platinum wires form smaller vesicles than electroformation on ITO slides; however, the size and physical separation of the wires can impact the size of the GUVs formed. Vesicles made by gentle hydration consistently have more lamellae or nested vesicles (Fig. A.4), and vesicles made by emulsion transfer consistently have defects of lipid aggregates or nested vesicles (Fig. A.5). Vesicles extruded through 100 nm membrane filters are too small to be resolved (Fig. A.6).

Vesicles made by electroformation and gentle hydration exhibit liquid-liquid phase separation of their membranes, consistent with the tendency for membranes to demix when they contain mixtures of high- T_{melt} lipids, low- T_{melt} lipids, and cholesterol [16]. In contrast, the vesicles prepared by emulsion transfer did not exhibit liquid-liquid phase separation at room temperature, indicating that the lipid composition of emulsion transfer vesicles differed from the lipid composition of the other vesicles (Fig. A.5).

Electroformation and gentle hydration create vesicles with minor offsets in lipid ratios

Our central result is that three methods of producing giant vesicles (electroformation on ITO slides, electroformation on platinum wires, and gentle hydration) result in similar percentages of lipids in the membranes. Moreover, these percentages are similar to that of the master stock solution. These similarities are shown in the first four stacked bars in Fig. 3.3A.

Another way to visualize the minor differences in lipid ratios between the three methods is to zoom into a region of the pseudo-ternary diagram in Fig. 3.3B. Lipid compositions of vesicles made by the two electroformation methods (triangles and circles) and the gentle hydration method (squares) cluster around the master stock solution (star). Fig. 3.3B shows that electroforming vesicles on ITO slides and on platinum wires shifts lipid mole ratios from the master stock solution by roughly 3.5 mol% and 1.5 mol%, respectively. Similarly, gentle

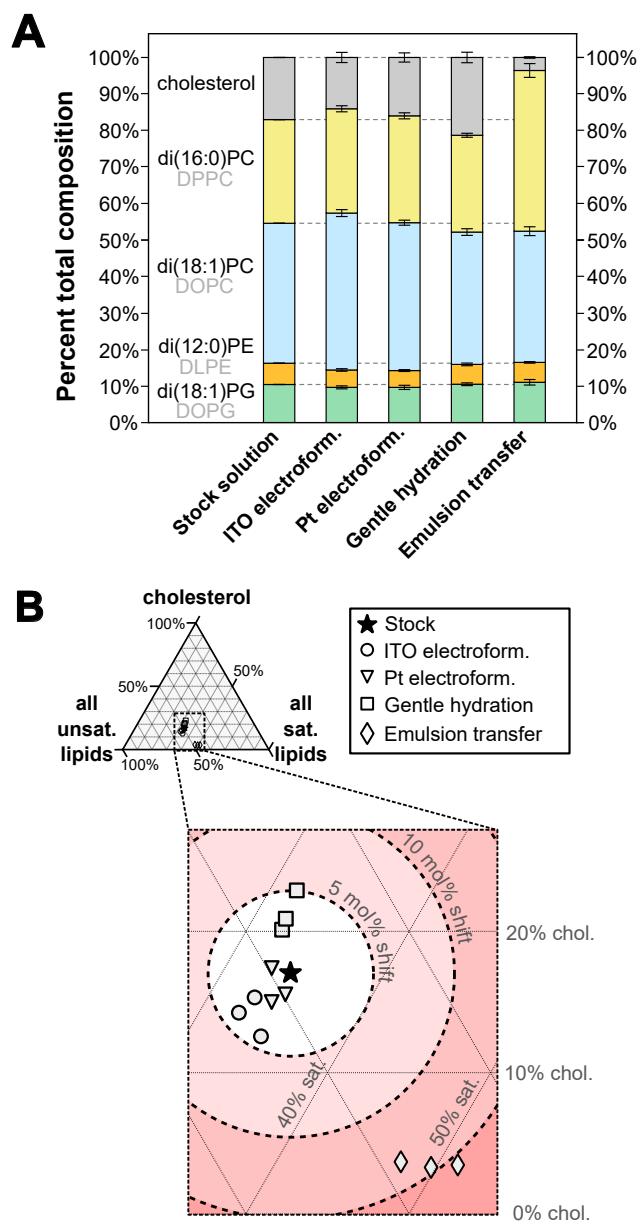


Figure 3.3: **Lipid percentages in 5-component vesicles produced by different methods.** **A)** Percent of each lipid component in the master stock solution and in the three independent vesicle solutions of each technique made from the master stock solution. Values are averages, and error bars above each section of the bar chart are standard deviations of three independent experiments. Full data appear in Tab. A.1, A.5, and A.6. **B)** Lipid percentages for the three independent solutions of each technique plotted on a pseudo-ternary diagram, where the three vertices represent cholesterol, the sum of the saturated lipids (di(16:0)PC and di(12:0)PE), and the sum of the unsaturated lipids (di(18:1)PC and di(18:1)PG).

hydration of vesicles shifts lipid mole ratios by roughly 4 mol%, in the direction of increasing cholesterol. The data in Fig. 3.3 also show that reproducibility of the electroformation and hydration methods is high, based on the close clustering of data from three independent experiments. The range of sample-to-sample lipid ratios for each method is within ± 2 mol%.

Our result that electroformation and gentle hydration do not produce vesicles with wildly different mole fractions of cholesterol is consistent with reports that the maximum amount of cholesterol that can be incorporated into membranes is roughly equivalent for vesicles made by electroformation (between 65 and 70 mol% [217]), gentle hydration (61 mol% [243] or ≤ 63 mol% [214]), and a third method, rapid solvent exchange (66 ± 1 mol% [214]). Recent ToF-SIMS data disagree with these results, but have low reproducibility: in two independent experiments, the amount of cholesterol in GUVs made by electroformation was either roughly one-quarter or two thirds of that in GUVs made by gentle hydration [232].

Shifts in lipid compositions in Fig. 3.3 are largely due to different mole fractions of cholesterol in vesicles with respect to the master stock solution. In contrast, only small shifts of ≈ 1 mol% are seen in PE-lipid and PG-lipids (Fig. A.7). These shifts are the same magnitude as sample-to-sample differences of independent experiments. The small shift in di(12:0)PE seems surprising in light of previous studies using lipid mixtures extracted from rabbit sarcoplasmic reticulum: PE-lipids were grossly over-represented in the lipids left behind on a glass substrate [205]. The particular lipid we use, di(12:0)PE, may integrate better into vesicles than other PE lipids because it is in a liquid, lamellar phase (rather than a gel phase or an inverted hexagonal phase). In contrast, the small shift in the charged PG-lipid is not as surprising, at least for gentle hydration. Blosser et al. found no statistically significant shift in the mole fraction of diphytanoylPG lipids with respect to a stock solution for vesicles that were made by gentle hydration [78]. Similarly, Angelova found no significant difference in the mole fractions of charged (PS-lipids) and uncharged lipids (PC-lipids) between a vesicle solution made by gentle hydration and a lipid film left behind on a glass surface [205].

How will the minor shifts in lipid ratios we observe in Fig. 3.3 impact how the biophysics community interprets data from GUVs? It depends on how experiments are designed. Broad

conclusions derived from experiments that increment stock lipid compositions by ≈ 5 mol% will likely apply equally well to vesicles electroformed on ITO slides or on platinum electrodes, and may slightly differ when applied to vesicles made by gentle hydration. In contrast, detailed conclusions that depend on incrementing lipid compositions by only ≈ 1 mol% will likely apply only to vesicles made by a single method and will likely be affected by sample-to-sample differences. More detailed conclusions are difficult to extract from the data in Fig. 3.3 because only the percentages of the lipids (rather than their absolute values) are relevant. For example, an increase in the ratio of cholesterol to phospholipids could be due to an absolute increase in cholesterol, an absolute decrease in phospholipids, or both.

Emulsion transfer results in too little cholesterol in vesicles

Emulsion transfer forms vesicles with less cholesterol. Unlike the electroformation and gentle hydration methods, the emulsion transfer method creates large shifts in lipid compositions of vesicles (Fig. 3.3). When compared to the master stock solution, the emulsion phase transfer method incorporated only $\approx 20\%$ of the expected amount of cholesterol. This result is consistent with previous reports of low cholesterol in vesicle membranes made by emulsion techniques such as cDICE ($<1\%$ of the expected cholesterol [?]), double-layer cDICE (25-35% of the expected cholesterol [221]), emulsion phase transfer (28-50% of the expected cholesterol [220]), and droplet shooting size-filtration (33-50% of the expected cholesterol [244]), as discussed in [219]. The problem likely arises because cholesterol lacks a large polar headgroup to drive it out of bulk oil, toward an interface with water. The problem can be mitigated, but not eliminated, by switching from heavy [219] to light mineral oil or adding higher levels of cholesterol to the oil than the target membrane level [220].

Too much saturated and long-chain PC-lipids in vesicles made by emulsion transfer

We were surprised to find that the emulsion transfer method also vastly skews the ratio of the PC-lipids; di(16:0)PC is over-represented by a factor of ≈ 21.5 in the vesicles compared

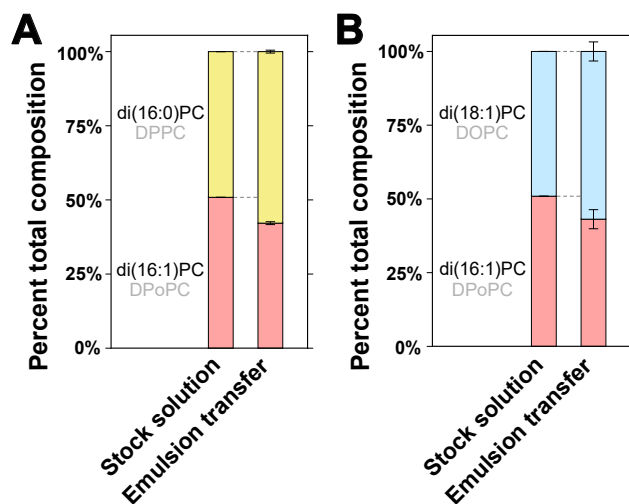


Figure 3.4: **Emulsion phase transfer incorporates more saturated and long-chain lipids into vesicles.** **A)** Ratio of lipids in vesicles made from a stock, 50:50 mixture of two PC-lipids with chain lengths of 16 carbons, one saturated and one unsaturated. **B)** Lipid composition of vesicles made from a stock solution containing two unsaturated PC lipids, one with a chain length of 18 carbons and one with a chain length of 16 carbons. In both panels, values are averages, and error bars above each section of the bar chart are standard deviations of three independent experiments. Full data appear in Tab. A.2 and A.3.

to the master stock solution (Fig. 3.3). The effect is so large that nearly all loss of cholesterol in emulsion transfer vesicles appears to be counteracted by a gain in di(16:0)PC. To our knowledge, shifts in phospholipid compositions have not previously been measured in emulsion transfer vesicles.

Two structural characteristics of di(16:0)PC could have caused it to be over-represented relative to di(18:1)PC in vesicles made by emulsion transfer: chain length and saturation. To determine whether each of these characteristics is salient on its own, we designed two additional experiments. In the first experiment, we made a 50:50 stock solution of lipids that differ only in their degree of unsaturation: di(16:0)PC and di(16:1)PC. We found that vesicles made by emulsion phase transfer from this stock solution contained significantly more saturated lipid, in a ratio of 60:40 (Fig. 3.4A). The stock solution did not contain cholesterol, so the over-representation of the saturated lipid is not due to known, favorable interactions

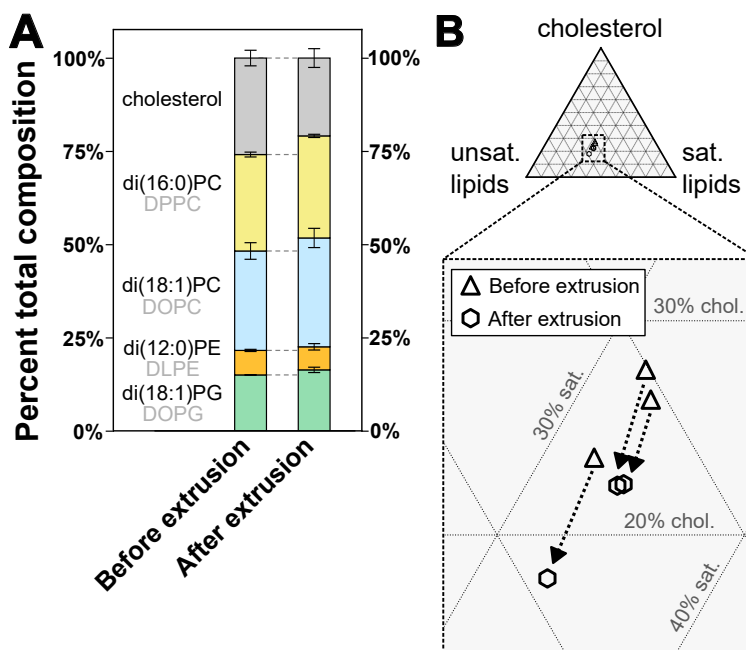


Figure 3.5: **Extrusion of giant vesicles decreases their cholesterol content.** **A)** Percentage of all five lipids in vesicles made via gentle hydration, before and after extrusion through a 0.1 μM filter. Values are averages, and error bars above each section of the bar chart are standard deviations of three independent experiments. **B)** Mole fractions of each experiment plotted on a pseudo-ternary diagram, before and after extrusion. The three vertices correspond to cholesterol, the sum of the saturated lipids (di(16:0)PC and di(12:0)PE), and the sum of the unsaturated lipids (di(18:1)PC and di(18:1)PG). Full data appear in Tab. A.5 and A.6 These gentle hydration samples were prepared and measured separately from samples comparing the four other methods.

between cholesterol and saturated lipids [245]. In the second experiment, we made a 50:50 stock solution of lipids that differ only in their chain length: di(16:1)PC and di(18:1)PC. We found that vesicles made by emulsion phase transfer from this stock solution contained 3-10 mol% more of the longer-chain lipid, but with lower reproducibility (Fig. 3.4B).

Extrusion of vesicles results in lower cholesterol fractions

Some powerful techniques of assessing membrane phase behavior use giant vesicles whereas others (e.g., electron microscopy and neutron scattering [17, 246, 247]) require ≈ 100 nm

vesicles, produced by extruding vesicles through polycarbonate filters. Here, we conducted a new series of experiments to compare ratios of lipids in solutions of giant vesicles generated by gentle hydration with ratios from the same solutions after extrusion (Fig. A.6).

We find decreases in cholesterol due to extrusion (Fig. 3.5). In terms of absolute numbers, these shifts are not huge, a decrease of 5.0 ± 3.3 mol% cholesterol, where the uncertainty is the standard deviation for three independent experiments. In terms of the total percent of cholesterol, the shifts are significant, roughly 1/5 of cholesterol is lost upon extrusion of vesicles made by gentle hydration. This value is in between reports of no loss of cholesterol from some membranes (specifically, for binary membranes of 33% cholesterol with di(18:1)PC or di(14:0)PC or for ternary mixtures of 2:1:3 PC-lipids/eggPC/cholesterol) and a loss of $\approx 1/3$ to $\approx 1/2$ of cholesterol from other membranes (namely for binary membranes of 33% cholesterol with 16:0/18:1PC, di(16:0)PC, or di(20:4)PC) [218]. In other words, no clear trend has been uncovered to explain how lipid unsaturation affects the loss of cholesterol from vesicles upon extrusion.

We find that the decrease in cholesterol upon extrusion is offset by smaller increases in PC-lipids (1.4 ± 0.7 mol% for di(16:0)PC, and 1.5 ± 0.8 mol% for di(18:1)PC, respectively). Shifts in PE- and PG-lipids are insignificant (0.4 ± 0.9 mol% for di(12:0)PE and 2.5 ± 3.4 mol% for di(18:1)PG). As before, the main conclusion is that experiments that report results at high precision (e.g., 1 mol%) will be sensitive to how vesicles are made and to sample-to-sample differences.

3.5 Caveats

In the sections above, we tested whether several methods of making vesicles skew the ratio of lipids in membranes. Many unexplored variations on each method exist. For example, we made vesicles by gentle hydration in water rather than in salt solutions, and the vesicles formed on a glass surface rather than on polymer-coated substrates [248, 249] or on tracing paper [250]. Similarly, we converted giant vesicles into smaller vesicles by extruding them rather than by freeze/thaw cycles or sonication.

Similar caveats apply to the choice of master stock solution. Many lipid mixtures are equally relevant and may produce different shifts in lipid ratios. Whenever lipid stocks contain small fractions of some lipids (like the PE-and PG-lipids in our sample), small shifts in their mole fractions will be observed, even if the percent change is high. Although we found small shifts in all lipid fractions for most methods, it is worth bearing in mind that small shifts can result in big changes, especially in lipid phase behavior. If a membrane lies near a phase boundary, a tiny shift in its lipid composition can lead a previously uniform membrane to demix into coexisting phases, or a liquid membrane to turn into a gel phase. For researchers who are comparing vesicles made by different methods, a best practice is to choose a ratio of lipids that lies in the middle of whatever phase region is desired.

3.6 Conclusions

In summary, electroformation and gentle hydration, the most common methods of producing GUVs, result in minor shifts (≤ 5 mol%) in the lipid ratio relative to a stock solution and minor (± 2 mol%) sample-to-sample variations for independent experiments. Researchers will find the magnitudes of these shifts to be either comfortably small or alarmingly large, depending on how they design their experiments. For example, experiments that report concentrations incremented by only ≈ 1 mol% will be highly sensitive to the vesicle-making method and to sample-to-sample differences. An additional method (emulsion transfer) results in large shifts. Although it was previously known that vesicles made by emulsion transfer contain much less cholesterol than the stock solutions from which they are made, we found the surprising result that emulsion transfer vesicles also contain less unsaturated lipid and less shorter-chain lipid. Extrusion of vesicles can further decrease a membrane's cholesterol content.

Chapter 4

MEMBRANE-SENSING PROPERTIES OF THE SQUALENE MONOOXYGENASE DEGRON

This chapter was written in collaboration with Sharona E. Gordon and Sarah L. Keller. All experiments were conducted by Heidi M.J. Weakly.

4.1 Introduction

4.1.1 Cholesterol synthesis and the enzymatic role of squalene monooxygenase

Plasma membranes of animal cells contain high fractions of cholesterol (roughly 0.8 moles of cholesterol for every mole of phospholipids) [251], which contributes to the membrane's structural integrity [6]. Cholesterol levels in organelle membranes are much lower. For example, the endoplasmic reticulum (ER) contains roughly 0.05 moles for every mole of phospholipids [252,253]. Cells have evolved intricate mechanisms to regulate cholesterol levels and maintain homeostasis [251]. Enzymes play a key role in this process [252,253]. Regulated by gene expression, protein localization, and post-translational modifications, enzymes can activate or deactivate metabolic synthesis depending on the needs of the cell.

Cells synthesize new cholesterol in the endoplasmic reticulum (ER) via the mevalonate pathway. Two steps in the mevalonate pathway are controlled by rate-limiting enzymes (Fig. 4.1). The first of these steps involves the formation of mevalonate acid and is catalyzed by the HMG-CoA reductase (HMGCR) enzyme [254]. HMGCR is a well-characterized enzyme and the therapeutic target for agents that lower cholesterol levels, i.e., statins. The second rate-limiting step involves the enzyme squalene monooxygenase (SM), also known as squalene epoxidase [255]. Squalene monooxygenase converts squalene to 2,3(S)-monooxidosqualene, which is subsequently converted to cholesterol through a multi-step pathway [256].

Squalene monooxygenase is a potential therapeutic target for treating and preventing cholesterol-related diseases. Videlicet, a statin that inhibits HMGCR has an undesired side effect of preventing synthesis of necessary molecules from the mevalonate pathway such as ubiquinone and dolichol [257,258]. Targeting SM, which enters the mevalonate pathway after ubiquinone and dolichol are produced, is a promising alternative to current statin therapies.

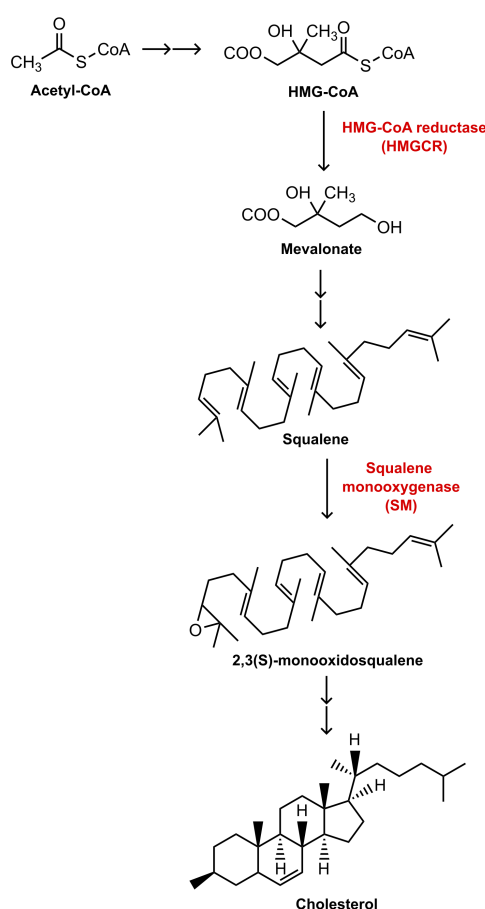


Figure 4.1: **HMG-CoA reductase and squalene monooxygenase control rate-limiting steps in cholesterol synthesis.** A simplified depiction of the mevalonate pathway in which de novo cholesterol is synthesized. Multi-step reactions are denoted by double arrows. HMG-CoA reductase (HMGCR) converts HMG-CoA into mevalonate. In several reactions downstream, squalene monooxygenase (SM) catalyzes the conversion of squalene substrate to form 2,3(S)-monooxidosqualene. The final, major product of the reaction pathway is cholesterol.

4.1.2 *Squalene monooxygenase: structure*

Broadly, the architecture of squalene monooxygenase (SM) is divided into two parts - an N-terminal regulatory domain and a C-terminal catalytic domain. The catalytic domain composes the bulk of the protein and contains the binding sites for flavin adenosine dinucleotide (FAD) co-factor, squalene, and SM inhibitors. Crystal structures of human squalene monooxygenase with small molecule inhibitors provide details of the conformational changes necessary for squalene and inhibitor binding [259]. The catalytic domain also contains two potential transmembrane domains.

This thesis chapter focuses on the regulatory domain, which contains the first 100 amino acids of SM (SM100). The regulatory domain is necessary for cholesterol-dependent degradation, and it retains this function even when it is isolated from the catalytic domain [260]. The N and C termini of SM100 are both known to be cytosolic, but the structure and binding of the N-terminal regulatory domain are less well characterized, for two main reasons. First, the hydrophobicity of SM100 has impeded studies of full-length SM [259,260]. Second, unlike the catalytic domain, SM100 contains small disordered regions that have not been resolved with X-ray crystallography [261]. In the last decade, pivotal studies have successfully validated two membrane-embedded structures within SM100 - a re-entrant loop [262] and an amphipathic helix [261]. These studies [261,262] utilized extensive mutations, circular dichroism, and protein expression assays to determine that the re-entrant loop and amphipathic helix undergo structural changes in response to excess cholesterol.

4.1.3 *Degron mechanisms of squalene monooxygenase*

To restore protein homeostasis in eukaryotes, damaged proteins can be cleared by proteasomes or lysosomes [263]. Generally, proteasomes eliminate short-lived proteins and soluble misfolded proteins via the ubiquitin-protease system, whereas lysosomes degrade long-lived proteins and insoluble protein aggregates via endocytic, phagocytic or autophagic pathways [264].

When cholesterol is in excess in the endoplasmic reticulum (presumably $>5\%$ [252]), SM undergoes cholesterol-accelerated degradation by the ubiquitin-proteasome system, mediated by the E3 ubiquitin ligase MARCH6 [265]. This process is an excellent example of feedback inhibition: squalene monooxygenase is required for cholesterol synthesis, while excess cholesterol accelerates the degradation of SM. When protein degradation is regulated intrinsically by a specific amino acid sequence, the sequence is termed a degron. Degrons contain common structural features that promote degradation, including ubiquitination sites (e.g., lysine amino acids) and unstable secondary structures such as amphipathic helices or intrinsically disordered regions [266, 267]. Deg1, a degron evolutionary similar to SM100, has been employed in multiple studies to uncover the mechanisms of protein degradation [268, 269].

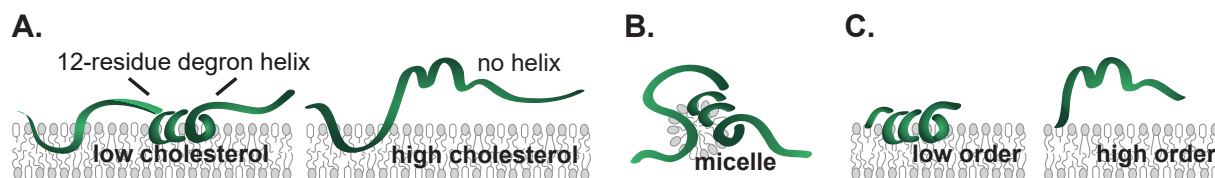


Figure 4.2: Structure and membrane binding mechanisms of the regulatory domain of squalene monooxygenase (SM100). **A)** Working model for the interaction of SM100 and membranes. At low membrane cholesterol levels, the degron region forms a short amphipathic helix that associates with the membrane. At high membrane cholesterol levels, the amphipathic helix is displaced from the membrane. This process unravels the protein and exposes the hydrophobic residues that created the amphipathic helix. **B)** Chua et al. 2017 confirmed the structure of SM100 in detergent micelles that lack other physical properties of lipid membranes. **C)** This chapter will investigate the binding and structure of the degron region in lipid membranes to understand the role of biochemical properties (e.g., due to cholesterol mole fraction) and biophysical properties (e.g., due to membrane order).

Chua et al. were the first to identify a degron sequence in SM [261]. Their proposed mechanism for cholesterol sensing is that squalene monooxygenase binds to membranes with low cholesterol by forming an amphipathic helix. As cholesterol levels increase, the amphipathic helix is expelled from the membrane and undergoes a structural change, initiating squalene monooxygenase degradation [261] (Fig. 4.2A). Interestingly, there are several examples of

proteins that are regulated by sterols including the HMGR enzyme in the mevalonate pathway [91] and Niemann-Pick C1 protein, which is required for the transport of LDL-derived (ingested) cholesterol into cells [270]. However, these proteins contain specific sterol-sensing domains [271] that are not present in SM100. To date, it is not yet known if SM100 binds to cholesterol.

Key evidence is still missing to prove that cholesterol concentration is the mechanism by which the degnon binds to membranes. Past work has measured the cholesterol-dependent degradation of SM100 in cell membranes (by delivering cholesterol to membranes with cyclodextrin), whereas SM helicity has been measured only in detergent micelles [261] (Fig. 4.2B). Physical properties of the membrane may also influence degnon binding: lipid packing defects and membrane curvature are known to drive the binding of amphipathic helices of various proteins. For example, Sikdar et al. used molecular dynamic simulations to show that partitioning of the hepatitis A virus-2B peptide into membrane bilayers is predominantly driven by sensing of lipid packing defects, rather than sensing of cholesterol [272]. Levels of other lipids including plasmalogens and unsaturated fatty acids can increase or decrease SM protein levels [273, 274], suggesting the membrane-sensing mechanisms of SM are more complex than a simple model in which SM senses only the mole fraction of cholesterol in a membrane.

4.2 Aims and hypothesis

Prior work with squalene monooxygenase has demonstrated its cholesterol-dependent function. Through extensive mutagenesis and evolutionary comparisons, scientists have identified that the function of the degnon is sequence-specific and positively correlates with the hydrophobicity of the degnon region. Our ultimate aim is to identify the mechanistic details that influence the degnon's binding to membranes. In the near term, the goal of this chapter is to develop an approach to test:

Aim 1. What conditions allow the SM degnon to bind to the membrane?

Aim 2. What is the mechanism of membrane binding?

Aim 3. Does lipid order influence the binding of the degnon to the membrane? (Fig 1C).

4.2.1 Peptide and protein design

To investigate the binding of squalene monooxygenase to membranes in response to cholesterol levels, I first designed a synthesized peptide (Ser43 - Gly77) containing the SM degnon sequence, with the goal of mimicking the function of the native squalene monooxygenase degnon. I modified the peptide with an N-terminal biotin-aminohexanoic linker (Biotin-Ahx) and C-terminal amidation. The aminohexanoic linker provides additional space to ensure recognition of the full peptide sequence when biotin is bound to avidin/streptavidin/Strep-Tactin[®] [275]. I also mutated the sequence with a single amino acid substitution (Phe63 to Trp63) to enable fluorescence detection of the degnon in membranes.

In parallel, I utilized bacterial purification to express a longer portion of the regulatory domain (SM50-100). To do so, I had to overcome challenges in cloning small peptides (< 100 amino acids). Small peptides have a propensity to be degraded by endogenous proteases in *E. coli* expression systems; this is especially true for sequences with disordered structures like SM100 [276]. Another challenge is that small peptides can easily become over-expressed. When the volume of peptide becomes too high for the *E. coli* control machinery, the peptide forms insoluble aggregates, also known as inclusion bodies [277]. Inclusion bodies require complex processes to recover and purify the peptide [278]. These challenges cannot be solved by simply expressing a longer sequence, as Padyana et al. have reported difficulty in expressing full-length native squalene monooxygenase. Their crystallography experiments had to employ an N-terminally truncated version of SM (residues 118-574) [259]. One strategy to improve expression and purification of short peptide sequences in *E. coli* is to fuse the peptide sequence to a larger protein. To test this approach, I linked SM50-100 to Maltose Binding Protein (MBP). Additionally, I incorporated a site for the Tobacco Etch Virus (TEV) protease between the MBP and SM50-100 sequence to aid in the future cleavage of SM50-100 from MBP.

4.3 Materials and Methods

4.3.1 Materials

All phospholipids were obtained from Avanti Polar Lipids (Alabaster, AL) and were used without further purification. Two peptides based on the squalene monooxygenase degron Biotin-Ahx-GSGSYRCRHRNGLLGRQQSGSQWALFSDILSGLPFIG-NH₂ and Ac-Lys(Biotin)-GSGSYRCRHRNGLLGRQQSGSQWALFSDILSGLPFIG-NH₂ were synthesized and purified by Eton Bioscience (San Diego, CA). The identity of the peptides was confirmed by HPLC and mass spectroscopy by the commercial supplier. Cloning reagents, including restriction enzymes, were purchased from New England Biolabs (NEB).

4.3.2 Constructs, cloning, and bacterial culture

To construct the MBP-SM50-100 fusion protein, a double-stranded DNA fragment with amino acids 50-100 of the regulatory domain was purchased from Integrated DNA Technologies (IDT) (Full sequence in Appendix B). This fragment will be referred to as the “SM gene block” or “gene block” throughout the methods. A flexible, glycine-serine linker (GSSGSSG) and free cysteine to enable the conjugation of fluorescent labels were added to the N-terminal side of the SM gene block. An Avi-tag (GLNDIFEAQKIEWHE), which contains a biotinylation site for the *E. coli* biotin ligase BirA, was added to the C-terminus. The ends of the gene block included restriction enzyme sites (HindIII and XhoI) to insert the fragment into the parent vector via traditional cloning. The final sequence was codon optimized to promote gene expression in *E. coli*. The quality of the gene block was confirmed by capillary electrophoresis and mass spectrometry by the supplier (IDT). The lyophilized SM gene block was resuspended in Tris-EDTA (TE) buffer at 10 ng/ μ L.

The MBP vector and SM gene block insert were cloned using traditional cloning techniques (restriction digest, ligation, and transformation) following NEB protocols. The MBP backbone was treated with Quick CIP from NEB. CIP is a derivative of calf intestinal alkaline phosphatase added to prevent recirculation during ligation by dephosphorylation of

the free 5' and 3' ends. The insert and vector were mixed 3:1 by mass. MBP-SM50-100 was transformed into *E. coli* cells (DH5 α) with a 2-hour outgrowth in SOC media. The culture was spread on selection plates and allowed to grow overnight. The final selection had distinct, single colonies and more colonies than the vector only (negative control). Multiple colonies were selected and grown overnight in sterile Luria Broth. Plasmid DNA was purified (QIAprep Spin Miniprep Kit, QIAGEN) and sequenced with a single oligo primer (CAGCAGCCAACTCAGCTTCC) (Eurofins).

Upon sequence confirmation, the MBP-SM50-100 plasmid was transformed in BL-21(DE3) cells via heat shock and grown overnight on selection plates. One colony was collected and grown overnight in 5 mL of Luria Broth. A 60 mL solution of culture medium was prepared (Terrific Broth, 1% glucose, and antibiotic) and inoculated with the overnight culture at 1:500. When the optical density reached 0.9, 1 mM IPTG was added to induce protein expression. The culture was incubated overnight at 18 °C. Cells were pelleted by centrifuging the culture medium at 5000 rpm for 25 minutes at 4 °C. The supernatant was discarded and all pellets were stored at -20 °C until further purification.

4.3.3 Protein purification

Cell pellets were resuspended in lysis buffer (Pierce protease inhibitor and 2 mM 2-mercaptoethanol) and then lysed with an Avestin Emusiflex C3 (Bee International, South Easton, MA). The lysed cell solution was centrifuged at 18,000 rpm (40,000 rcf) for 30 min at 4 °C. The cleared lysate solution was decanted and added to amylose resin (NEB) for batch binding. The resin was washed and equilibrated with column buffer (25 mM HEPES, 150 mM NaCl, pH 7.4), before binding. Following 1 hr of mixing at 4 °C, the resin solution was gently pipetted into a disposable column (Cytiva Life Sciences). The column was gently flushed with a column volume of wash buffer to decrease nonspecific binding. The wash step was completed 5x, each with one column volume of buffer. The protein was eluted using 10 mM maltose in column buffer. The protein fractions were supplemented with a 10% (by vol.) glycerol solution, flash-frozen in liquid nitrogen, and stored at -80 °C.

4.3.4 *Size exclusion chromatography (SEC)*

Purified MBP-SM50-100 and cleaved SM50-100 were analyzed using size exclusion chromatography (SEC) (GE AKTA Explorer). The evening before FLPC analysis, the fusion protein was cleaved with Tobacco Etch Virus (TEV) protease (expressed and purified in-house) at 4 °C. TEV conditions were based on optimization experiments (Fig. B.1). A Superdex 75 10/300 GL column (Cytiva Life Sciences) was equilibrated with 1x protein buffer (20 mM HEPES, 100 mM NaCl, pH 7.4) at 0.8 mL/min at room temperature. Before injection on the column, the protein solution was filtered through a regenerated cellulose membrane (pore size 0.2 μ M). As a secondary purification, 1 mL fractions were collected for gel analysis and subsequent use.

4.3.5 *Bimane-C3-maleimide labeling*

A 10 mM stock of bimane-C3-maleimide (Molecular Probes, Inc.) was solubilized in dimethyl sulfoxide (DMSO) and diluted before subsequent experiments with protein. For fluorescence studies, bimane-C3-maleimide was diluted to final concentration 0.25 μ M in 200 μ L of 20 mM HEPES, 100 mM NaCl. Protein was added in excess at a final concentration of 0.75 μ M to bind as much probe as possible. Bimane-C3-maleimide is a convenient label because its fluorescence intensity increases as it binds to cysteine. A Horbia Fluorlog 3 was used to measure the emission spectra of bimane-C3-maleimide with protein. Emission reached equilibrium after 30 min., indicating the binding reaction between bimane-C3-maleimide and the Cys49 was complete (Fig. B.2).

4.3.6 *Cy3b-maleimide labeling*

For the co-sedimentation assays, MBP-SM50-100 was labeled with Cy3b-maleimide (AAT Bioquest, Pleasanton, CA) at Cys49. All labeling experiments utilized a 2.5 mM stock of Cy3b-maleimide in DMSO (stored at -20 °C). To remain within the loading volume capacity of the purification columns, the total volume of all reactions was 75 μ L. Before labeling, MBP-

SM50-100 was treated with 2.5x molar excess of tris(2-carboxyethyl)phosphine (TCEP) for 20 min. TCEP is a reducing agent that disrupts disulfide bonds, including any at position Cys49, that would prevent cysteine-maleimide conjugation. Then, TCEP was removed by gravity filtration with a Bio-Spin 6 column from Bio-Rad. Next, the labeling reaction was prepared by mixing 20 μ M TCEP-treated MBP-SM50-100 with 80 μ M Cy3b-maleimide in 20 mM HEPES, 100 mM NaCl, pH 7.4. The solution was briefly centrifuged and left to react for 2 hr. at room temperature. Free dye was removed using a new Bio-Spin 6 column. Fractions from the columns were collected and analyzed using in-gel fluorescence to confirm the removal of the free dye.

4.3.7 Vesicle preparation

Vesicles, also known as liposomes, were prepared using sonication or extrusion methods. Lipid solutions in chloroform contained mixtures of these lipids: DOPC (di18:1 PC), cholesterol, and 10 mol% DOPG (di18:1 PG). In the co-sedimentation assays, cholesterol constituted 10 or 50 mol% of the total vesicle composition.

Vesicles were prepared by placing the sample in a water bath above the melting temperature of all lipid species and sparging with nitrogen gas for 1-2 min. to create a lipid film. Afterward, the sample was placed under vacuum for 2 hrs. to remove any residual chloroform. The dry lipid film was hydrated with buffer (20 mM HEPES, 100 mM NaCl, pH 7.4) to a final concentration of 1-10 mg/ml and briefly vortexed. To prepare vesicles with an average radius of 50 nm, vesicles were tip-sonicated (Brandon Sonifier 450, VWR Scientific) at 50% duty cycle and 1-2 output power for 4 min. or until the solution turned from opaque to clear.

To form vesicle solutions with higher curvature (smaller radii), vesicle solutions were passed multiple times through various sizes of polycarbonate filters using a miniextruder (Avanti Polar Lipids). A custom-built heat block was utilized to interface the miniextruder with two 1 mL gas-tight syringes (Hamilton Co.) and two dual syringe pumps (Genie TouchTM, Kent Scientific Co.). The syringe pumps eliminated pressure leaks that had oc-

curred when the vesicles were extruded by hand in initial tests.

The miniextruder apparatus was assembled by prewetting two, 10 mm polyethylene filter supports (WhatmanTM) and a single polycarbonate filter (Nucleopore Track-Etch Membrane, WhatmanTM) with buffer. To minimize loss of the vesicle solution, 1.0 mL of buffer was passed through the entire assembly before the sample was extruded. Vesicles were passed 9 times through membrane filters with 0.1 μm pores. For each sample, a small fraction was reserved and analyzed on a particle sizer (Wyatt DynaPro Plate Reader III).

4.3.8 Co-sedimentation assay

Co-sedimentation assays to quantify protein-lipid vesicle interactions followed previously established methods [279]. In this experiment, vesicles and protein were mixed in 200 μL of solution at a ratio of 1:100 or 1:500 protein to lipid, where lipid refers to the total cholesterol concentration in the sample. Samples were allowed to come to equilibrium for 30 min. and then centrifuged in a Beckman Coulter OptimaTM Ultracentrifuge (TA100.1 rotor) at 80,000 rpm (279,000 rcf) for 1 hr at 4 °C. Immediately following ultracentrifugation, the sample tubes were carefully removed from the rotor, and the supernatant was separated from the vesicle pellets. The pellets were resuspended in 15 μL of buffer (20 mM HEPES, 100 mM NaCl, pH 7.4) and transferred to new 0.2 mL tubes. All samples were analyzed using SDS-PAGE gels loaded with equivalent fractions of supernatant and resuspended cell pellet. For gels with fluorescently labeled protein, the gel was imaged on an Amersham ImageQuant 800 (Cytiva), and then stained for 1 hr with Quick Coomassie Blue. Before imaging, gels stained with Quick Coomassie Blue were destained with DI water overnight. To quantify the extent of membrane-bound protein, the integrated intensity of the vesicle pellet band was compared to the integrated intensity of the pellet + supernatant. Images were processed with Fiji (ImageJ). In brief, regions of interest were created around each band (representing the sample), and at the top of the gel (representing the background). The total integrated intensity of the background was then subtracted from the total integrated intensity of the corresponding band.

4.3.9 Fluorescence quenching assays

Fluorescence emission spectra were measured using a Horiba Fluorolog 3 spectrophotometer. To probe protein-lipid interactions with bimane-C3-maleimide, all samples were pipetted into a 1-cm quartz cuvette. The samples were excited with a wavelength of 380 nm and emission was recorded from 400 nm to 640 nm. The excitation and emission slits were both set to 3 nm bandwidth. At higher concentrations of protein, the slits were adjusted to 2 nm to remain within the linear range of the fluorometer. Initial measurements with only buffer (no protein or lipid vesicles) were taken and later used for background subtraction. Lipid vesicles were added at a concentration of 100 μM and measurements were immediately taken to establish a t_0 baseline. The emission spectra were measured again after 5 and 10 min. at room temperature. The samples were not mixed between measurements. By adding more vesicles to the same sample cell, this workflow was repeated for solutions containing 500 μM and 1000 μM lipid vesicles. Vesicle additions were performed with concentrated stocks to prevent over-dilution of bimane-C3-maleimide-SM100. For all titrations, the final concentration of bimane-labeled protein was within $\leq 5\%$ of the initial concentration. All data were analyzed and plotted in MATLAB (Mathworks, Inc.).

4.4 Results and Discussion

4.4.1 Peptide Solubility

I began experiments in this chapter with commercially synthesized peptides. However, the solubility of these peptides presented multiple challenges that we attributed to the peptides' electrostatic charge (+3.0 at pH 7.0) and hydrophobicity (39 % of total residues are hydrophobic). Qualitative experiments demonstrated the peptides were insoluble under neutral conditions in both water and buffer (30 mM HEPES, 130 mM KCl, pH 7.4).

A common strategy to enhance solubility is to hydrate basic peptides in 10-30% acetic acid or to dissolve hydrophobic peptides in an organic solvent such as methanol or DMSO, then to follow with a water or buffer dilution. Initially, this strategy seemed promising. I found

that the peptides were soluble at 1 mM with 18 % glacial acetic acid; however, the acetic acid concentration reduced the solution pH to 2.0. Despite its efficacy in solubilizing the peptide, the acidic environment precluded fluorescent labeling of the peptide via cysteine-maleimide chemistry. Unfortunately, readjustment of the solution pH to ~ 7.0 , resulted in precipitation of the peptide. I could not test the potential impact of higher buffer concentrations (i.e., HEPES) or different buffers such as Tris or MOPS due to the limited amount of commercially sourced peptide.

I performed alternative tests to determine the effects of organic solvents on peptide solubility as follows: first, I dissolved 1 mM of each peptide was dissolved in 100% DMSO. While both peptide solutions were translucent in 100% DMSO, the solution became turbid after minimal additions with buffer. Surprisingly, the buffer was only 18% of the total volume when the peptides precipitated. Given our inability to achieve peptide dissolution under the required experimental conditions (pH 7.0-7.4 and $\leq 1\%$ DMSO), we redirected our efforts to designing and producing the fusion protein, MBP-SM100. The fusion protein offered multiple advantages compared to the synthesized peptide, e.g., superior solubility and the capability to produce larger protein quantities via bacterial expression for further analyses.

4.4.2 MBP-SM50-100 and SM50-100 Biochemical Validation

I assessed the purity of the fusion protein (MBP-SM50-100), before and after cleavage by TEV protease, using size exclusion chromatography (SEC) with a Cytiva Superdex 75, 10/300 on a GE AKTA Explorer. Before TEV cleavage (Fig. 4.3A), the chromatograph for MBP-SM50-100 showed a set of early elution peaks representing aggregates of the fusion protein. A single peak at a higher elution volume was representative of soluble and monodisperse MBP-SM50-100. After TEV cleavage (Fig. 4.3B), the single peak disappears and is replaced by two peaks corresponding to the MBP and SM50-100 fractions. The shift of the peaks in figure 4.3C indicates that the protein was cut to completion.

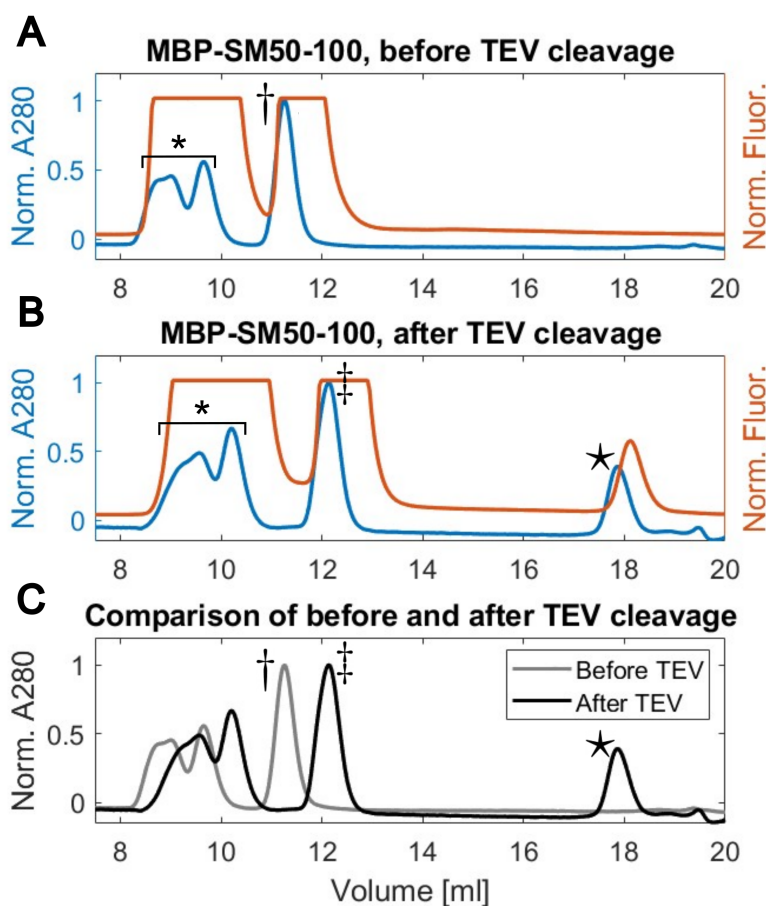


Figure 4.3: **SEC analysis of MBP-SM50-100 and SM50-100 shows the proteins are soluble and mono-dispersed.** Normalized absorption at 280 nm (blue curve) and normalized fluorescence intensity (excitation at 280nm, emission at 340nm) (orange curve) of MBP-SM50-100 on a Cytiva Superdex 75, 10/300 A) before TEV cleavage and B) SM50-100 after TEV. The y-axis represents the elution volume. The first set of peaks [*] represents oligomers or aggregates of the fusion protein, MBP-SM50-100. [†] is mono-disperse MBP-SM50-100. After cleavage (B), the fusion protein is separated into two, new peaks: MBP [†] and SM50-100 [★]. C) The MBP peaks ([*] and [†]) shift to higher elution volumes after TEV cleavage, indicating the protein was cut to completion.

4.4.3 Degron binding to lipid vesicles

I conducted co-sedimentation experiments to test the binding of the fusion protein, MBP-SM50-100, to vesicles with varying cholesterol concentrations. The results, depicted in Fig.

4.4, showed no clear binding of the fusion protein to vesicles containing 10 mol% or 50 mol% cholesterol. While the fluorescent intensity of the low cholesterol condition was more intense than that of the high cholesterol condition, both were similar to the negative control.

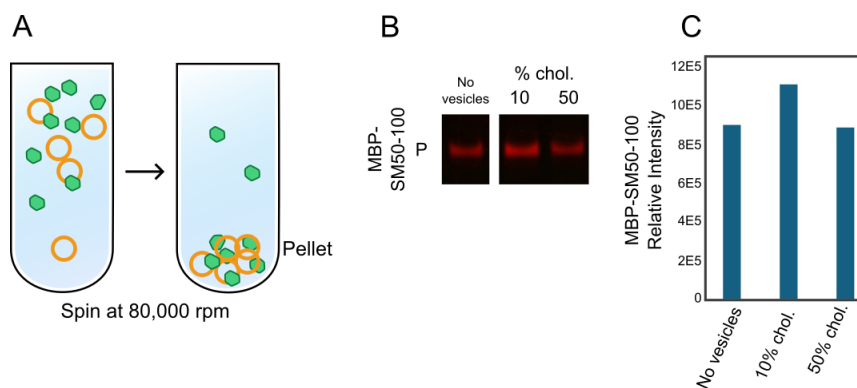


Figure 4.4: **MBP-SM50-100 binding to lipid vesicles.** **A)** Co-sedimentation assays were used to measure the membrane-bound fraction (pellet, P) of MBP-SM50-100 (labeled with Cy3b-maleimide). Vesicles (10% and 50% cholesterol (chol.), 25 μ M total lipid) were incubated with MBP-SM50-100 (70 nM) for 30 min and then ultracentrifuged at 80,000 rpm (279,000 xg) for 1 hr. **B)** In-gel fluorescence of membrane-bound MBP-SM50-100 at 10 mol% and 50 mol% cholesterol and a negative control, no vesicles. **C)** Quantification of the intensity of each band in B).

One explanation for this outcome is that the MBP component of the fusion protein prevents the binding of the degnon to the membrane. This is a plausible explanation, given that MBP is roughly five times larger than SM50-100 and may therefore impede protein-lipid interactions. Additionally, the negative control's fluorescence intensity may have been affected by protein aggregates, which also sediment with vesicles, so could skew the results. Finally, it is also plausible that the degnon may require vesicles with either a lower cholesterol concentration or a higher curvature to bind effectively. Future investigation is necessary to determine the effects of each variable on degnon binding.

Another method to access protein-lipid interactions and binding is with fluorescence quenching, in which the fluorescent emission intensity decreases due to interactions between the fluorescent probe and a quencher (i.e., the non-polar tails of the membrane). Bimane is

a good candidate for quenching because its fluorescence has been well characterized and it is likely small enough to prevent perturbations of the protein's structure on its own [280]. To test the interaction of the N-terminal half of SM50-100 with vesicles, I labeled Cys49 with bimane-C3-maleimide and measured the emission spectra of bimane with and without lipid vesicles. As shown in Fig. 4.5, titration of bimane-C3-SM50-100 with 100 μM , 500 μM , and 1000 μM lipid vesicles does not affect the emission spectrum. This negative result could indicate that the N-terminal of SM50-100 is not interacting with vesicles under the experimental conditions or that the Cys49 position is too buried within the protein to detect environmental changes.

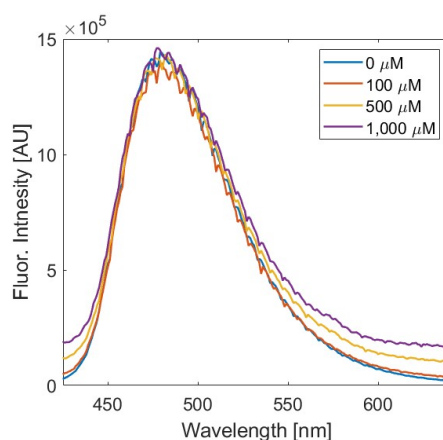


Figure 4.5: **Fluorescence emission spectra of Bimane-labeled MBP-SM50-100 with lipid vesicles.** A) Intensity was measured at 0 μM , 100 μM , 500 μM , and 1000 μM total lipid. All measurements were taken 10 min after the addition of lipid vesicles to the sample cell. Vesicle composition was 95 mol% POPC and 5 mol% DOPG.

4.5 Conclusions and Future Work

In this chapter, I outline an approach to test the interactions of squalene monooxygenase with membranes of different biochemical and biophysical properties. By utilizing lipid vesicles, I can precisely tune membrane features such as the concentration of cholesterol, membrane order (i.e., packing), and membrane size. My preliminary results show that MBP-SM50-

100 does not bind to low-cholesterol vesicles (≤ 10 mol %). In co-sedimentation assays to measure the fraction of membrane-bound MBP-SM50-100, no significant difference was detected between low-cholesterol vesicles and high-cholesterol vesicles. Although I did not observe cholesterol-dependent changes in binding (Fig. 4.4 C), my SEC analysis of MBP-SM50-100 indicates that the protein is susceptible to aggregation (Fig. 4.3), meaning the protein can sediment in the absence of vesicles [281]. There are several options for improving the reliability of the co-sedimentation experiments; these include repeating the experiments with protein purified from SEC or testing the cleaved protein (SM50-100). Alternatively, binding could be assessed with a flotation assay, which is not sensitive to protein aggregates.

To employ an alternative assay to test for binding of MBP-SM50-100 of membranes, I labeled Cys49 with bimane-C3-maleimide. I then attempted to measure changes in the emission spectrum when MBP-SM50-100 was mixed with vesicles containing 10 mol% and 50 mol% cholesterol. My experiments revealed no change in the fluorescent emission of bimane. As before, the MBP may be too large to allow binding of the degon. Alternatively, Cys49 may be too distant from the membrane-bound region or too buried within the protein to detect significant changes in bimane fluorescence.

Each experiment I have conducted to date has not definitively shown binding of SM50-100 to membranes, but each experiment also has significant caveats. In future work, I plan to probe interactions of the degon region and membranes using tryptophan mutants of the degon. To test this approach, we choose two sites to mutate from phenylalanine (Phe) to tryptophan (Trp): Phe63 and Phe66. I initiated a collaboration with theorists (Mark Uline and Roberto Gambarini at the University of South Carolina), who conducted all-atom molecular simulations of these mutants (residues 61-73) with membranes. Their initial simulations revealed that both protein mutants insert into 100 % DOPC membranes at 0.1 M NaCl. However, the Phe66 Trp mutant binds to the membrane faster (40 ns) than either the Phe63 Trp mutant or the native sequence, which require 170 ns and 335 ns, respectively. Given these results, future work could measure tryptophan fluorescence to elucidate interactions of the Phe66 Trp mutant with the membrane and to further understand

the mechanisms and structural configurations of the degron. Moreover, these experiments could be conducted with vesicles composed of a range of cholesterol concentrations.

A challenge of using tryptophan fluorescence to detect membrane binding is that SM must be separated from MBP. This is because tryptophan residues in MBP may make it difficult to determine which parts of the tryptophan emission spectra are due to interactions of SM with the membrane. One solution to this problem could be to cleave MBP from SM50-100 at the TEV site. However, although the SEC results validate the solubility and monodispersity of cleaved SM, further controls are needed to confirm its stability. For example, analyzing centrifuged solutions of cleaved SM could confirm the protein does not form aggregates after SEC purification.

In summary, many unanswered questions remain about how squalene monooxygenase interacts with membranes. Decades of studies in cells have provided some information about its structure and the mechanisms involved in its degradation. However, using cell-based assays to determine binding has limitations, as there are many intermediate steps between membrane binding and protein expression that are not well understood. Therefore, using protein expression levels to determine membrane binding is just the first step in understanding the binding mechanisms of squalene monooxygenase.

Our goal is to answer questions about SM by measuring its binding to membranes in a method that is as direct as possible and that uses model systems in which we can precisely tune membrane properties. Furthermore, we would like to continue exploring the relationship between membrane curvature, membrane order, and degron binding. Even if we find that binding of the degron to membranes is cholesterol-dependent, we still need to understand the role of membrane curvature and order. We hypothesize that these variables play a crucial role in degron binding and that specific conditions can trigger the displacement of the degron. To test this hypothesis, future research can employ extruded vesicles with high curvatures (similar to ER membranes) and could assess the role of membrane order by using vesicles comprised of varying ratios of saturated and unsaturated lipids.

In conclusion, we have presented an approach for measuring the binding of squalene

monooxygenase to membranes and subsequent structural changes. Our approach leverages protein mutants and multiple assays to detect changes in the environment of the protein. We envision future experiments that may offer new insights into the mechanism of squalene monooxygenase and may improve our understanding of cholesterol synthesis and regulation.

Chapter 5

STEP-UP: STUDENTS WRITE BIOPHYSICS CONTENT FOR WIKIPEDIA

The content held in this chapter was designed for educational purposes and may be shared and adapted for educational, non-commercial, purposes under fair use.

5.1 *What is STEP-UP?*

Science Teaching Experience Program for Upcoming PhDs (STEP-UP) is a year-long, training program at the University of Washington (UW), in which graduate students develop and implement student-centered curricula as the instructors of record for upper division STEM courses [282]. The program focuses on evidence-based teaching practices that support active learning and promote equitable classroom environments [283]. Broadly, the program is broken into two parts. First, the STEP-UP cohort of roughly 20 graduate students complete a one-quarter course, in which they learn course design, pedagogical theory, and teaching strategies. The cohort practices implementing these skills in a mock classroom with undergraduate volunteers. In the program's second half, STEP-UP participants design and teach undergraduate courses at UW. Most often, the courses are taught by a team of three instructors, and the teaching load is divided among different units within the course. I designed the course, *The Molecular Mechanisms of Life and Death* (BIOL 410B), for the STEP-UP program, with my co-instructors Nicole Marsh and Cassidy Hagan. We taught the course in the Spring Quarter of 2024. Most of the 23 students were senior undergraduates; 82% described the course as "in their major". The *Biophysics WikiProject* I designed was the final assessment of my biophysics unit. This thesis chapter presents course materials for the *Biophysics WikiProject* (Appendix C) and offers insights and recommendations to enhance

project implementation and student learning in future iterations.

5.2 Inspiration: Why ask students to edit Wikipedia?

In 2023, Wikipedia comprised more than 63 million articles, and *English Wikipedia* attracted 84 billion views [284]. These statistics reflect why Wikipedia is consistently one of the 10 most popular websites in the world [285]. Despite Wikipedia's far-reaching audience, only 19% of *English Wikipedia* biographies are about women. An encouraging aspect is that gender gaps on Wikipedia can be addressed, as its open-source format allows anyone to create and edit content. Many communities, such as *500 Women Scientists*, have worked to design and implement programming to ensure the contributions of women and minorities in science, technology, engineering, and mathematics (STEM) are reflected in the world's largest free encyclopedia. One example of these types of events is a "Wiki-thon", which brings together individuals to learn how to edit Wikipedia among a community of supportive peers.

After attending *Wikipedia Edit for Change 2022*, hosted by the University of California Berkeley Libraries, I was inspired to teach my students how to edit Wikipedia, with the goal that our edits would contribute toward making Wikipedia a platform that more accurately represents the diversity of sciences and scientists. Furthermore, as Wikipedia is frequently the first place undergraduates interact with new science topics, I was inspired to work with my students to create free, accessible content about biophysics. My course plan leveraged the lessons I learned from my Wiki-thon experience, and utilized the process to frame the problem and the course assignment, and motivated my students to translate topics in biophysics for general audiences.

5.3 Project Design

The biophysics unit of the course utilized a combination of academic papers and online resources to teach biophysical concepts, techniques, and applications. The WikiProject was introduced in the first lecture of the unit. The objectives of the initial classroom session were that students would be able to:

1. Describe biophysics and themes in biophysics
2. Ask scientific questions about a biological system that could be answered with biophysics
3. Discuss the importance and limitations of Wikipedia
4. Navigate Wikipedia and analyze content for editing
5. Identify a subject for the WikiProject

5.3.1 Introduction to Wikipedia

With permission from the UC Berkeley Library, I adapted content from the Wiki-thon for the course. In the first lecture, students were introduced to the content policies of Wikipedia, which are summarized below.

Neutral point of view. All content should be impartial and written in a neutral tone. All major points of view and theories must be presented equally.

Verifiability and Notability. All content must be supported by independent, published materials with citations in the text. Whenever possible, it is recommended to use academic and peer-reviewed publications. Other reliable sources might include university-level textbooks, books published by reputable publishing houses, journals, and mainstream newspapers. Wikipedia uses notability tests to determine if a topic should have its own article. Content that does not pass these tests will be flagged and possibly removed from Wikipedia. Notability and verifiability are interconnected. Topics are accepted as notable if they exhibit “significant coverage” from reputable and independent sources [286]

No original content. Wikipedia is first and foremost an encyclopedia. All content must be summarized from other sources. Original content such as stories, poems, or blogs should not be shared on Wikipedia.

Conflict of Interest. Wikipedia advises that users do not edit or create any content that could be a conflict of interest. It was emphasized that the goal was to remain unbiased and impartial. As an example for our class, we discussed how we could not write a biography about a current instructor or research supervisor.

Following a discussion of these policies, I taught students how to add a source or update an existing source on a Wikipedia page. Students learned about *Wikipedia Talk Pages* and *WikiProject Groups*, both of which are resources on Wikipedia for determining and discussing what content on Wikipedia needs revision.

Students learned that the *Talk* page is a forum to discuss what content needs revision in light of other Wikipedia edits. In class, students browsed through a couple of *Talk* pages and shared some brief conclusions from the page with their peers, and then the classroom. *Talk* pages also include a rating of the quality of the material, determined by various Wikipedia groups.

Finally, I taught students about the sandbox feature, a separate page that allows for drafting changes to articles, without augmenting or removing content from the official Wikipedia page. We discussed that we would be drafting our edits to Wikipedia using the Sandbox feature.

5.3.2 Project Score

By completing the WikiProject students would learn to critically analyze scientific content on Wikipedia, evaluate gaps in biophysics knowledge, and create new Wikipedia content based on course material and their research. I presented an outline of the WikiProject in a handout following the first lecture (Appendix C).

Students were given the option to either edit an existing Wikipedia page on a biophysical topic or create a new Wikipedia page for a scientist. Students were required to sign up for a topic in a shared Google sheet, and they were allowed to change their subject as many times as they wanted. However, each student needed to have a unique, biophysics-related subject that was distinct from their peers. I provided the students with a non-exhaustive list of biophysics subjects before the start of the session (Appendix C). Each topic was labeled with the quality of the current page (A, B, C, start, or stub) and an importance indicator (Top, High, Mid, or Low), determined by scientific WikiProject groups. The importance

indicator highlighted the probability that a topic would be searched. This information was provided to help students determine which topics would be easiest to improve, which would have the most impact on Wikipedia articles or a combination of these factors.

Step-by-step details of how I instructed the students to complete the project are contained in Appendix C. Briefly, I required that students submit four documents that formed the scaffold of the WikiProject. (1) To interact with and critically analyze text, students had to read and summarize a current Wikipedia article related to a biophysics topic and then generate a list of content items for improvement. Students were explicitly told that although additional technical content of the Wikipedia article might need revision, anything unrelated to biophysics was outside the project's scope. Students were encouraged to leave non-biophysics suggestions on the *Talk* page. If the students choose to create a new page for a scientist, they were tasked with finding and summarizing three independent sources on their scientist. (2) The second document contained the primary research component. Students were required to use the university library databases to find and read a paper or to explore the content of a scientist's web page to find research themes and publications. The goal of the document was to guide students in summarizing and paraphrasing the results of their literature research. The final two documents were (3) their proposal, drafted in their Wikipedia sandbox, and (4) a one-page (or less) description of their proposal.

5.3.3 *Project timeline and deadlines*

One goal that guided my design of the WikiProject was building trust with the students by inspiring them to choose topics of interest to them and support their exploration. Expectations, the project deadline, and the assessment criteria were shared upfront, including the grading rubric uploaded to Canvas (Appendix C).

Students had four weeks to complete the project, and the submission was due one week after the final class period. This deadline allowed students to choose subjects discussed on the last day of the biophysics unit.

Students were encouraged to start their projects early and submit their work for feedback

before the project deadline. Specifically, the students were presented with two optional deadlines, in which they could submit the first two documents of the assignment and receive instructor feedback. (Appendix C, Proposal, Important Dates). In other words, students could complete research portions of the project early to ask questions and ensure they were meeting the objectives of the project. I implemented this by creating optional assignments on the course website for students to upload their material by the (optional) deadlines. For students who took advantage of this option, I uploaded feedback to Canvas before the next class session.

5.4 Challenges and recommendations

As with any new course, the end of the quarter revealed areas for improvement. Two categories of future improvement are summarized here: self-reflections and suggestions from student evaluation.

5.4.1 Self-reflections on the Biophysics Wikiproject

1. Students would benefit from more examples of how to edit and improve Wikipedia.

When I first presented this project to my students, I indicated that choosing to create a new page on a scientist might take 1-2 hours longer than editing an existing page, given that creating a new page would require finding multiple, independent sources describing the scientist. Upon reflection, I think that mentioning 1-2 more hours of work may have deterred some students from making pages for scientists (roughly 20% students made new scientist biographies).

Separately, to practice with Wikipedia's structure and syntax, I drafted a new page for a scientist using Wikipedia's sandbox, and I submitted the draft to Wikipedia for review (using features in the sandbox). I think students would have benefited from some documentation of this process (e.g., a video summarizing the major points). Seeing the steps involved in creating the page and the final draft may have inspired others to create new Wikipedia pages.

Within “the Propose an Edit to Wikipedia” handout (Appendix C), I encouraged students to be creative with their edits. I gave an example of creating a helpful table to summarize information that might be overwhelming if presented in only text. I think exploring more of these types of examples, either in class or through an additional, small assignment, would have prompted students to brainstorm ideas for improving different pages. The additional examples could have provided scaffolding to approach the project more creatively.

I can only speculate about how students eventually chose to fulfill the project, but it seemed that most students found a review article on a topic and used material within the review to supplement an existing page. My intent was the opposite: that students would have found gaps in a Wikipedia page, and then conducted online research to add new information.

2. Adding one in-class work session could prevent many problems that students encountered with Wikipedia syntax.

A common issue in the final project submission was formatting. A significant number of students had problems with Wikipedia’s sandbox feature - both using it and generating a .pdf document of their sandbox. A few students submitted their projects essentially in coding language, which made it difficult for me to read their projects to grade them.

I think many of these issues could be eliminated in the future by requiring that students work with the sandbox feature during a class session. Unfortunately, the biophysics unit constituted only one of three units. Thus, additional in-class time for live practice could not be accommodated. If time permits in future sessions, I would recommend that each student practice using the sandbox to write roughly a half page of class notes. In addition to the syntax, they could practice other important features for articles such as including citations, creating subheadings, and adding embedded links to other Wikipedia pages. At the end of that session, students would then submit their notes in the same format required for the final project.

3. Incentives could be better structured so that more work done by students is submitted to Wikipedia.

Many students created interesting and well-described edits for Wikipedia. Though stu-

dents were only tasked with creating proposals; they were not required to upload their edits to Wikipedia's main page.

Students were offered three extra credit points (on top of the project's 100 total points) if they submitted their proposal to Wikipedia (after they made any necessary changes given by the instructor). The large majority of proposals only required minor edits such as including the source the student used for a specific statement or adding 1-2 sentences for clarification. Unfortunately, some students with excellent proposals did not upload their edits to Wikipedia, because it did not seem worthwhile for them to implement the small changes or because they were not motivated by the small number of extra points.

If more instruction time were available, it would be feasible for an instructor to require students to submit their proposals and also to require students to make edits in response to the instructor's suggestions. However, this cannot be accomplished in a timeline as brief as three weeks. In at least one case, a student did not include adequate scientific sources or included substantial information that was misrepresented. If this information had been uploaded to Wikipedia, it would have diminished rather than improved the quality of the posted material. My course lacked the time to work with the students through iterative rounds of edits that would have been necessary for all of them to produce high-quality edits suitable for posting on Wikipedia.

5.4.2 Suggestions from student evaluation

In the course evaluations, many students had good suggestions for improving the WikiProject. One suggestion, consistent with my observations, was to create a short video about navigating Wikipedia on Canvas so that students could reference it throughout the project. I agree this would benefit students, especially if they missed class sessions introducing the basics of Wikipedia or in-class work sessions (if offered).

Another interesting idea presented by several students was turning the WikiProject into a group project. The students suggested breaking up the components of the Wikipedia page and assigning them to different group members. For a senior undergraduate course, I found it

more appropriate for each student to create an individual proposal, tailored to their interests.

An excellent suggestion was to have students peer-edit each other's proposals. The student, who made this suggestion, pointed out that peer-editing would also allow students to learn about a topic they didn't personally research. I also think this is a great idea for future implementations. If class time permits, an entire period could be dedicated to each student sharing their proposal.

5.5 *Final thoughts and conclusions*

On the first day of instruction, none of the students could describe biophysics or what ideas might be related to biophysics. Designing and teaching this course was a tremendous amount of work. In the end, it was rewarding to see students build confidence in the material and begin to ask questions about scientific research. In an open-ended question on the student evaluations, I asked the students: "What is your advice to future students taking this biophysics module?" The answers overwhelmingly encouraged future students to not be afraid of asking questions. Unbeknownst to my students, my goals for this course were 1) to build students' confidence in their abilities to read and analyze scientific papers and 2) to teach students to ask effective questions. The student evaluations reflect that progress was made toward both of these goals.

My favorite pieces of advice that students offered for future students are below:

"Don't be afraid of physics! Applying physics to biology can lead to neat experiments and results. Don't be afraid to ask questions as well."

"Come to class ready to make some inferences and hypothesize about scientific data. There aren't exams and you aren't tested on any knowledge, so perhaps the most useful thing you can get out of this class is an understanding of how these ideas and concepts apply to biological research happening right now."

In summary, I would assign the WikiProject again. However, I would work to improve the implementation by providing the students with more examples and methods for editing content on Wikipedia. Furthermore, I would require students to interact with the sandbox feature to improve their user experience and understanding of the various tools well before the project deadline. Overall, I think the students had a positive experience. In the student evaluations, 92% of students said they “strongly agree ” or “agree” that they now have the skills to edit content on Wikipedia in the future. In addition, 52% of students “agree” that they are now more interested in improving Wikipedia (through edits of scientific or other content) than they were before this course.

I encourage future instructors to build on the materials I developed and insights I have outlined to create an engaging learning opportunity for students and to improve Wikipedia so that it contains better scientific content and representation. The objectives of the WikiProject are aimed at the highest levels of Bloom’s taxonomy (analyze, evaluate, and create). Removing the syntaxial barriers for students to focus on the deeper work should be the primary goal of most future augmentations.

Chapter 6

CONCLUSIONS AND FUTURE DIRECTIONS

This thesis employs lipid vesicles as a model for cellular membranes to ask questions about protein-lipid interactions. First, utilizing lipids vesicles composed of lipids ratios that phase separate, we asked whether we could couple 2D phase separation in membranes to 3D protein condensates. Specifically, our initial goal was to quantify the effects of coupled phase behavior on the miscibility temperature of membranes. This question proved challenging given that experimental conditions optimized for membranes are typically incompatible with experimental conditions optimized for proteins. In chapter 2, we characterized the experimental challenges researchers face when coupling membrane phase separation to protein condensates. To help future researchers circumvent these challenges, we summarized numerous experimental tools for researchers to employ. Given the current, immense interest in protein phase separation and the fact that new areas of the phase diagram (the pre-wetting regime) are not yet well understood, we anticipate more researchers will seek to investigate coupling between membrane phase separation and protein phase separation; we hope our review will provide insight and value to those investigations.

In chapter 3, we examined whether common methods of making lipid vesicles capture intended lipid ratios using mass spectroscopy. Lipid vesicles were formed from an identical master stock containing five different lipid species and then compared to the parent stock. We measured shifts in cholesterol for gentle hydration ($\sim 20\%$ increase) and ITO electroformation ($\sim 80\%$ decrease). In the ITO electroformation and emulsion phase transfer techniques, we measured shifts in the PC-lipid incorporation ratio dependent on the level of chain saturation. For all methods of vesicle formation, we observed small deviations in the population-averaged lipid ratios. We found that lipid ratios within a single technique

are highly reproducible. Future researchers could leverage our results in many ways. For example, researchers could zero in on specific lipid ratios in their experiments (e.g., ternary lipid compositions or mixtures of various ratios of cholesterol and PC-lipids). Researchers could use our results as a starting point to investigate the mechanisms of lipid incorporation. They could also expand our results to examine how the lipid composition of vesicles depends on other parameters, such as vesicle size or variables specific to the technique (e.g., different re-hydration solvents in gentle hydration techniques or different oils in emulsion phase transfer techniques).

In chapter 4, we developed an approach to probe interactions of squalene monooxygenase, a rate-limiting enzyme in cholesterol synthesis, with membranes. We describe the design and characterization of an analog protein (residues 50-100) for testing membrane interactions with squalene monooxygenase's degnon. By combining a co-sedimentation assay with single tryptophan mutants of squalene monooxygenase, we captured preliminary data supporting the feasibility of this approach to directly measure the influence of membrane cholesterol levels on degnon binding. Furthermore, we designed tryptophan mutants to determine the structure of degnon in response to cholesterol levels and membrane binding. Cholesterol concentration is one possible variable that influences the mechanism of binding. We anticipate that future investigators will use the tools and experimental approaches we have developed to test the influence of other important membrane properties (such as lipid order and membrane curvature) on squalene monooxygenase.

Building on the biophysics research in this thesis, chapter 5 describes new educational curricula to increase student understanding of biophysical subjects and techniques by editing biophysics content on Wikipedia. The chapter outlines a Wikipedia project for college-level courses, presents grading materials, and discusses improvements for future educational implementations of the project.

BIBLIOGRAPHY

- [1] J. Ubach, X. Zhang, X. Shao, T. C. Südhof, and J. Rizo, “Ca²⁺ binding to synaptotagmin: how many Ca²⁺ ions bind to the tip of a C2-domain?,” *The EMBO Journal*, vol. 17, no. 14, pp. 3921–3930, 1998.
- [2] K. C. Courtney, T. Mandal, N. Mehta, L. Wu, Y. Li, D. Das, Q. Cui, and E. R. Chapman, “Synaptotagmin-7 outperforms synaptotagmin-1 to promote the formation of large, stable fusion pores via robust membrane penetration,” *Nature Communications*, vol. 14, no. 1, p. 7761, 2023.
- [3] V. A. Fadok, D. L. Bratton, S. C. Frasch, M. L. Warner, and P. M. Henson, “The role of phosphatidylserine in recognition of apoptotic cells by phagocytes,” *Cell Death & Differentiation*, vol. 5, no. 7, pp. 551–562, 1998.
- [4] R. Koynova and M. Caffrey, “Phases and phase transitions of the phosphatidylcholines,” *BBA - Reviews on Biomembranes*, vol. 1376, no. 1, pp. 91–145, 1998.
- [5] N. Fuller and R. P. Rand, “The influence of lysolipids on the spontaneous curvature and bending elasticity of phospholipid membranes.,” *Biophysical Journal*, vol. 81, no. 1, pp. 243–254, 2001.
- [6] P. L. Yeagle, “Modulation of membrane function by cholesterol,” *Biochimie*, vol. 73, no. 10, pp. 1303–1310, 1991.
- [7] G. N. Levine, J. F. Keaney, and J. A. Vita, “Cholesterol Reduction in Cardiovascular Disease — Clinical Benefits and Possible Mechanisms,” *New England Journal of Medicine*, vol. 332, no. 8, pp. 512–521, 1995.
- [8] A. J. Brown, “Cholesterol, Statins and Cancer,” *Clinical and Experimental Pharmacology and Physiology*, vol. 34, no. 3, pp. 135–141, 2007.
- [9] S. L. Veatch and S. L. Keller, “Separation of liquid phases in giant vesicles of ternary mixtures of phospholipids and cholesterol,” *Biophysical Journal*, vol. 85, no. 5, pp. 3074–3083, 2003.
- [10] I. Levental, F. J. Byfield, P. Chowdhury, F. Gai, T. Baumgart, and P. A. Janmey, “Cholesterol-dependent phase separation in cell-derived giant plasma-membrane vesicles,” *The Biochemical Journal*, vol. 424, no. 2, pp. 163–167, 2009.

- [11] S. P. Rayermann, G. E. Rayermann, C. E. Cornell, A. J. Merz, and S. L. Keller, “Hallmarks of Reversible Separation of Living, Unperturbed Cell Membranes into Two Liquid Phases,” *Biophysical Journal*, vol. 113, no. 11, pp. 2425–2432, 2017.
- [12] S. L. Veatch and S. L. Keller, “Organization in Lipid Membranes Containing Cholesterol,” *Physical Review Letters*, vol. 89, no. 26, p. 268101, 2002.
- [13] T. Baumgart, S. Das, W. W. Webb, and J. T. Jenkins, “Membrane Elasticity in Giant Vesicles with Fluid Phase Coexistence,” *Biophysical Journal*, vol. 89, no. 2, pp. 1067–1080, 2005.
- [14] Y. Z. Yoon, J. P. Hale, P. G. Petrov, and P. Cicuta, “Mechanical properties of ternary lipid membranes near a liquid-liquid phase separation boundary,” *Journal of Physics. Condensed Matter: An Institute of Physics Journal*, vol. 22, no. 6, p. 062101, 2010.
- [15] K. J. Wilson, H. Q. Nguyen, J. Gervay-Hague, and S. L. Keller, “Sterol-lipids enable large-scale, liquid-liquid phase separation in membranes of only 2 components,” *bioRxiv*, p. 2024.02.02.578692, 2024.
- [16] S. L. Veatch and S. L. Keller, “Seeing spots: Complex phase behavior in simple membranes,” *BBA - Molecular Cell Research*, vol. 1746, no. 3, pp. 172–185, 2005.
- [17] C. E. Cornell, A. Mileant, N. Thakkar, K. K. Lee, and S. L. Keller, “Direct imaging of liquid domains in membranes by cryo-electron tomography,” *Proceedings of the National Academy of Sciences*, vol. 117, no. 33, pp. 19713–19719, 2020.
- [18] S. D. Connell, G. Heath, P. D. Olmsted, and A. Kisil, “Critical point fluctuations in supported lipid membranes,” *Faraday Discussions*, vol. 161, no. 0, pp. 91–111, 2013.
- [19] J. V. Bleecker, P. A. Cox, and S. L. Keller, “Mixing Temperatures of Bilayers Not Simply Related to Thickness Differences between Lo and Ld Phases,” *Biophysical Journal*, vol. 110, no. 11, pp. 2305–2308, 2016.
- [20] P. Heftberger, B. Kollmitzer, A. Rieder, H. Amenitsch, and G. Pabst, “In Situ Determination of Structure and Fluctuations of Coexisting Fluid Membrane Domains,” *Biophysical Journal*, vol. 108, no. 4, pp. 854–862, 2015.
- [21] S. L. Veatch, I. V. Polozov, K. Gawrisch, and S. L. Keller, “Liquid Domains in Vesicles Investigated by NMR and Fluorescence Microscopy,” *Biophysical Journal*, vol. 86, no. 5, pp. 2910–2922, 2004.

- [22] I. Ionova, V. Livshits, and D. Marsh, “Phase Diagram of Ternary Cholesterol/Palmitoylsphingomyelin/Palmitoyl-oleoyl-Phosphatidylcholine Mixtures: Spin-Label EPR Study of Lipid-Raft Formation,” *Biophysical Journal*, vol. 102, no. 8, pp. 1856–1865, 2012.
- [23] C. P. Brangwynne, C. R. Eckmann, D. S. Courson, A. Rybarska, C. Hoegel, J. Gharakhani, F. Jülicher, and A. A. Hyman, “Germline P Granules Are Liquid Droplets That Localize by Controlled Dissolution/Condensation,” *Science*, vol. 324, no. 5935, pp. 1729–1732, 2009.
- [24] I. A. Antifeeva, A. V. Fonin, A. S. Fefilova, O. V. Stepanenko, O. I. Povarova, S. A. Silonov, I. M. Kuznetsova, V. N. Uversky, and K. K. Turoverov, “Liquid-liquid phase separation as an organizing principle of intracellular space: overview of the evolution of the cell compartmentalization concept,” *Cellular and molecular life sciences: CMLS*, vol. 79, no. 5, p. 251, 2022.
- [25] P. Li, S. Banjade, H.-C. Cheng, S. Kim, B. Chen, L. Guo, M. Llaguno, J. V. Hollingsworth, D. S. King, S. F. Banani, P. S. Russo, Q.-X. Jiang, B. T. Nixon, and M. K. Rosen, “Phase transitions in the assembly of multivalent signalling proteins,” *Nature*, vol. 483, no. 7389, pp. 336–340, 2012.
- [26] S. Banjade and M. K. Rosen, “Phase transitions of multivalent proteins can promote clustering of membrane receptors,” *eLife*, vol. 3, p. e04123, 2014.
- [27] C. P. Brangwynne, P. Tompa, and R. V. Pappu, “Polymer physics of intracellular phase transitions,” *Nature Physics*, vol. 11, no. 11, pp. 899–904, 2015.
- [28] T. J. Nott, E. Petsalaki, P. Farber, D. Jervis, E. Fussner, A. Plochowietz, T. D. Craggs, D. P. Bazett-Jones, T. Pawson, J. D. Forman-Kay, and A. J. Baldwin, “Phase Transition of a Disordered Nuage Protein Generates Environmentally Responsive Membraneless Organelles,” *Molecular Cell*, vol. 57, no. 5, pp. 936–947, 2015.
- [29] C. W. Pak, M. Kosno, A. S. Holehouse, S. B. Padrick, A. Mittal, R. Ali, A. A. Yunus, D. R. Liu, R. V. Pappu, and M. K. Rosen, “Sequence Determinants of Intracellular Phase Separation by Complex Coacervation of a Disordered Protein,” *Molecular Cell*, vol. 63, no. 1, pp. 72–85, 2016.
- [30] A. G. Larson, D. Elnatan, M. M. Keenen, M. J. Trnka, J. B. Johnston, A. L. Burlingame, D. A. Agard, S. Redding, and G. J. Narlikar, “Liquid droplet formation by HP1 suggests a role for phase separation in heterochromatin,” *Nature*, vol. 547, no. 7662, pp. 236–240, 2017.

- [31] X. Su, J. A. Ditlev, E. Hui, W. Xing, S. Banjade, J. Okrut, D. S. King, J. Taunton, M. K. Rosen, and R. D. Vale, “Phase separation of signaling molecules promotes T cell receptor signal transduction,” *Science*, vol. 352, no. 6285, pp. 595–599, 2016.
- [32] J. A. Ditlev, A. R. Vega, D. V. Köster, X. Su, T. Tani, A. M. Lakoduk, R. D. Vale, S. Mayor, K. Jaqaman, and M. K. Rosen, “A composition-dependent molecular clutch between T cell signaling condensates and actin,” *eLife*, vol. 8, 2019.
- [33] H. J. Sharpe, T. J. Stevens, and S. Munro, “A Comprehensive Comparison of Transmembrane Domains Reveals Organelle-Specific Properties,” *Cell*, vol. 142, no. 1, pp. 158–169, 2010.
- [34] D. Marsh, “Lateral Pressure Profile, Spontaneous Curvature Frustration, and the Incorporation and Conformation of Proteins in Membranes,” *Biophysical Journal*, vol. 93, no. 11, pp. 3884–3899, 2007.
- [35] V. A. Frolov, A. V. Shnyrova, and J. Zimmerberg, “Lipid Polymorphisms and Membrane Shape,” *Cold Spring Harbor Perspectives in Biology*, vol. 3, no. 11, p. a004747, 2011.
- [36] H. M. J. Weakly and S. L. Keller, “Coupling liquid phases in 3D condensates and 2D membranes: Successes, challenges, and tools,” *Biophysical Journal*, 2023.
- [37] C. H. Moeller and W. W. Thomson, “An ultrastructural study of the yeast tonoplast during the shift from exponential to stationary phase,” *Journal of Ultrastructure Research*, vol. 68, no. 1, pp. 28–37, 1979.
- [38] A. Toulmay and W. A. Prinz, “Direct imaging reveals stable, micrometer-scale lipid domains that segregate proteins in live cells,” *Journal of Cell Biology*, vol. 202, no. 1, pp. 35–44, 2013.
- [39] C.-W. Wang, Y.-H. Miao, and Y.-S. Chang, “A sterol-enriched vacuolar microdomain mediates stationary phase lipophagy in budding yeast,” *Journal of Cell Biology*, vol. 206, no. 3, pp. 357–366, 2014.
- [40] C. L. Leveille, C. E. Cornell, A. J. Merz, and S. L. Keller, “Yeast cells actively tune their membranes to phase separate at temperatures that scale with growth temperatures,” *Proceedings of the National Academy of Sciences*, vol. 119, no. 4, p. e2116007119, 2022.
- [41] A. Molliex, J. Temirov, J. Lee, M. Coughlin, A. P. Kanagaraj, H. J. Kim, T. Mittag, and J. P. Taylor, “Phase Separation by Low Complexity Domains Promotes Stress Granule Assembly and Drives Pathological Fibrillization,” *Cell*, vol. 163, no. 1, pp. 123–133, 2015.

- [42] J. A. Riback, C. D. Katanski, J. L. Kear-Scott, E. V. Pilipenko, A. E. Rojek, T. R. Sosnick, and D. A. Drummond, “Stress-Triggered Phase Separation Is an Adaptive, Evolutionarily Tuned Response,” *Cell*, vol. 168, no. 6, pp. 1028–1040.e19, 2017.
- [43] S. Kroschwald, S. Maharana, D. Mateju, L. Malinovska, E. Nüske, I. Poser, D. Richter, and S. Alberti, “Promiscuous interactions and protein disaggregases determine the material state of stress-inducible RNP granules,” *eLife*, vol. 4, p. e06807, 2015.
- [44] O. Beutel, R. Maraspini, K. Pombo-García, C. Martin-Lemaitre, and A. Honigmann, “Phase Separation of Zonula Occludens Proteins Drives Formation of Tight Junctions,” *Cell*, vol. 179, no. 4, pp. 923–936.e11, 2019.
- [45] K. J. Day, G. Kago, L. Wang, J. B. Richter, C. C. Hayden, E. M. Lafer, and J. C. Stachowiak, “Liquid-like protein interactions catalyse assembly of endocytic vesicles,” *Nature Cell Biology*, vol. 23, no. 4, pp. 366–376, 2021.
- [46] W. Ma and C. Mayr, “A Membraneless Organelle Associated with the Endoplasmic Reticulum Enables 3UTR-Mediated Protein-Protein Interactions,” *Cell*, vol. 175, no. 6, pp. 1492–1506.e19, 2018.
- [47] J. E. Lee, P. I. Cathey, H. Wu, R. Parker, and G. K. Voeltz, “Endoplasmic reticulum contact sites regulate the dynamics of membraneless organelles,” *Science (New York, N.Y.)*, vol. 367, no. 6477, p. eaay7108, 2020.
- [48] X. Yu, L. Zhang, J. Shen, Y. Zhai, Q. Jiang, M. Yi, X. Deng, Z. Ruan, R. Fang, Z. Chen, X. Ning, and Z. Jiang, “The STING phase-separator suppresses innate immune signalling,” *Nature Cell Biology*, vol. 23, no. 4, pp. 330–340, 2021.
- [49] L.-P. Bergeron-Sandoval, S. Kumar, H. K. Heris, C. L. A. Chang, C. E. Cornell, S. L. Keller, P. François, A. G. Hendricks, A. J. Ehrlicher, R. V. Pappu, and S. W. Michnick, “Endocytic proteins with prion-like domains form viscoelastic condensates that enable membrane remodeling,” *Proceedings of the National Academy of Sciences*, vol. 118, no. 50, p. e2113789118, 2021.
- [50] W. T. Snead, A. P. Jalihal, T. M. Gerbich, I. Seim, Z. Hu, and A. S. Gladfelter, “Membrane surfaces regulate assembly of ribonucleoprotein condensates,” *Nature Cell Biology*, vol. 24, no. 4, pp. 461–470, 2022.
- [51] P. Sengupta, B. Baird, and D. Holowka, “Lipid rafts, fluid/fluid phase separation, and their relevance to plasma membrane structure and function,” *Seminars in cell & developmental biology*, vol. 18, no. 5, pp. 583–590, 2007.

- [52] D. Marsh, “Cholesterol-induced fluid membrane domains: A compendium of lipid-raft ternary phase diagrams,” *Biochimica et Biophysica Acta*, vol. 1788, no. 10, pp. 2114–2123, 2009.
- [53] A. R. Honerkamp-Smith, S. L. Veatch, and S. L. Keller, “An introduction to critical points for biophysicists; observations of compositional heterogeneity in lipid membranes,” *Biochimica et Biophysica Acta*, vol. 1788, no. 1, pp. 53–63, 2009.
- [54] F. A. Heberle and G. W. Feigenson, “Phase Separation in Lipid Membranes,” *Cold Spring Harbor Perspectives in Biology*, vol. 3, no. 4, p. a004630, 2011.
- [55] S. F. Banani, H. O. Lee, A. A. Hyman, and M. K. Rosen, “Biomolecular condensates: organizers of cellular biochemistry,” *Nature Reviews Molecular Cell Biology*, vol. 18, no. 5, pp. 285–298, 2017.
- [56] S. Alberti, “The wisdom of crowds: regulating cell function through condensed states of living matter,” *Journal of Cell Science*, vol. 130, no. 17, pp. 2789–2796, 2017.
- [57] A. E. Posey, A. S. Holehouse, and R. V. Pappu, “Phase Separation of Intrinsically Disordered Proteins,” *Methods in Enzymology*, vol. 611, pp. 1–30, 2018.
- [58] E. M. Langdon and A. S. Gladfelter, “A New Lens for RNA Localization: Liquid-Liquid Phase Separation,” *Annual Review of Microbiology*, vol. 72, no. 1, pp. 255–271, 2018.
- [59] D. Bracha, M. T. Walls, and C. P. Brangwynne, “Probing and engineering liquid-phase organelles,” *Nature Biotechnology*, vol. 37, no. 12, pp. 1435–1445, 2019.
- [60] T. Hirose, K. Ninomiya, S. Nakagawa, and T. Yamazaki, “A guide to membraneless organelles and their various roles in gene regulation,” *Nature Reviews Molecular Cell Biology*, vol. 24, no. 4, pp. 288–304, 2023.
- [61] M. R. Moldover and J. W. Cahn, “An Interface Phase Transition: Complete to Partial Wetting,” *Science*, vol. 207, no. 4435, pp. 1073–1075, 1980.
- [62] C. Ebner and W. F. Saam, “New Phase-Transition Phenomena in Thin Argon Films,” *Physical Review Letters*, vol. 38, no. 25, pp. 1486–1489, 1977.
- [63] H. Nakanishi and M. E. Fisher, “Multicriticality of Wetting, Prewetting, and Surface Transitions,” *Physical Review Letters*, vol. 49, no. 21, pp. 1565–1568, 1982.

- [64] P. G. de Gennes, “Wetting: statics and dynamics,” *Rev. Mod. Phys.*, vol. 57, no. 3, pp. 827–863, 1985.
- [65] M. Rouches, S. L. Veatch, and B. B. Machta, “Surface densities prewet a near-critical membrane,” *Proceedings of the National Academy of Sciences*, vol. 118, no. 40, p. e2103401118, 2021.
- [66] X. Zhao, G. Bartolucci, A. Honigmann, F. Jülicher, and C. A. Weber, “Thermodynamics of wetting, prewetting and surface phase transitions with surface binding,” *New Journal of Physics*, vol. 23, no. 12, p. 123003, 2021.
- [67] M. R. Helfrich, L. K. Mangeney-Slavin, M. S. Long, K. Y. Djoko, and C. D. Keating, “Aqueous Phase Separation in Giant Vesicles,” *Journal of the American Chemical Society*, vol. 124, no. 45, pp. 13374–13375, 2002.
- [68] Y. Li, R. Lipowsky, and R. Dimova, “Transition from Complete to Partial Wetting within Membrane Compartments,” *Journal of the American Chemical Society*, vol. 130, no. 37, pp. 12252–12253, 2008.
- [69] R. Lipowsky, “Response of Membranes and Vesicles to Capillary Forces Arising from Aqueous Two-Phase Systems and Water-in-Water Droplets,” *The Journal of Physical Chemistry B*, vol. 122, no. 13, pp. 3572–3586, 2018.
- [70] H. Kusumaatmaja, A. I. May, M. Feeney, J. F. McKenna, N. Mizushima, L. Frigerio, and R. L. Knorr, “Wetting of phase-separated droplets on plant vacuole membranes leads to a competition between tonoplast budding and nanotube formation,” *Proceedings of the National Academy of Sciences*, vol. 118, no. 36, p. e2024109118, 2021.
- [71] S. Botterbusch and T. Baumgart, “Interactions between Phase-Separated Liquids and Membrane Surfaces,” *Applied Sciences*, vol. 11, no. 3, p. 1288, 2021.
- [72] A. Mangiarotti, N. Chen, Z. Zhao, R. Lipowsky, and R. Dimova, “Wetting and complex remodeling of membranes by biomolecular condensates,” *Nature Communications*, vol. 14, no. 1, p. 2809, 2023.
- [73] Y. Lee, S. Park, F. Yuan, C. C. Hayden, L. Wang, E. M. Lafer, S. Q. Choi, and J. C. Stachowiak, “Transmembrane coupling of liquid-like protein condensates,” *Nature Communications*, vol. 14, no. 1, p. 8015, 2023.
- [74] D. Sun, X. Zhao, T. Wiegand, G. Bartolucci, C. Martin-Lemaitre, S. W. Grill, A. A. Hyman, C. Weber, and A. Honigmann, “Assembly of tight junction belts by surface condensation and actin elongation,” *bioRxiv*, 2023.

- [75] G. Paccione, M. Robles-Ramos, C. Alfonso, M. Sobrinos-Sanguino, W. Margolin, S. Zorrilla, B. Monterroso, and G. Rivas, “Lipid Surfaces and Glutamate Anions Enhance Formation of Dynamic Biomolecular Condensates Containing Bacterial Cell Division Protein FtsZ and Its DNA-Bound Regulator SlmA,” *Biochemistry*, vol. 61, no. 22, pp. 2482–2489, 2022.
- [76] H.-Y. Wang, S. H. Chan, S. Dey, I. Castello-Serrano, M. K. Rosen, J. A. Ditlev, K. R. Levental, and I. Levental, “Coupling of protein condensates to ordered lipid domains determines functional membrane organization,” *Science Advances*, vol. 9, no. 17, p. eadf6205, 2023.
- [77] C. C. Vequi-Suplicy, K. A. Riske, R. L. Knorr, and R. Dimova, “Vesicles with charged domains,” *Biochimica et Biophysica Acta*, vol. 1798, no. 7, pp. 1338–1347, 2010.
- [78] M. C. Blosser, J. B. Starr, C. W. Turtle, J. Ashcraft, and S. L. Keller, “Minimal effect of lipid charge on membrane miscibility phase behavior in three ternary systems,” *Biophysical Journal*, vol. 104, no. 12, pp. 2629–2638, 2013.
- [79] L. Babl, A. Merino-Salomón, N. Kanwa, and P. Schwille, “Membrane mediated phase separation of the bacterial nucleoid occlusion protein Noc,” *Scientific Reports*, vol. 12, no. 1, p. 17949, 2022.
- [80] A. T. Hammond, F. A. Heberle, T. Baumgart, D. Holowka, B. Baird, and G. W. Feigenson, “Crosslinking a lipid raft component triggers liquid ordered-liquid disordered phase separation in model plasma membranes,” *Proceedings of the National Academy of Sciences*, vol. 102, no. 18, pp. 6320–6325, 2005.
- [81] B. B. Machta, E. Gray, M. Nouri, N. L. C. McCarthy, E. M. Gray, A. L. Miller, N. J. Brooks, and S. L. Veatch, “Conditions that Stabilize Membrane Domains Also Antagonize n-Alcohol Anesthesia,” *Biophysical Journal*, vol. 111, no. 3, pp. 537–545, 2016.
- [82] C. E. Cornell, N. L. C. McCarthy, K. R. Levental, I. Levental, N. J. Brooks, and S. L. Keller, “n-Alcohol Length Governs Shift in Lo-Ld Mixing Temperatures in Synthetic and Cell-Derived Membranes,” *Biophysical Journal*, vol. 113, no. 6, pp. 1200–1211, 2017.
- [83] S. S. W. Leung and J. Thewalt, “Link between Fluorescent Probe Partitioning and Molecular Order of Liquid Ordered-Liquid Disordered Membranes,” *The Journal of Physical Chemistry B*, vol. 121, no. 6, pp. 1176–1185, 2017.

- [84] A. P. Liu and D. A. Fletcher, “Actin Polymerization Serves as a Membrane Domain Switch in Model Lipid Bilayers,” *Biophysical Journal*, vol. 91, no. 11, pp. 4064–4070, 2006.
- [85] A. Mangiarotti, M. Siri, N. W. Tam, Z. Zhao, L. Malacrida, and R. Dimova, “Biomolecular condensates modulate membrane lipid packing and hydration,” *Nature Communications*, vol. 14, no. 1, p. 6081, 2023.
- [86] I.-H. Lee, M. Y. Imanaka, E. H. Modahl, and A. P. Torres-Ocampo, “Lipid Raft Phase Modulation by Membrane-Anchored Proteins with Inherent Phase Separation Properties,” *ACS Omega*, vol. 4, no. 4, pp. 6551–6559, 2019.
- [87] J. K. Chung, W. Y. C. Huang, C. B. Carbone, L. M. Nocka, A. N. Parikh, R. D. Vale, and J. T. Groves, “Coupled membrane lipid miscibility and phosphotyrosine-driven protein condensation phase transitions,” *Biophysical Journal*, vol. 120, no. 7, p. 1257, 2021.
- [88] F. Yuan, H. Alimohamadi, B. Bakka, A. N. Trementozzi, K. J. Day, N. L. Fawzi, P. Rangamani, and J. C. Stachowiak, “Membrane bending by protein phase separation,” *Proceedings of the National Academy of Sciences*, vol. 118, no. 11, 2021.
- [89] J. Ureña, A. Knight, and I.-H. Lee, “Membrane Cargo Density-Dependent Interaction between Protein and Lipid Domains on the Giant Unilamellar Vesicles,” *Langmuir*, vol. 38, no. 15, pp. 4702–4712, 2022.
- [90] Z. Liu, A. Yethiraj, and Q. Cui, “Sensitive and selective polymer condensation at membrane surface driven by positive co-operativity,” *Proceedings of the National Academy of Sciences*, vol. 120, no. 15, p. e2212516120, 2023.
- [91] C. S. Scheve, P. A. Gonzales, N. Momin, and J. C. Stachowiak, “Steric Pressure between Membrane-Bound Proteins Opposes Lipid Phase Separation,” *Journal of the American Chemical Society*, vol. 135, no. 4, pp. 1185–1188, 2013.
- [92] Z. I. Imam, L. E. Kenyon, A. Carrillo, I. Espinoza, F. Nagib, and J. C. Stachowiak, “Steric pressure among membrane-bound polymers opposes lipid phase separation,” *Langmuir*, vol. 32, no. 15, pp. 3774–3784, 2016.
- [93] R. Dimova and C. Marques, *The Giant Vesicle Book*. CRC Press, Taylor & Francis Group, 2019.
- [94] U. Mennicke and T. Salditt, “Preparation of Solid-Supported Lipid Bilayers by Spin-Coating,” *Langmuir*, vol. 18, no. 21, pp. 8172–8177, 2002.

- [95] P. Lenz, C. M. Ajo-Franklin, and S. G. Boxer, "Patterned supported lipid bilayers and monolayers on poly(dimethylsiloxane)," *Langmuir*, vol. 20, no. 25, pp. 11092–11099, 2004.
- [96] M. Montal and P. Mueller, "Formation of Bimolecular Membranes from Lipid Monolayers and a Study of Their Electrical Properties," *Proceedings of the National Academy of Sciences*, vol. 69, no. 12, pp. 3561–3566, 1972.
- [97] H.-R. Lee, Y. Lee, S. S. Oh, and S. Q. Choi, "Ultra-Stable Freestanding Lipid Membrane Array: Direct Visualization of Dynamic Membrane Remodeling with Cholesterol Transport and Enzymatic Reactions," *Small*, vol. 16, no. 40, p. 2002541, 2020.
- [98] A.-S. Cans, M. Andes-Koback, and C. D. Keating, "Positioning Lipid Membrane Domains in Giant Vesicles by Micro-organization of Aqueous Cytoplasm Mimic," *Journal of the American Chemical Society*, vol. 130, no. 23, pp. 7400–7406, 2008.
- [99] C. Love, J. Steinkühler, D. T. Gonzales, N. Yandrapalli, T. Robinson, R. Dimova, and T.-Y. D. Tang, "Reversible pH-Responsive Coacervate Formation in Lipid Vesicles Activates Dormant Enzymatic Reactions," *Angewandte Chemie International Edition*, vol. 59, no. 15, pp. 5950–5957, 2020.
- [100] J. Zhao, J. Wu, and S. L. Veatch, "Adhesion Stabilizes Robust Lipid Heterogeneity in Supercritical Membranes at Physiological Temperature," *Biophysical Journal*, vol. 104, no. 4, pp. 825–834, 2013.
- [101] V. D. Gordon, M. Deserno, C. M. J. Andrew, S. U. Egelhaaf, and W. C. K. Poon, "Adhesion promotes phase separation in mixed-lipid membranes," *Europhysics Letters*, vol. 84, no. 4, p. 48003, 2008.
- [102] S. L. Veatch, "Electro-formation and fluorescence microscopy of giant vesicles with co-existing liquid phases," *Methods in Molecular Biology (Clifton, N.J.)*, vol. 398, pp. 59–72, 2007.
- [103] T. P. d. Souza, G. V. Bossa, P. Stano, F. Steiniger, S. May, P. L. Luisi, and A. Fahr, "Vesicle aggregates as a model for primitive cellular assemblies," *Physical Chemistry Chemical Physics*, vol. 19, no. 30, pp. 20082–20092, 2017.
- [104] S. W. Hui, T. L. Kuhl, Y. Q. Guo, and J. Israelachvili, "Use of poly(ethylene glycol) to control cell aggregation and fusion," *Colloids and Surfaces B: Biointerfaces*, vol. 14, no. 1, pp. 213–222, 1999.

- [105] R. Lipowsky, “Spontaneous tubulation of membranes and vesicles reveals membrane tension generated by spontaneous curvature,” *Faraday Discussions*, vol. 161, no. 0, pp. 305–331, 2012.
- [106] T. Bhatia, T. Robinson, and R. Dimova, “Membrane permeability to water measured by microfluidic trapping of giant vesicles,” *Soft Matter*, vol. 16, no. 31, pp. 7359–7369, 2020.
- [107] M. Rahimi, D. Regan, M. Arroyo, A. B. Subramaniam, H. A. Stone, and M. Staykova, “Shape Transformations of Lipid Bilayers Following Rapid Cholesterol Uptake,” *Biophysical Journal*, vol. 111, no. 12, pp. 2651–2657, 2016.
- [108] M. Staykova, D. P. Holmes, C. Read, and H. A. Stone, “Mechanics of surface area regulation in cells examined with confined lipid membranes,” *Proceedings of the National Academy of Sciences of the United States of America*, vol. 108, no. 22, pp. 9084–9088, 2011.
- [109] J. C. Stachowiak, C. C. Hayden, and D. Y. Sasaki, “Steric confinement of proteins on lipid membranes can drive curvature and tubulation,” *Proceedings of the National Academy of Sciences of the United States of America*, vol. 107, no. 17, pp. 7781–7786, 2010.
- [110] B. Sorre, A. Callan-Jones, J. Manzi, B. Goud, J. Prost, P. Bassereau, and A. Roux, “Nature of curvature coupling of amphiphysin with membranes depends on its bound density,” *Proceedings of the National Academy of Sciences*, vol. 109, no. 1, pp. 173–178, 2012.
- [111] N. Rodriguez, F. Pincet, and S. Cribier, “Giant vesicles formed by gentle hydration and electroformation: A comparison by fluorescence microscopy,” *Colloids and Surfaces B: Biointerfaces*, vol. 42, no. 2, pp. 125–130, 2005.
- [112] A. Roux, D. Cuvelier, P. Nassoy, J. Prost, P. Bassereau, and B. Goud, “Role of curvature and phase transition in lipid sorting and fission of membrane tubules,” *The EMBO Journal*, vol. 24, no. 8, pp. 1537–1545, 2005.
- [113] M. Heinrich, A. Tian, C. Esposito, and T. Baumgart, “Dynamic sorting of lipids and proteins in membrane tubes with a moving phase boundary,” *Proceedings of the National Academy of Sciences*, vol. 107, no. 16, pp. 7208–7213, 2010.
- [114] R. Parthasarathy, C. H. Yu, and J. T. Groves, “Curvature-modulated phase separation in lipid bilayer membranes,” *Langmuir*, vol. 22, no. 11, pp. 5095–5099, 2006.

- [115] C. Prévost, H. Zhao, J. Manzi, E. Lemichez, P. Lappalainen, A. Callan-Jones, and P. Bassereau, “IRSp53 senses negative membrane curvature and phase separates along membrane tubules,” *Nature Communications*, vol. 6, no. 1, p. 8529, 2015.
- [116] T. Portet, S. E. Gordon, and S. L. Keller, “Increasing Membrane Tension Decreases Miscibility Temperatures; an Experimental Demonstration via Micropipette Aspiration,” *Biophysical Journal*, vol. 103, no. 8, pp. L35–L37, 2012.
- [117] A. G. Ayuyan and F. S. Cohen, “Raft Composition at Physiological Temperature and pH in the Absence of Detergents,” *Biophysical Journal*, vol. 94, no. 7, pp. 2654–2666, 2008.
- [118] T. Hamada, Y. Kishimoto, T. Nagasaki, and M. Takagi, “Lateral phase separation in tense membranes,” *Soft Matter*, vol. 7, no. 19, pp. 9061–9068, 2011.
- [119] K. Oglecka, P. Rangamani, B. Liedberg, R. S. Kraut, and A. N. Parikh, “Oscillatory phase separation in giant lipid vesicles induced by transmembrane osmotic differentials,” *eLife*, vol. 3, p. e03695, 2014.
- [120] Y. Sakuma, T. Taniguchi, T. Kawakatsu, and M. Imai, “Tubular Membrane Formation of Binary Giant Unilamellar Vesicles Composed of Cylinder and Inverse-Cone-Shaped Lipids,” *Biophysical Journal*, vol. 105, no. 9, pp. 2074–2081, 2013.
- [121] J. Steinkühler, P. De Tillieux, R. L. Knorr, R. Lipowsky, and R. Dimova, “Charged giant unilamellar vesicles prepared by electroformation exhibit nanotubes and transbilayer lipid asymmetry,” *Scientific Reports*, vol. 8, no. 1, p. 11838, 2018.
- [122] S. K. Lim, P. Rangamani, M. Nallani, A. S. W. Wong, H.-P. M. d. Hoog, A. N. Parikh, M. Nallani, Sandin, Sara, and Liedberg, Bo, “Spontaneous formation of nanometer scale tubular vesicles in aqueous mixtures of lipid and block copolymer amphiphiles,” *Soft Matter*, vol. 13, no. 6, pp. 1107–1115, 2017.
- [123] E. L. Talbot, J. Kotar, L. D. Michele, and P. Cicuta, “Directed tubule growth from giant unilamellar vesicles in a thermal gradient,” *Soft Matter*, vol. 15, no. 7, pp. 1676–1683, 2019.
- [124] N. Khalifat, M. Rahimi, A.-F. Bitbol, M. Seigneuret, J.-B. Fournier, N. Puff, M. Arroyo, and M. I. Angelova, “Interplay of Packing and Flip-flop in Local Bilayer Deformation. How Phosphatidylglycerol Could Rescue Mitochondrial Function in a Cardiolipin-deficient Yeast Mutant,” *Biophysical Journal*, vol. 107, no. 4, pp. 879–890, 2014.

- [125] C. van der Wel, D. Heinrich, and D. J. Kraft, “Microparticle Assembly Pathways on Lipid Membranes,” *Biophysical Journal*, vol. 113, no. 5, pp. 1037–1046, 2017.
- [126] M. Karimi, J. Steinkühler, D. Roy, R. Dasgupta, R. Lipowsky, and R. Dimova, “Asymmetric Ionic Conditions Generate Large Membrane Curvatures,” *Nano Letters*, vol. 18, no. 12, pp. 7816–7821, 2018.
- [127] N. A. Schenk, P. J. Dahl, M. G. Hanna, A. Audhya, G. G. Tall, J. D. Knight, and A. Anantharam, “A simple supported tubulated bilayer system for evaluating protein-mediated membrane remodeling,” *Chemistry and physics of lipids*, vol. 215, pp. 18–28, 2018.
- [128] Y. Liu, J. Agudo-Canalejo, A. Grafmüller, R. Dimova, and R. Lipowsky, “Patterns of Flexible Nanotubes Formed by Liquid-Ordered and Liquid-Disordered Membranes,” *ACS Nano*, vol. 10, no. 1, pp. 463–474, 2016.
- [129] R. Dasgupta, M. S. Miettinen, N. Fricke, R. Lipowsky, and R. Dimova, “The glycolipid GM1 reshapes asymmetric biomembranes and giant vesicles by curvature generation,” *Proceedings of the National Academy of Sciences*, vol. 115, no. 22, pp. 5756–5761, 2018.
- [130] D. Thid, J. J. Benkoski, S. Svedhem, B. Kasemo, and J. Gold, “DHA-induced changes of supported lipid membrane morphology,” *Langmuir: the ACS journal of surfaces and colloids*, vol. 23, no. 11, pp. 5878–5881, 2007.
- [131] B. K. Yoon, J. A. Jackman, M. C. Kim, and N.-J. Cho, “Spectrum of Membrane Morphological Responses to Antibacterial Fatty Acids and Related Surfactants,” *Langmuir*, vol. 31, no. 37, pp. 10223–10232, 2015.
- [132] H. G. Franquelim, A. Khmelinskaia, J.-P. Sobczak, H. Dietz, and P. Schwille, “Membrane sculpting by curved DNA origami scaffolds,” *Nature Communications*, vol. 9, no. 1, p. 811, 2018.
- [133] H. G. Franquelim, H. Dietz, and P. Schwille, “Reversible membrane deformations by straight DNA origami filaments,” *Soft Matter*, vol. 17, no. 2, pp. 276–287, 2021.
- [134] Y. A. Domanov and P. K. J. Kinnunen, “Antimicrobial Peptides Temporins B and L Induce Formation of Tubular Lipid Protrusions from Supported Phospholipid Bilayers,” *Biophysical Journal*, vol. 91, no. 12, pp. 4427–4439, 2006.
- [135] A. Arouri, V. Kiessling, L. Tamm, M. Dathe, and A. Blume, “Morphological Changes Induced by the Action of Antimicrobial Peptides on Supported Lipid Bilayers,” *The Journal of Physical Chemistry B*, vol. 115, no. 1, pp. 158–167, 2011.

- [136] W. T. Snead, W. F. Zeno, G. Kago, R. W. Perkins, J. B. Richter, C. Zhao, E. M. Lafer, and J. C. Stachowiak, “BAR scaffolds drive membrane fission by crowding disordered domains,” *Journal of Cell Biology*, vol. 218, no. 2, pp. 664–682, 2018.
- [137] F. Yuan, C. T. Lee, A. Sangani, J. R. Houser, L. Wang, E. M. Lafer, P. Rangamani, and J. C. Stachowiak, “The ins and outs of membrane bending by intrinsically disordered proteins,” *Science Advances*, vol. 9, no. 27, p. eadg3485, 2023.
- [138] A. Yamada, S. Lee, P. Bassereau, and C. N. Baroud, “Trapping and release of giant unilamellar vesicles in microfluidic wells,” *Soft Matter*, vol. 10, no. 32, pp. 5878–5885, 2014.
- [139] T. Robinson, “Microfluidic Handling and Analysis of Giant Vesicles for Use as Artificial Cells: A Review,” *Advanced Biosystems*, vol. 3, no. 6, p. e1800318, 2019.
- [140] M. J. Sarmiento, M. Prieto, and F. Fernandes, “Reorganization of lipid domain distribution in giant unilamellar vesicles upon immobilization with different membrane tethers,” *Biochimica et Biophysica Acta*, vol. 1818, no. 11, pp. 2605–2615, 2012.
- [141] T. Robinson and P. S. Dittrich, “Observations of Membrane Domain Reorganization in Mechanically Compressed Artificial Cells,” *ChemBioChem*, vol. 20, no. 20, pp. 2666–2673, 2019.
- [142] J. Steinkühler, R. L. Knorr, Z. Zhao, T. Bhatia, S. M. Bartelt, S. Wegner, R. Dimova, and R. Lipowsky, “Controlled division of cell-sized vesicles by low densities of membrane-bound proteins,” *Nature Communications*, vol. 11, no. 1, p. 905, 2020.
- [143] C. A. Stanich, A. R. Honerkamp-Smith, G. G. Putzel, C. S. Warth, A. K. Lamprecht, P. Mandal, E. Mann, T.-A. D. Hua, and S. L. Keller, “Coarsening Dynamics of Domains in Lipid Membranes,” *Biophysical Journal*, vol. 105, no. 2, pp. 444–454, 2013.
- [144] H. A. Stone and A. Ajdari, “Hydrodynamics of particles embedded in a flat surfactant layer overlying a subphase of finite depth,” *Journal of Fluid Mechanics*, vol. 369, pp. 151–173, 1998.
- [145] Y. Kaizuka and J. T. Groves, “Structure and Dynamics of Supported Intermembrane Junctions,” *Biophysical Journal*, vol. 86, no. 2, pp. 905–912, 2004.
- [146] B. L. Stottrup, S. L. Veatch, and S. L. Keller, “Nonequilibrium Behavior in Supported Lipid Membranes Containing Cholesterol,” *Biophysical Journal*, vol. 86, no. 5, pp. 2942–2950, 2004.

- [147] K. J. Seu, A. P. Pandey, F. Haque, E. A. Proctor, A. E. Ribbe, and J. S. Hovis, “Effect of Surface Treatment on Diffusion and Domain Formation in Supported Lipid Bilayers,” *Biophysical Journal*, vol. 92, no. 7, pp. 2445–2450, 2007.
- [148] A. Honigmann, C. Walter, F. Erdmann, C. Eggeling, and R. Wagner, “Characterization of horizontal lipid bilayers as a model system to study lipid phase separation,” *Biophysical Journal*, vol. 98, no. 12, pp. 2886–2894, 2010.
- [149] A. V. Samsonov, I. Mihalyov, and F. S. Cohen, “Characterization of cholesterol-sphingomyelin domains and their dynamics in bilayer membranes,” *Biophysical Journal*, vol. 81, no. 3, pp. 1486–1500, 2001.
- [150] M. D. Collins and S. L. Keller, “Tuning lipid mixtures to induce or suppress domain formation across leaflets of unsupported asymmetric bilayers,” *Proceedings of the National Academy of Sciences*, vol. 105, no. 1, pp. 124–128, 2008.
- [151] K. Funakoshi, H. Suzuki, and S. Takeuchi, “Lipid Bilayer Formation by Contacting Monolayers in a Microfluidic Device for Membrane Protein Analysis,” *Analytical Chemistry*, vol. 78, no. 24, pp. 8169–8174, 2006.
- [152] J. S. H. Danial, B. Cronin, C. Mallik, and M. I. Wallace, “On demand modulation of lipid composition in an individual bilayer,” *Soft Matter*, vol. 13, no. 9, pp. 1788–1793, 2017.
- [153] S. R. Kirchner, A. Ohlinger, T. Pfeiffer, A. S. Urban, F. D. Stefani, A. Deak, A. A. Lutich, and J. Feldmann, “Membrane composition of jetted lipid vesicles: a Raman spectroscopy study,” *Journal of Biophotonics*, vol. 5, no. 1, pp. 40–46, 2012.
- [154] J. C. Stachowiak, D. L. Richmond, T. H. Li, A. P. Liu, S. H. Parekh, and D. A. Fletcher, “Unilamellar vesicle formation and encapsulation by microfluidic jetting,” *Proceedings of the National Academy of Sciences*, vol. 105, no. 12, pp. 4697–4702, 2008.
- [155] D. L. Richmond, E. M. Schmid, S. Martens, J. C. Stachowiak, N. Liska, and D. A. Fletcher, “Forming giant vesicles with controlled membrane composition, asymmetry, and contents,” *Proceedings of the National Academy of Sciences*, vol. 108, no. 23, pp. 9431–9436, 2011.
- [156] R. S. Gunderson and A. R. Honerkamp-Smith, “Liquid-liquid phase transition temperatures increase when lipid bilayers are supported on glass,” *Biochimica et Biophysica Acta*, vol. 1860, no. 10, pp. 1965–1971, 2018.

- [157] A. B. Subramaniam, G. Guidotti, V. N. Manoharan, and H. A. Stone, “Glycans pattern the phase behaviour of lipid membranes,” *Nature Materials*, vol. 12, no. 2, pp. 128–133, 2013.
- [158] M. B. Klenow, J. C. Jeppesen, and A. C. Simonsen, “Membrane rolling induced by bacterial toxins,” *Soft Matter*, vol. 16, no. 6, pp. 1614–1626, 2020.
- [159] M. Chung, R. D. Lowe, Y.-H. M. Chan, P. V. Ganesan, and S. G. Boxer, “DNA-tethered membranes formed by giant vesicle rupture,” *Journal of Structural Biology*, vol. 168, no. 1, pp. 190–199, 2009.
- [160] M. Chung and S. G. Boxer, “Stability of DNA-Tethered Lipid Membranes with Mobile Tethers,” *Langmuir*, vol. 27, no. 9, pp. 5492–5497, 2011.
- [161] Y. Kaizuka and J. T. Groves, “Bending-mediated superstructural organizations in phase-separated lipid membranes,” *New Journal of Physics*, vol. 12, no. 9, p. 095001, 2010.
- [162] M. H. Jensen, E. J. Morris, and A. C. Simonsen, “Domain Shapes, Coarsening, and Random Patterns in Ternary Membranes,” *Langmuir*, vol. 23, no. 15, pp. 8135–8141, 2007.
- [163] K. Yokota, A. Toyoki, K. Yamazaki, and T. Ogino, “Behavior of raft-like domain in stacked structures of ternary lipid bilayers prepared by self-spreading method,” *Japanese Journal of Applied Physics*, vol. 53, no. 5S1, p. 05FA11, 2014.
- [164] F. Roder, O. Birkholz, O. Beutel, D. Paterok, and J. Piehler, “Spatial Organization of Lipid Phases in Micropatterned Polymer-Supported Membranes,” *Journal of the American Chemical Society*, vol. 135, no. 4, pp. 1189–1192, 2013.
- [165] O. Purruicker, A. Förtig, R. Jordan, and M. Tanaka, “Supported Membranes with Well-Defined Polymer Tethers—Incorporation of Cell Receptors,” *ChemPhysChem*, vol. 5, no. 3, pp. 327–335, 2004.
- [166] N. Bunjes, E. K. Schmidt, A. Jonczyk, F. Rippmann, D. Beyer, H. Ringsdorf, P. Gräber, W. Knoll, and R. Naumann, “Thiopeptide-Supported Lipid Layers on Solid Substrates,” *Langmuir*, vol. 13, no. 23, pp. 6188–6194, 1997.
- [167] A. B. Subramaniam, S. Lecuyer, K. S. Ramamurthi, R. Losick, and H. A. Stone, “Particle/Fluid Interface Replication as a Means of Producing Topographically Patterned Polydimethylsiloxane Surfaces for Deposition of Lipid Bilayers,” *Advanced Materials*, vol. 22, no. 19, pp. 2142–2147, 2010.

- [168] E. J. Miller, K. Voitchovsky, and M. Staykova, “Substrate-led cholesterol extraction from supported lipid membranes,” *Nanoscale*, vol. 10, no. 34, pp. 16332–16342, 2018.
- [169] L. Feriani, L. Cristofolini, and P. Cicuta, “Soft pinning of liquid domains on topographical hemispherical caps,” *Chemistry and Physics of Lipids*, vol. 185, pp. 78–87, 2015.
- [170] M. Rinaldin, S. L. D. ten Haaf, E. J. Vegter, C. van der Wel, P. Fonda, L. Giomi, and D. J. Kraft, “Supported lipid membranes with designed geometry,” 2021.
- [171] T.-Y. Yoon, B. Okumus, F. Zhang, Y.-K. Shin, and T. Ha, “Multiple intermediates in SNARE-induced membrane fusion,” *Proceedings of the National Academy of Sciences*, vol. 103, no. 52, pp. 19731–19736, 2006.
- [172] K. A. Runas and N. Malmstadt, “Low levels of lipid oxidation radically increase the passive permeability of lipid bilayers,” *Soft Matter*, vol. 11, no. 3, pp. 499–505, 2014.
- [173] J. Litz, N. Thakkar, T. Portet, and S. Keller, “Depletion with Cyclodextrin Reveals Two Populations of Cholesterol in Model Lipid Membranes,” *Biophysical Journal*, vol. 110, no. 3, pp. 635–645, 2016.
- [174] P. M. Bendix, M. S. Pedersen, and D. Stamou, “Quantification of nano-scale inter-membrane contact areas by using fluorescence resonance energy transfer,” *Proceedings of the National Academy of Sciences*, vol. 106, no. 30, pp. 12341–12346, 2009.
- [175] K. A. Runas, S. J. Acharya, J. J. Schmidt, and N. Malmstadt, “Addition of Cleaved Tail Fragments during Lipid Oxidation Stabilizes Membrane Permeability Behavior,” *Langmuir*, vol. 32, no. 3, pp. 779–786, 2016.
- [176] C. M. Ajo-Franklin, C. Yoshina-Ishii, and S. G. Boxer, “Probing the Structure of Supported Membranes and Tethered Oligonucleotides by Fluorescence Interference Contrast Microscopy,” *Langmuir*, vol. 21, no. 11, pp. 4976–4983, 2005.
- [177] D. J. Estes and M. Mayer, “Giant liposomes in physiological buffer using electroformation in a flow chamber,” *Biochimica et Biophysica Acta*, vol. 1712, no. 2, pp. 152–160, 2005.
- [178] S. Knecht, D. Ricklin, A. N. Eberle, and B. Ernst, “Oligohis-tags: mechanisms of binding to Ni²⁺-NTA surfaces,” *Journal of Molecular Recognition*, vol. 22, no. 4, pp. 270–279, 2009.

- [179] C. C. Hayden, J. S. Hwang, E. A. Abate, M. S. Kent, and D. Y. Sasaki, “Directed Formation of Lipid Membrane Microdomains as High Affinity Sites for His-Tagged Proteins,” *Journal of the American Chemical Society*, vol. 131, no. 25, pp. 8728–8729, 2009.
- [180] Z. Feng, X. Chen, X. Wu, and M. Zhang, “Formation of biological condensates via phase separation: Characteristics, analytical methods, and physiological implications,” *The Journal of Biological Chemistry*, vol. 294, no. 40, pp. 14823–14835, 2019.
- [181] J. W. Yu, J. M. Mendrola, A. Audhya, S. Singh, D. Keleti, D. B. DeWald, D. Murray, S. D. Emr, and M. A. Lemmon, “Genome-Wide Analysis of Membrane Targeting by *S. cerevisiae* Pleckstrin Homology Domains,” *Molecular Cell*, vol. 13, no. 5, pp. 677–688, 2004.
- [182] K. Carvalho, L. Ramos, C. Roy, and C. Picart, “Giant Unilamellar Vesicles Containing Phosphatidylinositol(4,5)bispophosphate: Characterization and Functionality,” *Biophysical Journal*, vol. 95, no. 9, pp. 4348–4360, 2008.
- [183] Y.-H. Wang, A. Collins, L. Guo, K. B. Smith-Dupont, F. Gai, T. Svitkina, and P. A. Janmey, “Divalent Cation-Induced Cluster Formation by Polyphosphoinositides in Model Membranes,” *Journal of the American Chemical Society*, vol. 134, no. 7, pp. 3387–3395, 2012.
- [184] S. Shukla, R. Jin, J. Robustelli, Z. E. Zimmerman, and T. Baumgart, “PIP2 Reshapes Membranes through Asymmetric Desorption,” *Biophysical Journal*, vol. 117, no. 5, pp. 962–974, 2019.
- [185] M. S. Long, C. D. Jones, M. R. Helfrich, L. K. Mangeney-Slavin, and C. D. Keating, “Dynamic microcompartmentation in synthetic cells,” *Proceedings of the National Academy of Sciences of the United States of America*, vol. 102, no. 17, pp. 5920–5925, 2005.
- [186] S. S. Bordovsky, C. S. Wong, G. D. Bachand, J. C. Stachowiak, and D. Y. Sasaki, “Engineering Lipid Structure for Recognition of the Liquid Ordered Membrane Phase,” *Langmuir*, vol. 32, no. 47, pp. 12527–12533, 2016.
- [187] K. Edwards, M. Johnsson, G. Karlsson, and M. Silvander, “Effect of polyethyleneglycol-phospholipids on aggregate structure in preparations of small unilamellar liposomes,” *Biophysical Journal*, vol. 73, no. 1, pp. 258–266, 1997.
- [188] A. R. Strom, A. V. Emelyanov, M. Mir, D. V. Fyodorov, X. Darzacq, and G. H. Karpen, “Phase separation drives heterochromatin domain formation,” *Nature*, vol. 547, no. 7662, pp. 241–245, 2017.

- [189] R. Oshidari, R. Huang, M. Medghalchi, E. Y. W. Tse, N. Ashgriz, H. O. Lee, H. Wyatt, and K. Mekhail, “DNA repair by Rad52 liquid droplets,” *Nature Communications*, vol. 11, no. 1, p. 695, 2020.
- [190] S. Kilic, A. Lezaja, M. Gatti, E. Bianco, J. Michelena, R. Imhof, and M. Altmeyer, “Phase separation of 53BP1 determines liquid-like behavior of DNA repair compartments,” *The EMBO Journal*, vol. 38, no. 16, p. e101379, 2019.
- [191] P. A. Beales and T. K. Vanderlick, “Partitioning of Membrane-Anchored DNA between Coexisting Lipid Phases,” *The Journal of Physical Chemistry B*, vol. 113, no. 42, pp. 13678–13686, 2009.
- [192] R. Rubio-Sánchez, S. E. Barker, M. Walczak, P. Cicuta, and L. D. Michele, “A Modular, Dynamic, DNA-Based Platform for Regulating Cargo Distribution and Transport between Lipid Domains,” *Nano Letters*, vol. 21, no. 7, pp. 2800–2808, 2021.
- [193] Y. Bagheri, A. A. Ali, P. Keshri, J. Chambers, A. Gershenson, and M. You, “Imaging Membrane Order and Dynamic Interactions in Living Cells with a DNA Zipper Probe,” *Angewandte Chemie International Edition*, vol. 61, no. 6, p. e202112033, 2022.
- [194] E. P. Diamandis and T. K. Christopoulos, “The biotin-(strept)avidin system: principles and applications in biotechnology,” *Clinical Chemistry*, vol. 37, no. 5, pp. 625–636, 1991.
- [195] S. Chiruvolu, S. Walker, J. Israelachvili, F. J. Schmitt, D. Leckband, and J. A. Zasadzinski, “Higher order self-assembly of vesicles by site-specific binding,” *Science*, vol. 264, no. 5166, pp. 1753–1756, 1994.
- [196] S. A. Walker and J. A. Zasadzinski, “Electrostatic Control of Spontaneous Vesicle Aggregation,” *Langmuir*, vol. 13, no. 19, pp. 5076–5081, 1997.
- [197] N. Momin, S. Lee, A. K. Gadok, D. J. Busch, G. D. Bachand, C. C. Hayden, J. C. Stachowiak, and D. Y. Sasaki, “Designing lipids for selective partitioning into liquid ordered membrane domains,” *Soft Matter*, vol. 11, no. 16, pp. 3241–3250, 2015.
- [198] K. You, Q. Huang, C. Yu, B. Shen, C. Sevilla, M. Shi, H. Hermjakob, Y. Chen, and T. Li, “PhaSepDB: a database of liquid–liquid phase separation related proteins,” *Nucleic Acids Research*, vol. 48, no. D1, pp. D354–D359, 2020.
- [199] K. M. Ruff, S. Roberts, A. Chilkoti, and R. V. Pappu, “Advances in Understanding Stimulus-Responsive Phase Behavior of Intrinsically Disordered Protein Polymers,” *Journal of Molecular Biology*, vol. 430, no. 23, pp. 4619–4635, 2018.

- [200] Y. Bagheri, M. Rouches, B. B. Machta, and S. L. Veatch, “Experimental investigations of coupled polymer and membrane phase transitions,” *Biophysical Journal*, vol. 122, no. 3, p. 78a, 2023.
- [201] H. M. J. Weakly, K. J. Wilson, G. J. Goetz, E. L. Pruitt, A. Li, L. Xu, and S. L. Keller, “Common methods of making giant vesicles (except emulsion techniques) capture intended lipid ratios,” *bioRxiv*, 2024.
- [202] F. Olson, C. A. Hunt, F. C. Szoka, W. J. Vail, and D. Papahadjopoulos, “Preparation of liposomes of defined size distribution by extrusion through polycarbonate membranes,” *BBA - Biomembranes*, vol. 557, no. 1, pp. 9–23, 1979.
- [203] S. Sugiura, T. Kuroiwa, T. Kagota, M. Nakajima, S. Sato, S. Mukataka, P. Walde, and S. Ichikawa, “Novel Method for Obtaining Homogeneous Giant Vesicles from a Monodisperse Water-in-Oil Emulsion Prepared with a Microfluidic Device,” *Langmuir*, vol. 24, no. 9, pp. 4581–4588, 2008.
- [204] T. F. Zhu and J. W. Szostak, “Preparation of Large Monodisperse Vesicles,” *PLoS ONE*, vol. 4, no. 4, p. e5009, 2009.
- [205] Angelova, M.I., *Lipid Swelling and Liposome Formation in Electric Fields*. PhD Thesis, Institute of Biophysics, Bulgarian Academy of Sciences, Sofia, 1988.
- [206] S. E. Ghellab, Q. Li, T. Fuhs, H. Bi, and X. Han, “Electroformation of double vesicles using an amplitude modulated electric field,” *Colloids and Surfaces B: Biointerfaces*, vol. 160, pp. 697–703, 2017.
- [207] T. Ip, Q. Li, N. Brooks, and Y. Elani, “Manufacture of Multilayered Artificial Cell Membranes through Sequential Bilayer Deposition on Emulsion Templates,” *Chem-BioChem*, vol. 22, no. 13, pp. 2275–2281, 2021.
- [208] S. Pautot, B. J. Frisken, and D. A. Weitz, “Engineering asymmetric vesicles,” *Proceedings of the National Academy of Sciences*, vol. 100, no. 19, pp. 10718–10721, 2003.
- [209] Y. Elani, S. Purushothaman, P. J. Booth, J. M. Seddon, N. J. Brooks, R. V. Law, and O. Ces, “Measurements of the effect of membrane asymmetry on the mechanical properties of lipid bilayers,” *Chemical Communications*, vol. 51, no. 32, pp. 6976–6979, 2015.
- [210] M. Doktorova, F. A. Heberle, B. Eicher, R. F. Standaert, J. Katsaras, E. London, G. Pabst, and D. Marquardt, “Preparation of asymmetric phospholipid vesicles: The next generation of cell membrane models,” *Nature protocols*, vol. 13, no. 9, pp. 2086–2101, 2018.

- [211] K. Akashi, H. Miyata, H. Itoh, and K. Kinoshita, "Preparation of giant liposomes in physiological conditions and their characterization under an optical microscope," *Biophysical Journal*, vol. 71, no. 6, pp. 3242–3250, 1996.
- [212] L. M. Dominak and C. D. Keating, "Polymer Encapsulation within Giant Lipid Vesicles," *Langmuir*, vol. 23, no. 13, pp. 7148–7154, 2007.
- [213] M. Abkarian, E. Loiseau, and G. Massiera, "Continuous droplet interface crossing encapsulation (cDICE) for high throughput monodisperse vesicle design," *Soft Matter*, vol. 7, no. 10, pp. 4610–4614, 2011.
- [214] J. Huang, J. T. Buboltz, and G. W. Feigenson, "Maximum solubility of cholesterol in phosphatidylcholine and phosphatidylethanolamine bilayers," *BBA - Biomembranes*, vol. 1417, no. 1, pp. 89–100, 1999.
- [215] R. M. Epanand, D. W. Hughes, B. G. Sayer, N. Borochoy, D. Bach, and E. Wachtel, "Novel properties of cholesterol-dioleoylphosphatidylcholine mixtures," *Biochimica et biophysica acta*, vol. 1616, no. 2, pp. 196–208, 2003.
- [216] S. R. Shaikh, V. Cherezov, M. Caffrey, S. P. Soni, D. LoCasio, W. Stillwell, and S. R. Wassall, "Molecular Organization of Cholesterol in Unsaturated Phosphatidylethanolamines: X-ray Diffraction and Solid State ^2H NMR Reveal Differences with Phosphatidylcholines," *Journal of the American Chemical Society*, vol. 128, no. 16, pp. 5375–5383, 2006.
- [217] M. M. Stevens, A. R. Honerkamp-Smith, and S. L. Keller, "Solubility Limits of Cholesterol, Lanosterol, Ergosterol, Stigmasterol, and -Sitosterol in Electroformed Lipid Vesicles," *Soft matter*, vol. 6, no. 23, pp. 5882–5890, 2010.
- [218] M. Ibarguren, A. Alonso, B. G. Tenchov, and F. M. Goñi, "Quantitation of cholesterol incorporation into extruded lipid bilayers," *BBA - Biomembranes*, vol. 1798, no. 9, pp. 1735–1738, 2010.
- [219] M. Blosser, B. G. Horst, and S. L. Keller, "cDICE method produces giant lipid vesicles under physiological conditions of charged lipids and ionic solutions," *Soft Matter*, vol. 12, no. 35, pp. 7364–7371, 2016.
- [220] K. Karamdad, J. W. Hindley, G. Bolognesi, M. S. Friddin, R. V. Law, N. J. Brooks, O. Ces, and Y. Elani, "Engineering thermoresponsive phase separated vesicles formed via emulsion phase transfer as a content-release platform," *Chemical Science*, vol. 9, no. 21, pp. 4851–4858, 2018.

- [221] K. Dürre and A. R. Bausch, “Formation of phase separated vesicles by double layer cDICE,” *Soft Matter*, vol. 15, no. 47, pp. 9676–9681, 2019.
- [222] A. Gambhir, G. Hangyás-Mihályiné, I. Zaitseva, D. S. Cafiso, J. Wang, D. Murray, S. N. Pentylala, S. O. Smith, and S. McLaughlin, “Electrostatic Sequestration of PIP2 on Phospholipid Membranes by Basic/Aromatic Regions of Proteins,” *Biophysical Journal*, vol. 86, no. 4, pp. 2188–2207, 2004.
- [223] P. R. Cullis, M. J. Hope, and C. P. S. Tilcock, “Lipid polymorphism and the roles of lipids in membranes,” *Chemistry and Physics of Lipids*, vol. 40, no. 2, pp. 127–144, 1986.
- [224] J. N. van der Veen, J. P. Kennelly, S. Wan, J. E. Vance, D. E. Vance, and R. L. Jacobs, “The critical role of phosphatidylcholine and phosphatidylethanolamine metabolism in health and disease,” *BBA - Biomembranes*, vol. 1859, no. 9, Part B, pp. 1558–1572, 2017.
- [225] J. H. Lorent, K. R. Levental, L. Ganesan, G. Rivera-Longsworth, E. Sezgin, M. Doktorova, E. Lyman, and I. Levental, “Plasma membranes are asymmetric in lipid unsaturation, packing and protein shape,” *Nature Chemical Biology*, vol. 16, no. 6, pp. 644–652, 2020.
- [226] P. J. Brennan and H. Nikaido, “The Envelope of Mycobacteria,” *Annual Review of Biochemistry*, vol. 64, no. 1, pp. 29–63, 1995.
- [227] D. Marsh, *Handbook of Lipid Bilayers*. Boca Raton: CRC Press, 2 ed., 2013.
- [228] A. J. Verkleij, R. F. A. Zwaal, B. Roelofsen, P. Comfurius, D. Kastelijn, and L. L. M. van Deenen, “The asymmetric distribution of phospholipids in the human red cell membrane. A combined study using phospholipases and freeze-etch electron microscopy,” *BBA - Biomembranes*, vol. 323, no. 2, pp. 178–193, 1973.
- [229] S.-T. Yang, A. J. B. Kreutzberger, J. Lee, V. Kiessling, and L. K. Tamm, “The role of cholesterol in membrane fusion,” *Chemistry and Physics of Lipids*, vol. 199, pp. 136–143, 2016.
- [230] C. Dietrich, L. A. Bagatolli, Z. N. Volovyk, N. L. Thompson, M. Levi, K. Jacobson, and E. Gratton, “Lipid Rafts Reconstituted in Model Membranes,” *Biophysical Journal*, vol. 80, no. 3, pp. 1417–1428, 2001.
- [231] S. Pautot, B. J. Frisken, and D. A. Weitz, “Production of Unilamellar Vesicles Using an Inverted Emulsion,” *Langmuir*, vol. 19, no. 7, pp. 2870–2879, 2003.

- [232] D. S. Grusky, A. Bhattacharya, and S. G. Boxer, “Secondary Ion Mass Spectrometry of Single Giant Unilamellar Vesicles Reveals Compositional Variability,” *Journal of the American Chemical Society*, vol. 145, no. 50, pp. 27521–27530, 2023.
- [233] E. J. Findlay and P. G. Barton, “Phase behavior of synthetic phosphatidylglycerols and binary mixtures with phosphatidylcholines in the presence and absence of calcium ions,” *Biochemistry*, vol. 17, no. 12, pp. 2400–2405, 1978.
- [234] R. Koynova and M. Caffrey, “Phases and phase transitions of the hydrated phosphatidylethanolamines,” *Chemistry and Physics of Lipids*, vol. 69, no. 1, pp. 1–34, 1994.
- [235] A. Witkowska, L. Jablonski, and R. Jahn, “A convenient protocol for generating giant unilamellar vesicles containing SNARE proteins using electroformation,” *Scientific Reports*, vol. 8, no. 1, p. 9422, 2018.
- [236] A. Moga, N. Yandrapalli, R. Dimova, and T. Robinson, “Optimization of the Inverted Emulsion Method for High-Yield Production of Biomimetic Giant Unilamellar Vesicles,” *ChemBioChem*, vol. 20, no. 20, pp. 2674–2682, 2019.
- [237] E. G. Bligh and W. J. Dyer, “A rapid method of total lipid extraction and purification,” *Canadian Journal of Biochemistry and Physiology*, vol. 37, no. 8, pp. 911–917, 1959.
- [238] K. M. Hines, J. C. May, J. A. McLean, and L. Xu, “Evaluation of Collision Cross Section Calibrants for Structural Analysis of Lipids by Traveling Wave Ion Mobility-Mass Spectrometry,” *Analytical Chemistry*, vol. 88, no. 14, pp. 7329–7336, 2016.
- [239] K. M. Hines, J. Herron, and L. Xu, “Assessment of altered lipid homeostasis by HILIC-ion mobility-mass spectrometry-based lipidomics,” *Journal of Lipid Research*, vol. 58, no. 4, pp. 809–819, 2017.
- [240] A. Li, K. M. Hines, and L. Xu, “Lipidomics by HILIC-Ion Mobility-Mass Spectrometry,” *Methods in molecular biology (Clifton, N.J.)*, vol. 2084, pp. 119–132, 2020.
- [241] D. H. Ross, J. H. Cho, R. Zhang, K. M. Hines, and L. Xu, “LiPydomics: A Python Package for Comprehensive Prediction of Lipid Collision Cross Sections and Retention Times and Analysis of Ion Mobility-Mass Spectrometry-Based Lipidomics Data,” *Analytical Chemistry*, vol. 92, no. 22, pp. 14967–14975, 2020.
- [242] J. Herron, K. M. Hines, and L. Xu, “Assessment of altered cholesterol homeostasis by xenobiotics using ultra-high performance liquid chromatography-tandem mass spectrometry,” *Current protocols in toxicology*, vol. 78, no. 1, p. e65, 2018.

- [243] S. Garg, F. Castro-Roman, L. Porcar, P. Butler, P. J. Bautista, N. Krzyzanowski, and U. Perez-Salas, “Cholesterol solubility limit in lipid membranes probed by small angle neutron scattering and MD simulations,” *Soft Matter*, vol. 10, no. 46, pp. 9313–9317, 2014.
- [244] M. Morita, H. Onoe, M. Yanagisawa, H. Ito, M. Ichikawa, K. Fujiwara, H. Saito, and M. Takinoue, “Droplet-Shooting and Size-Filtration (DSSF) Method for Synthesis of Cell-Sized Liposomes with Controlled Lipid Compositions,” *ChemBioChem*, vol. 16, no. 14, pp. 2029–2035, 2015.
- [245] T. R. Shaw, K. C. Wissler, T. A. Schaffner, A. D. Gaffney, B. B. Machta, and S. L. Veatch, “Chemical potential measurements constrain models of cholesterol-phosphatidylcholine interactions,” *Biophysical Journal*, vol. 122, no. 6, pp. 1105–1117, 2023.
- [246] F. A. Heberle, M. Doktorova, H. L. Scott, A. D. Skinkle, M. N. Waxham, and I. Levental, “Direct label-free imaging of nanodomains in biomimetic and biological membranes by cryogenic electron microscopy,” *Proceedings of the National Academy of Sciences*, vol. 117, no. 33, pp. 19943–19952, 2020.
- [247] F. A. Heberle, M. Doktorova, S. L. Goh, R. F. Standaert, J. Katsaras, and G. W. Feigenson, “Hybrid and Nonhybrid Lipids Exert Common Effects on Membrane Raft Size and Morphology,” *Journal of the American Chemical Society*, vol. 135, no. 40, pp. 14932–14935, 2013.
- [248] K. S. Horger, D. J. Estes, R. Capone, and M. Mayer, “Films of Agarose Enable Rapid Formation of Giant Liposomes in Solutions of Physiologic Ionic Strength,” *Journal of the American Chemical Society*, vol. 131, no. 5, pp. 1810–1819, 2009.
- [249] A. Weinberger, F.-C. Tsai, G. Koenderink, T. Schmidt, R. Itri, W. Meier, T. Schmatko, A. Schröder, and C. Marques, “Gel-Assisted Formation of Giant Unilamellar Vesicles,” *Biophysical Journal*, vol. 105, no. 1, pp. 154–164, 2013.
- [250] J. Pazzi and A. B. Subramaniam, “Nanoscale Curvature Promotes High Yield Spontaneous Formation of Cell-Mimetic Giant Vesicles on Nanocellulose Paper,” *ACS Applied Materials & Interfaces*, vol. 12, no. 50, pp. 56549–56561, 2020.
- [251] Y. Lange and T. L. Steck, “Cholesterol homeostasis and the escape tendency (activity) of plasma membrane cholesterol,” *Progress in lipid research*, vol. 47, no. 5, pp. 319–332, 2008.

- [252] A. Radhakrishnan, J. L. Goldstein, J. G. McDonald, and M. S. Brown, "Switch-like Control of SREBP-2 Transport Triggered by Small Changes in ER Cholesterol: A Delicate Balance," *Cell Metabolism*, vol. 8, no. 6, pp. 512–521, 2008.
- [253] A. Sokolov and A. Radhakrishnan, "Accessibility of Cholesterol in Endoplasmic Reticulum Membranes and Activation of SREBP-2 Switch Abruptly at a Common Cholesterol Threshold," *The Journal of Biological Chemistry*, vol. 285, no. 38, pp. 29480–29490, 2010.
- [254] R. A. DeBose-Boyd, "Feedback regulation of cholesterol synthesis: sterol-accelerated ubiquitination and degradation of HMG CoA reductase," *Cell Research*, vol. 18, no. 6, pp. 609–621, 2008.
- [255] V. Howe, L. J. Sharpe, A. V. Prabhu, and A. J. Brown, "New insights into cellular cholesterol acquisition: promoter analysis of human *HMGCR* and *SQLE*, two key control enzymes in cholesterol synthesis," *Biochimica et Biophysica Acta (BBA) - Molecular and Cell Biology of Lipids*, vol. 1862, no. 7, pp. 647–657, 2017.
- [256] G. D. Prestwich, I. Abe, Y. F. Zheng, B. J. Robustell, and T. Dang, "Enzymatic cyclization of squalene analogs," *Pure Appl. Chem.*, vol. 71, no. 6, pp. 1127–1131, 1999.
- [257] I. C. Gelissen and A. J. Brown, "Drug targets beyond HMG-CoA reductase: Why venture beyond the statins?," *Frontiers in Biology*, vol. 6, no. 3, pp. 197–205, 2011.
- [258] L. Trapani, M. Segatto, P. Ascenzi, and V. Pallottini, "Potential role of nonstatin cholesterol lowering agents," *IUBMB Life*, vol. 63, no. 11, pp. 964–971, 2011.
- [259] A. K. Padyana, S. Gross, L. Jin, G. Cianchetta, R. Narayanaswamy, F. Wang, R. Wang, C. Fang, X. Lv, S. A. Biller, L. Dang, C. E. Mahoney, N. Nagaraja, D. Pirman, Z. Sui, J. Popovici-Muller, and G. A. Smolen, "Structure and inhibition mechanism of the catalytic domain of human squalene epoxidase," *Nature Communications*, vol. 10, no. 1, p. 97, 2019.
- [260] S. Gill, J. Stevenson, I. Kristiana, and A. J. Brown, "Cholesterol-dependent degradation of squalene monooxygenase, a control point in cholesterol synthesis beyond HMG-CoA reductase," *Cell Metabolism*, vol. 13, no. 3, pp. 260–273, 2011.
- [261] N. K. Chua, V. Howe, N. Jatana, L. Thukral, and A. J. Brown, "A conserved degron containing an amphipathic helix regulates the cholesterol-mediated turnover of human squalene monooxygenase, a rate-limiting enzyme in cholesterol synthesis," *The Journal of Biological Chemistry*, vol. 292, no. 49, pp. 19959–19973, 2017.

- [262] V. Howe, N. K. Chua, J. Stevenson, and A. J. Brown, “The Regulatory Domain of Squalene Monooxygenase Contains a Re-entrant Loop and Senses Cholesterol via a Conformational Change,” *Journal of Biological Chemistry*, vol. 290, no. 46, pp. 27533–27544, 2015.
- [263] I. Dikic, “Proteasomal and Autophagic Degradation Systems,” *Annual Review of Biochemistry*, vol. 86, pp. 193–224, 2017.
- [264] A. Ballabio and J. S. Bonifacino, “Lysosomes as dynamic regulators of cell and organismal homeostasis,” *Nature Reviews Molecular Cell Biology*, vol. 21, no. 2, pp. 101–118, 2020.
- [265] N. Zelcer, L. J. Sharpe, A. Loregger, I. Kristiana, E. C. L. Cook, L. Phan, J. Stevenson, and A. J. Brown, “The E3 Ubiquitin Ligase MARCH6 Degrades Squalene Monooxygenase and Affects 3-Hydroxy-3-Methyl-Glutaryl Coenzyme A Reductase and the Cholesterol Synthesis Pathway,” *Molecular and Cellular Biology*, vol. 34, no. 7, pp. 1262–1270, 2014.
- [266] M. Guharoy, P. Bhowmick, and P. Tompa, “Design Principles Involving Protein Disorder Facilitate Specific Substrate Selection and Degradation by the Ubiquitin-Proteasome System,” *The Journal of Biological Chemistry*, vol. 291, no. 13, pp. 6723–6731, 2016.
- [267] S. P. Melo, K. W. Barbour, and F. G. Berger, “Cooperation between an intrinsically disordered region and a helical segment is required for ubiquitin-independent degradation by the proteasome,” *The Journal of Biological Chemistry*, vol. 286, no. 42, pp. 36559–36567, 2011.
- [268] B. Medicherla, Z. Kostova, A. Schaefer, and D. H. Wolf, “A genomic screen identifies Dsk2p and Rad23p as essential components of ER-associated degradation,” *EMBO reports*, vol. 5, no. 7, pp. 692–697, 2004.
- [269] U. Lenk and T. Sommer, “Ubiquitin-mediated Proteolysis of a Short-lived Regulatory Protein Depends on Its Cellular Localization,” *Journal of Biological Chemistry*, vol. 275, no. 50, pp. 39403–39410, 2000.
- [270] N. Ohgami, D. C. Ko, M. Thomas, M. P. Scott, C. C. Y. Chang, and T.-Y. Chang, “Binding between the Niemann–Pick C1 protein and a photoactivatable cholesterol analog requires a functional sterol-sensing domain,” *Proceedings of the National Academy of Sciences*, vol. 101, no. 34, pp. 12473–12478, 2004.

- [271] P. E. Kuwabara and M. Labouesse, “The sterol-sensing domain: multiple families, a unique role?,” *Trends in Genetics*, vol. 18, no. 4, pp. 193–201, 2002.
- [272] S. Sikdar, M. Banerjee, and S. Vemparala, “Effect of cholesterol on the membrane partitioning dynamics of hepatitis A virus-2B peptide,” *Soft Matter*, vol. 17, no. 34, pp. 7963–7977, 2021.
- [273] M. Honsho, Y. Abe, and Y. Fujiki, “Dysregulation of Plasmalogen Homeostasis Impairs Cholesterol Biosynthesis,” *Journal of Biological Chemistry*, vol. 290, no. 48, pp. 28822–28833, 2015.
- [274] J. Stevenson, W. Luu, I. Kristiana, and A. Brown, “Squalene mono-oxygenase, a key enzyme in cholesterol synthesis, is stabilized by unsaturated fatty acids,” *Biochemical Journal*, vol. 461, no. 3, pp. 435–442, 2014.
- [275] H. Andresen, C. Grötzinger, K. Zarse, O. J. Kreuzer, E. Ehrentreich-Förster, and F. F. Bier, “Functional peptide microarrays for specific and sensitive antibody diagnostics,” *Proteomics*, vol. 6, no. 5, pp. 1376–1384, 2006.
- [276] N. Goda, N. Matsuo, T. Tenno, S. Ishino, Y. Ishino, S. Fukuchi, M. Ota, and H. Hiroaki, “An optimized Npro-based method for the expression and purification of intrinsically disordered proteins for an NMR study,” *Intrinsically Disordered Proteins*, vol. 3, no. 1, p. e1011004, 2015.
- [277] D. C. Williams, R. M. Van Frank, W. L. Muth, and J. P. Burnett, “Cytoplasmic Inclusion Bodies in *Escherichia coli* Producing Biosynthetic Human Insulin Proteins,” *Science*, vol. 215, no. 4533, pp. 687–689, 1982.
- [278] A. Singh, V. Upadhyay, A. K. Upadhyay, S. M. Singh, and A. K. Panda, “Protein recovery from inclusion bodies of *Escherichia coli* using mild solubilization process,” *Microbial Cell Factories*, vol. 14, no. 1, p. 41, 2015.
- [279] Y. Senju, P. Lappalainen, and H. Zhao, “Liposome Co-sedimentation and Co-flotation Assays to Study Lipid-Protein Interactions,” in *Phosphoinositides: Methods and Protocols* (R. J. Botelho, ed.), pp. 195–204, New York, NY: Springer US, 2021.
- [280] E. M. Kosower, H. Kanety, H. Dodiuk, and J. Hermolin, “Bimanes. 9. Solvent and substituent effects on intramolecular charge-transfer quenching of the fluorescence of syn-1,5-diazabicyclo[3.3.0]octadienediones (syn-9,10-dioxabimanes),” *The Journal of Physical Chemistry*, vol. 86, no. 8, pp. 1270–1277, 1982.

- [281] H. Zhao and P. Lappalainen, “A simple guide to biochemical approaches for analyzing protein–lipid interactions,” *Molecular Biology of the Cell*, vol. 23, no. 15, pp. 2823–2830, 2012.
- [282] S. M. L. Stowell, A. C. Churchill, A. K. Hund, K. C. Kelsey, M. D. Redmond, S. A. Seiter, and N. N. Barger, “Transforming Graduate Training in STEM Education,” *Bulletin of the Ecological Society of America*, vol. 96, no. 2, pp. 317–323, 2015.
- [283] S. Stromholt, B. Wiggins, and B. V. d. Mehden, “Practice-Based Teacher Education Benefits Graduate Trainees and Their Students Through Inclusive and Active Teaching Methods,” *Journal for STEM Education Research*, vol. 7, no. 1, 2024.
- [284] T. A. Press, “Here are the 25 most-viewed articles on Wikipedia in 2023,” *NPR*, 2023.
- [285] D. Jemielniak, “Wikipedia: Why is the common knowledge resource still neglected by academics?,” *GigaScience*, vol. 8, no. 12, p. giz139, 2019.
- [286] “Wikipedia:Notability,” 2024.

Appendix A

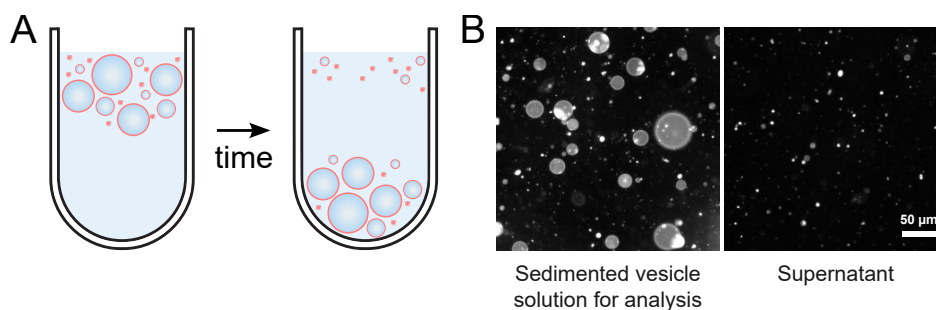
SUPPORTING MATERIALS: COMMON METHODS OF MAKING GIANT VESICLES (EXCEPT EMULSION TECHNIQUES) CAPTURE INTENDED LIPID RATIOS

Figure A.1: **Sedimenting vesicles removes some lipid aggregates.** **A)** Vesicles filled with a dense sucrose solution sink in an osmotically matched glucose solution. **B)** After sinking, large vesicles are observed only in the sedimented solution, and not in the supernatant. The vesicles in these images were made by emulsion phase transfer. The density of giant vesicles in the supernatant is representative of all techniques.

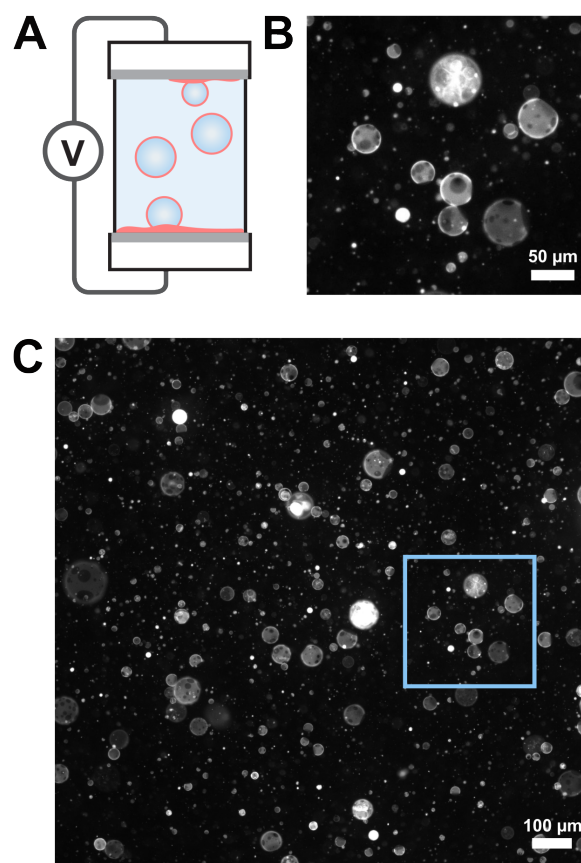


Figure A.2: **Representative fluorescence micrographs of vesicles made by electroformation on ITO-coated slides.** **A)** Schematic of ITO electroformation. **B)** Close-up of vesicles in the blue box in panel C. **C)** Full field of view of vesicles produced by electroformation on ITO slides. As expected, ITO electroformation produces the highest yield of giant, unilamellar vesicles (GUVs) of the four methods tested for producing vesicles. Some multilamellar vesicles, nested vesicles (large vesicles filled with multiple small vesicles) and some bright, lipid aggregates are also produced.

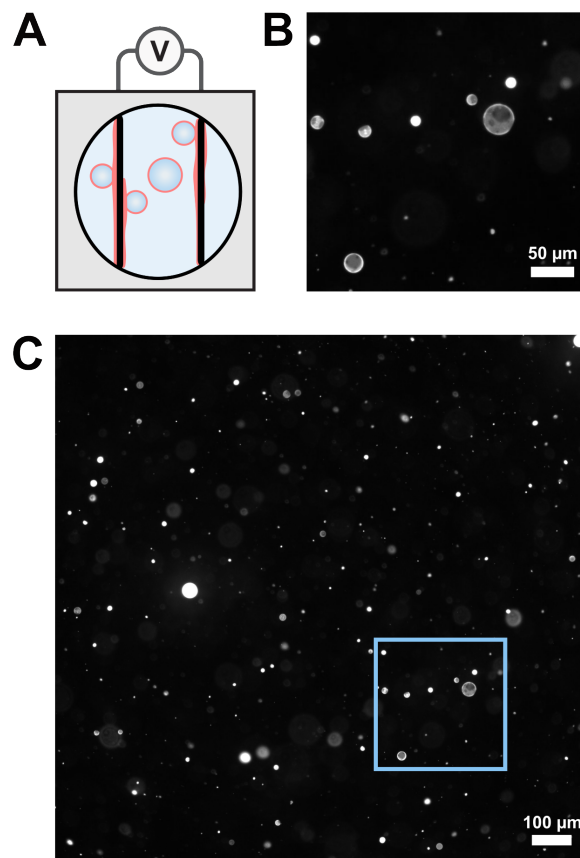


Figure A.3: **Representative fluorescence micrographs of vesicles made by electroformation on platinum wires.** **A)** Schematic of Pt electroformation. **B)** Close-up of vesicles in the blue box in panel C. **C)** Full field of view of vesicles produced by electroformation on Pt wires. The volume of stock solution used is low relative to the other methods and therefore produces a lower yield of vesicles at the same stock concentration.

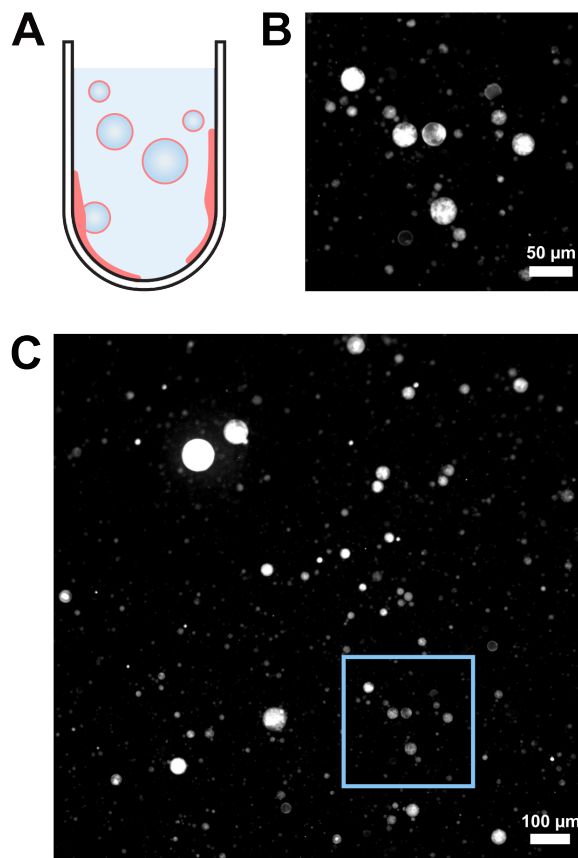


Figure A.4: **Representative fluorescence micrographs of vesicles made by gentle hydration for 24 hrs.** **A)** Schematic of gentle hydration. **B)** Close-up of vesicles in the blue box in panel C. **C)** Full field of view of vesicles produced by gentle hydration. As expected, the sample predominantly contains multilamellar vesicles and nested vesicles. When contrast is optimized for the bright, multi-layered vesicles, unilamellar vesicles in the same field of view can be too dim to be imaged.

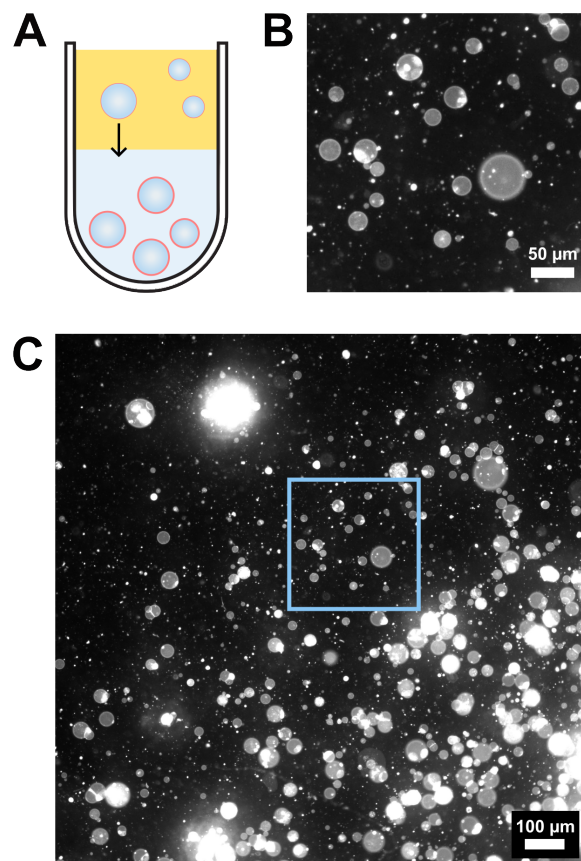


Figure A.5: **Representative fluorescence micrographs of vesicles made by emulsion phase transfer.** **A)** Schematic of emulsion phase transfer. **B)** Close-up of vesicles in the blue box in panel C. **C)** Full field of view of vesicles produced by emulsion phase transfer. The emulsion transfer method produces a high yield of giant unilamellar vesicles as well as defects including nested vesicles and lipid aggregates.

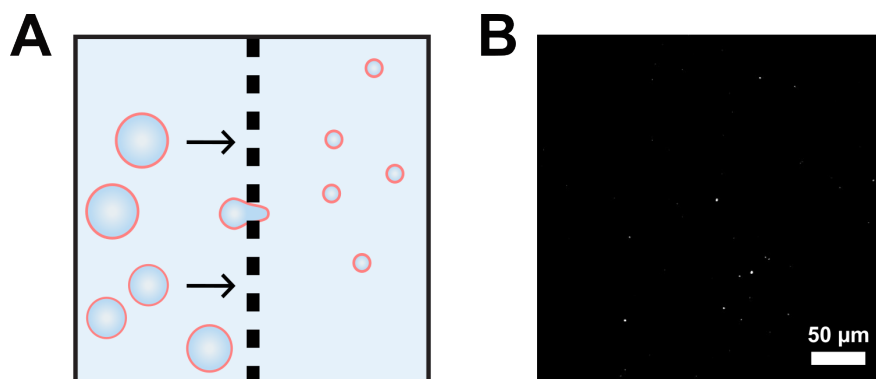


Figure A.6: **Vesicles after extrusion.** **A)** Schematic of extrusion. **B)** Representative fluorescence micrograph of vesicles after extrusion through a 100 nm diameter membrane filter. As expected, most vesicles are too small to be resolved with standard microscopy.

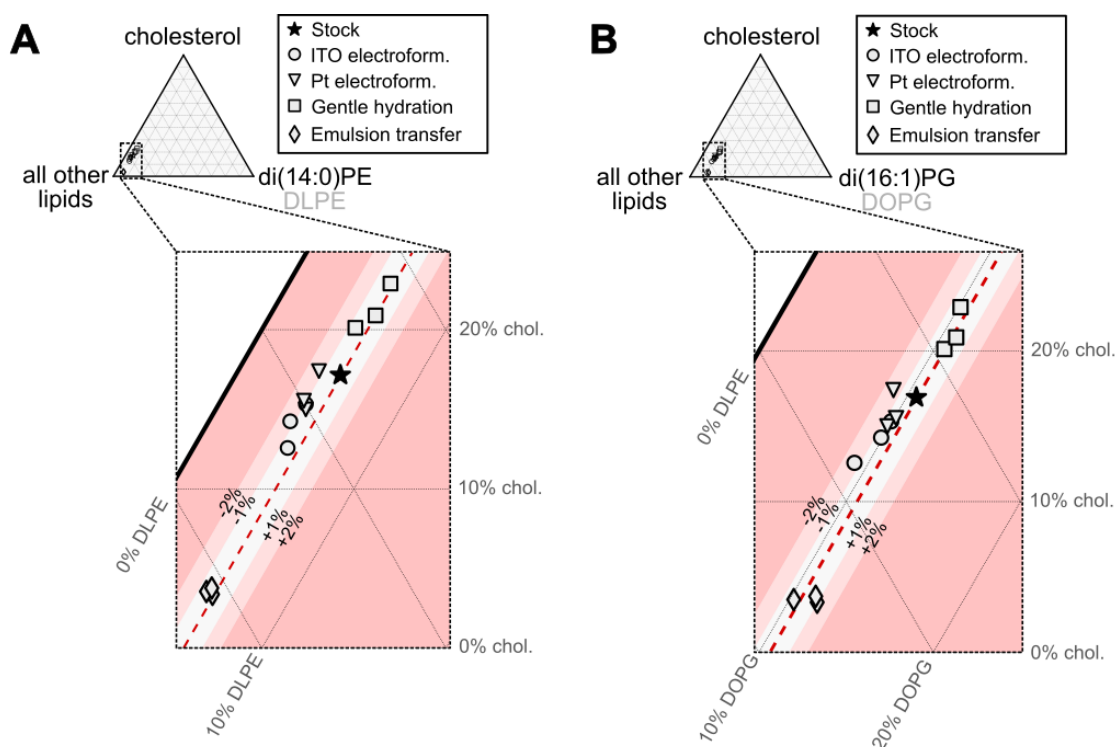


Figure A.7: Lipid percentages in 5-component vesicles produced by different methods, plotted as pseudo-ternary diagrams in which one vertex is di(12:0)PE or di(18:1)PG. Vesicles were prepared by four methods: electroformation on ITO slides, electroformation on platinum wires, gentle hydration, and emulsion phase transfer. Three independent preparations and experiments were run for each method. **A)** Lipid percentages of all solutions are plotted on a pseudo-ternary diagram, where the three vertices represent di(12:0)PE, cholesterol, and the sum of all other lipids. **B)** Lipid percentages of all solutions are plotted on a pseudo-ternary diagram, where the three vertices represent di(18:1)PE, cholesterol, and the sum of all other lipids. In both panels, the lipid percentages for the master stock solution are shown as a star. Deviations from the master stock solution in increments of 1% and 2% of DLPE or DOPG are shown as shaded regions.

Table A.1: Lipid compositions of five-component vesicles analyzed by mass spectrometry, expressed as percentages of total lipid

Method	Sample	Percentage of total lipid				
		Cholesterol	di(16:0)PC (DPPC)	di(18:1)PC (DOPC)	di(12:0)PE (DLPE)	di(18:1)PG (DOPG)
Stock solution	Master stock	17.0%	28.4%	38.3%	5.8%	10.4%
ITO electroform.	ITO 1	14.2%	28.0%	43.4%	4.4%	9.9%
	ITO 2	15.3%	28.1%	41.9%	4.7%	9.9%
	ITO 3	12.6%	29.5%	43.6%	5.1%	9.2%
Pt electroform.	Pt 1	17.4%	28.5%	40.7%	4.4%	9.0%
	Pt 2	15.0%	29.2%	41.1%	4.9%	9.9%
	Pt 3	15.5%	30.1%	39.7%	4.5%	10.1%
Gentle hydration	GH 1	22.9%	26.1%	35.3%	5.5%	10.1%
	GH 2	20.1%	27.1%	37.1%	5.0%	10.6%
	GH 3	20.9%	26.3%	36.2%	5.7%	10.9%
Emulsion transfer	Emulsion 1	3.4%	44.0%	35.4%	5.7%	11.6%
	Emulsion 2	3.5%	45.9%	35.1%	5.2%	10.2%
	Emulsion 3	3.8%	42.1%	37.3%	5.4%	11.3%

Table A.2: Percentages of lipids in GUVs made by emulsion transfer from a binary mixture of an unsaturated lipid and a saturated lipid

Method	Sample	Percentage of total lipid	
		di(16:0)PC	di(16:1)PC
Stock solution for lipid saturation experiments	Saturation stock	49.1%	50.9%
Emulsion transfer (ET)	ET saturation 1	58.2%	41.8%
	ET saturation 2	58.0%	42.0%
	ET saturation 3	57.3%	42.7%

Table A.3: Percentages of lipids in GUVs made by emulsion transfer from a binary mixture of lipids with different chain lengths

Method	Sample	Percentage of total lipid	
		di(18:1)PC	di(16:1)PC
Stock solution for lipid length experiments	Length stock	49.1%	50.9%
Emulsion phase transfer (ET)	ET length 1	58.8%	41.2%
	ET length 2	58.7%	41.3%
	ET length 3	53.1%	46.9%

Table A.4: Lipid compositions analyzed by mass spectrometry and expressed as percentages of total lipid for vesicles produced by gentle hydration (“before extrusion”) and then extruded (“after extrusion”). For example, “Experiment 1 – After” was made from an aliquot of the solution from “Experiment 1 – Before”.

Method	Sample	Cholesterol	Percentage of total lipid			
			di(16:0)PC (DPPC)	di(18:1)PC (DOPC)	di(12:0)PE (DLPE)	di(18:1)PG (DOPG)
Before extrusion	Exp. 1 - Before	23.6%	25.2%	29.2%	6.9%	15.0%
	Exp. 2 - Before	26.3%	26.5%	25.6%	6.5%	15.1%
	Exp. 3 - Before	27.7%	25.8%	25.2%	6.3%	14.9%
After extrusion	Exp. 1 - After	18.0%	27.9%	32.1%	5.2%	16.9%
	Exp. 2 - After	22.4%	27.3%	27.1%	6.7%	16.6%
	Exp. 3 - After	22.3%	27.0%	28.4%	6.7%	15.6%

Table A.5: Phospholipid abundances of five-component vesicles analyzed by mass spectrometry.

Lipid	di(15:0)PC (internal standard)	di(16:0) PC	di(18:1) PC	di(15:0)PE (internal standard)	di(12:0) PE	di(15:0)PG (internal standard)	di(18:1) PG
m/z	706.5	734.6	786.6	686.5	602.4	717.5	797.5
Retention time (minutes)	3.467	3.467	3.414	2.725	2.847	0.708	0.621
Calibrated retention time (minutes)	6.760	6.760	6.672	5.542	5.742	2.233	2.038
Collisional cross section (Å ²)	274.4	279.8	285.1	268.9	252.5	268.6	279.4
Master stock abundance	5617.5	17245.3	23270.3	4528.2	2853.3	4441.4	5016.5
ITO electroform. 1 abundance	6741.8	17442.6	27025.4	4434.9	1810.2	5385.0	4914.3
ITO electroform. 2 abundance	6857.4	24043.3	35779.5	4280.0	2523.2	5170.9	6393.5
ITO electroform. 3 abundance	7240.7	15652.1	23118.4	4920.6	1843.7	6871.4	4625.1
Pt. electroform. 1 abundance	6881.0	22694.3	32436.7	4665.2	2379.2	5772.2	6026.1
Pt. electroform. 2 abundance	6679.0	16801.5	23631.0	5039.4	2124.3	6748.9	5740.9
Pt. electroform. 3 abundance	5342.4	14477.7	19085.5	4548.3	1847.1	5020.5	4557.4
Gentle hydration 1 abundance	7353.0	30264.4	40917.1	5487.3	4792.2	5907.4	9413.3
Gentle hydration 2 abundance	7682.1	23456.5	32112.9	6630.8	3748.8	5247.5	6246.9
Gentle hydration 3 abundance	7625.5	22749.8	31393.1	5379.8	3504.5	5017.3	6195.7
Emulsion transfer 1 abundance	8370.8	9579.3	7712.5	5534.3	816.3	6091.2	1843.4
Emulsion transfer 2 abundance	8068.4	11843.5	9051.1	5553.9	931.3	5927.0	1931.0
Emulsion transfer 3 abundance	7626.0	9787.1	8667.5	5246.7	867.2	5531.6	1910.8

Table A.6: Cholesterol abundances of five-component vesicles analyzed by mass spectrometry.

	d7-cholesterol area (internal standard)	Cholesterol area
Master stock	3.21E+07	8.59E+06
ITO electroform. 1	2.68E+07	5.13E+06
ITO electroform. 2	2.76E+07	7.67E+06
ITO electroform. 3	2.53E+07	3.39E+06
Pt electroform 1	2.84E+07	8.33E+06
Pt electroform 2	2.61E+07	4.91E+06
Pt electroform 3	2.62E+07	5.33E+06
Gentle hydration 1	2.99E+07	1.57E+07
Gentle hydration 2	2.71E+07	8.93E+06
Gentle hydration 3	2.33E+07	8.05E+06
Emulsion transfer 1	2.23E+07	2.85E+05
Emulsion transfer 2	2.35E+07	3.88E+05
Emulsion transfer 3	3.67E+07	6.13E+05

Table A.7: Phospholipid abundances in GUVs made by emulsion transfer from a binary mixture of an unsaturated lipid and a saturated lipid

Lipid	di(15:0)PC	(16:0/18:1)PC		
	(internal standard)	di(16:0)PC	(internal standard)	di(16:1)PC
m/z	706.5	734.6	760.6	730.5
Retention time (minutes)	3.312	3.312	3.259	3.414
Calibrated retention time (minutes)	5.445	5.445	5.453	5.429
Collisional cross section (\AA^2)	239.9	249.9	248.7	240.9
Saturation stock abundance	14259.5	490722.3	12208.1	434934.4
ET saturation 1 abundance	54941.2	45862.2	52621.1	31490.8
ET saturation 2 abundance	58862.0	21123.8	55943.2	14554.5
ET saturation 3 abundance	57614.3	39973.9	54335.7	28099.2

Table A.8: Phospholipid abundances in GUVs made by emulsion transfer from a binary mixture of lipids with different chain lengths.

Lipid	(16:0/18:1)PC		
	(internal standard)	di(16:1)PC	di(18:1)PC
m/z	760.6	730.5	786.6
Retention time (minutes)	3.259	3.414	3.225
Calibrated retention time (minutes)	5.453	5.429	5.459
Collisional cross section (\AA^2)	248.7	240.9	254.0
Length stock abundance	8362.4	428416.6	412967.2
ET length 1 abundance	51197.1	13380.6	19090.4
ET length 2 abundance	53042.6	5718.8	8128.1
ET length 3 abundance	54721.9	10486.8	11892.0

Table A.9: Phospholipid abundances in GUVs produced by gentle hydration (“before extrusion”) and then extruded (“after extrusion”). For example, “After extrusion 1” was made from an aliquot of the solution from “Before extrusion 1”.

Lipid	di(15:0)PC (internal standard)	di(16:0)PC	di(18:1)PC	di(15:0)PE (internal standard)	di(12:0)PE	di(15:0)PG (internal standard)	di(18:1)PG
m/z	706.5	734.6	786.6	664.5	580.4	717.5	797.5
Retention time (minutes)	3.312	3.312	3.225	2.570	2.692	0.674	0.553
Calibrated retention time (minutes)	5.445	5.445	5.459	5.560	5.541	2.233	2.020
Collisional cross section (\AA^2)	239.9	249.9	254.0	232.0	216.8	239.8	248.4
Before extrusion 1 abundance	56822.3	84583.4	97994.1	85471.0	34719.6	36543.5	32416.2
Before extrusion 2 abundance	63191.0	113815.1	109639.1	101636.3	44984.7	39897.5	40816.1
Before extrusion 3 abundance	63430.2	159911.8	156115.9	95764.3	59014.5	30611.1	44526.0
After extrusion 1 abundance	54683.8	32544.4	37473.0	89296.3	9911.4	43706.7	15788.9
After extrusion 2 abundance	65041.1	65510.5	65082.1	96925.9	23877.9	37763.1	23185.0
After extrusion 3 abundance	50216.3	63415.0	66752.6	85189.5	26663.7	36801.5	26753.6

Table A.10: Cholesterol abundances in GUVs produced by gentle hydration (“before extrusion”) and then extruded (“after extrusion”). For example, “After extrusion 1” was made from an aliquot of the solution from “Before extrusion 1”.

Sample	Cholesterol area	d7-cholesterol area (internal standard)
Master stock	3.88E+08	1.61E+07
Before extrusion 1	4.26E+06	1.70E+07
Before extrusion 2	5.44E+06	1.69E+07
Before extrusion 3	8.02E+06	1.65E+07
After extrusion 1	1.09E+06	1.58E+07
After extrusion 2	2.47E+06	1.66E+07
After extrusion 3	2.89E+06	1.54E+07

Appendix B

**SUPPORTING MATERIALS: MEMBRANE-SENSING
PROPERTIES OF SQUALENE MONOOXYGENASE DEGRON****gBlock sequence for SM50-100:**

GTC GAT GAA GCT TTG AAA GAC GCG CAG ACT CGC ATC ACC AAA GAG AAT
CTT TAC TTC CAG GGC GGT AGC TCC GGC TCA TCC GGG TGT AAT GGC GGA
TTG CTT GGT CGT CAA CAA AGT GGA AGT CAA TTT GCC TTA TTT TCC GAT
ATT CTT TCG GGG CTT CCG TTC ATT GGG TTC TTT TGG GCC AAG AGC CCC
CCC GAG TCC GAA AAT AAA GAG CAA TTA GAA GCC CGC CGC CGT CGC AAA
GGT CTT AAT GAC ATT TTC GAA GCT CAA AAA ATT GAA TGG CAT GAG TAA
TAA CTC GAG CAC CAC

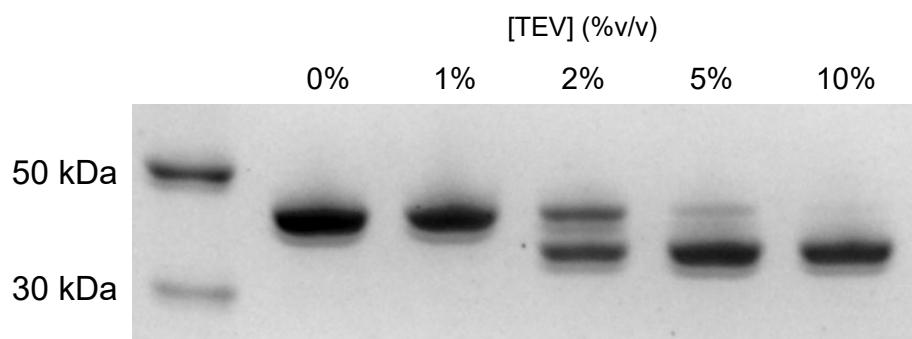


Figure B.1: **Optimization of MBP-SM50-100 cleavage by TEV protease.** Optimization of MBP-SM50-100 cleavage by TEV protease. Approximately 10 μ g of MBP-SM50-100 was cut overnight with TEV protease (1%, 2%, 5%, and 10% vol/vol) at 4 °C. Following cleavage, the samples were mixed with SDS detergent, briefly vortexed and analyzed by Coomassie Blue staining.

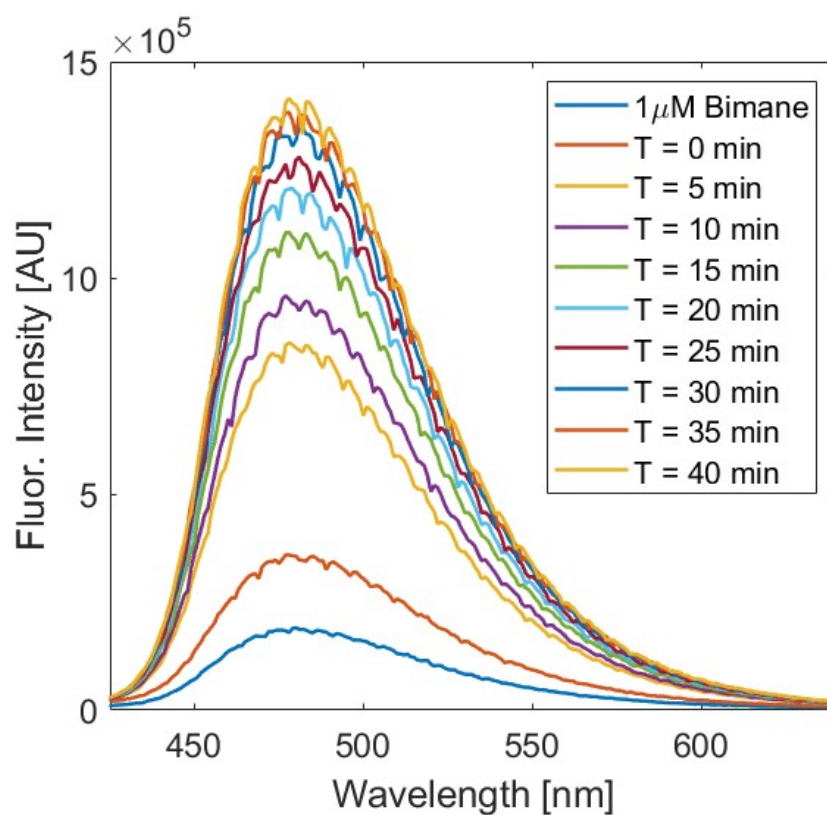


Figure B.2: **Fluorescent sensitivity of Bimane-C3-maleimide by cysteine conjugation.** $1 \mu\text{M}$ Bimane-C3-maleimide was mixed $1 \mu\text{M}$ MBP-SM50-100 to label protein via cysteine-maleimide chemistry. Fluorescence emission spectra were measured at various times after mixing in the fluorometer.

Appendix C

SUPPORTING MATERIALS: STEP-UP WIKIPEDIA ASSIGNMENT

The content held in this Appendix was designed for educational purposes and may be shared and adapted for educational, non-commercial, purposes under fair use.

Propose an Edit to Wikipedia

Introduction to Biophysics

123

SUMMARY

During this unit, we will explore current research in molecular and cellular biophysics. In each class we will discuss a different topic in biophysics and analyze 1-2 scientific paper(s). The goal of this assignment is to apply the knowledge and skills you have developed in this course and to communicate the significance of biophysics to the public by proposing an edit to Wikipedia.



For your proposal, you may choose to 1) edit an existing Wikipedia page on a biophysical topic or 2) create a new Wikipedia page for a scientist. At the end of the project, we will all submit our proposals to Wikipedia, improving access to biophysics.

PROJECT COMPONENTS

Option 1. Edit an existing Wikipedia page on a biophysics topic

1. Create a Wikipedia account with an anonymous username.
2. Choose a biophysics topic that interests you or choose one from the list of topics on Canvas.
3. Enter your name, username, and subject on the [class google sheet](#).
4. Read through the Wikipedia page on your topic and summarize the main points (~1 page).
5. Use the UW Library databases to find and summarize a review article on the topic.
6. Create a draft of your edits in your sandbox, including citations.
7. On Canvas, upload your summaries from steps 4-5, a .pdf of your sandbox proposal, and a short description of your changes.

Option 2. Create a new page for a biophysicist or biophysics-related scientist

1. Create a Wikipedia account with an anonymous username.
2. Choose a scientist who needs a Wikipedia page.
3. Enter your name, username, and the scientist's name on the [class google sheet](#).
4. Start by finding 3-4 resources on your scientist. Read and summarize the main points of each article (~1 page).
5. Use the UW Library databases or the scientist's lab website to find and summarize one of their scientific papers.
6. Create a draft of your edits in your sandbox, including citations.
7. On Canvas, upload your summaries from steps 4-5, a .pdf of your sandbox proposal, and a short paragraph describing why choose the scientist.

IMPORTANT DATES

Project due date: **May 16th, 2022, at 11:59pm**

The project is due after the end of the unit, to allow you to choose any topic related to the lecture material. The entire project should take 4-5 hours for you to complete.

Optional: If you would like to receive feedback on your proposal before the final due date, you can submit the materials from steps 4 and 5 on the following dates:

4/26/22: Upload your summary of the Wikipedia page or scientist references (Step 4)

5/3/22: Upload your summary from the scientific publication (Step 5)

DETAILS ABOUT STEP 4

Option 1. Biophysics Topic

124

The objective of step 4 is to read and understand the current Wikipedia page. You will summarize the major points of the page and generate notes on the sections/content that requires editing. It might be helpful to ask the following questions:

- How does this topic relate to themes or techniques in biophysics?
- Are the major points cited by reliable resources such as scientific journals or university textbooks?
- Is the language concise and clear enough that a non-expert could understand it?
- Is there anything that you should suggest in the Talk page for future revisions?

Remember the goal of the project is to improve topics related to biophysics. There will likely be other technical content on the page that needs revising, but that is beyond the requirements of the project. Please feel free to add these suggestions to the Talk page.

Option 2. Biophysicist/Scientist

In step 4, your task is to find 3-4 independent references about your scientist. Your sources may include newspapers (university-level or major newspapers) or online articles. The scientist's personal website and press releases from their institution are not considered independent resources. Summarize the main points, related to the scientist, and include the citation for each source. You may use APA, MLA, or Harvard press citation formats.

DETAILS ABOUT STEP 5

Use the UW library databases to select a review article on your topic (or written by your scientist). Focus on a subtopic (e.g., a specific cell type or receptor) and read through those sections. You do not need to read the entire paper. Include the title of the sub-section in the review and a summary of the main points. As you read, look up 1-2 articles cited in the review and read the corresponding abstract(s).

*If you are creating a Wikipedia page for a scientist, you will need to use one of their papers and their personal website to create a summary of their research

GRADING

Summary of the Wikipedia Page or Independent sources on scientist	20 points
Summary of the review article or scientific paper	30 points
Wikipedia proposal (.pdf of your sandbox)	40 points
1-paragraph explanation/description of your proposal	10 points
Wikipedia Edit Project (Total)	100 points

TIPS

- Start the assignment early. It will help to be further along if you get frustrated on the technical points of the Wikipedia sandbox during the editing stage.
- Feel free to get creative with your proposal! You may want to draft a new list or table for the Wikipedia page. Search chromatin on Wikipedia for examples.
- You may change your topic/scientist as many times as you want. If you change your topic, please update the google page to ensure that nobody else is already working on your topic and to alert others of your new topic.

Wikipedia Project: Biophysical Topics

Introduction to Biophysics

125

Biophysics covers a broad range of topics. Many of the subjects you discussed in your other courses (biochemistry, immunology, etc.) are likely related to physical principles or techniques. For your project, you may choose any topic if you can relate it to the themes of biophysics. For example, you may choose a specific protein or cell type that has unique physical or mechanical properties. Alternatively, you may choose an analytical technique and discuss the various applications of the technique.

If you need help choosing a topic, please feel free to explore this list of topics that need your skills to achieve *good article* status on Wikipedia. For each topic in the table below, the importance and quality of the current page is noted (Figure 1).

Subjects	Techniques	Scientists
Biophysics (Top/C)	AlphaFold (High/C)	Christopher Barnes
Biological Membrane (Top/C)	Atomic Force Microscopy (High/C)	Biophysics of viruses
Bleb (Cell Biology) (Mid/Stub)	Crystallography (High/Start)	
Calcium Imaging (Mid/Start)	FRET (Low/Start)	Alena Grabowski
Cell Migration (High/Start)	Super-Resolution Microscopy (Mid/B)	Applied biomechanics
Chromatin (High/B)		
Cilium (Top/C)		Gail Robertson
Collagen (High/C)		Biogenesis
Cytoskeleton (Top/C)		
DNA Condensation (Mid/Start)		Nancy Forde
Endocytosis (High/C)		Collagen mechanics
Intrinsically disordered proteins (Mid/Start)		
Lipid bilayer fusion (Mid/B)		Raghuveer Parthasarathy
Membrane biology (Mid/Stub)		Membranes; gut microbiota
Membrane Curvature (Low/Start)		
Membrane Fluidity (Mid/Start)		Sheila Patek
Nuclear Pore (Mid/C)		Evolutionary biomechanics
Osmotic Pressure (High/Start)		
Paraspeckle (Mid/Start)		Padmini Rangamani
Protein aggregation (High/Start)		Cell signaling
Protein-lipid interaction (Low/Start)		
Pseudopodia (High/Start)		Lena Ting
Rheology (Mid/C)		Neuromechanics
Signalosome (Start)		
Syncytiotrophoblast (Low/Start)		
Virophysics (Mid/Start)		

<p>+ GA</p>	<p>The article has attained good article status, having been examined by one or more impartial reviewers from WP:Good article nominations.</p> <p>More detailed criteria [show]</p>
<p>B</p>	<p>The article is mostly complete and without major problems but requires some further work to reach good article standards.</p> <p>More detailed criteria [show]</p>
<p>C</p>	<p>The article is substantial but is still missing important content or contains much irrelevant material. The article should have some references to reliable sources, but may still have significant problems or require substantial cleanup.</p> <p>More detailed criteria [show]</p>
<p>Start</p>	<p>An article that is developing but still quite incomplete. It may or may not cite adequate reliable sources.</p> <p>More detailed criteria [show]</p>
<p>Stub</p>	<p>A very basic description of the topic. Can be well-written, but may also have significant content issues.</p> <p>More detailed criteria [show]</p>

Figure 1. Description of the article quality ratings for WikiProjects (from Wikipedia: Content Assignment)

Rubric for Biophysics Wikipedia Proposal

BIOL410 B | Spring 2022

1 of 3

Components	Description of required material	Instructor comments
<p><i>Summary of current Wikipedia article</i> (If you chose a biophysics topic)</p>	<p>Summarizes the main points of the existing, published Wikipedia article using clear and concise language.</p> <p>Includes a brief description of the reliability of cited works and the level of technical language.</p> <p>May include notes on the content you plan to edit or expand upon in your proposal.</p>	<p>/20 points</p>
<p><i>Summary of references</i> (If you chose a scientist)</p>	<p>Bibliography of 3+ independent references that you will use to draft your Wikipedia page.</p> <p>For each reference, a concise description of the content about the scientist is included.</p>	<p>/20 points</p>
<p><i>Summary of scientific paper or review article</i></p>	<p>Using the literature to learn more about your topic.</p> <ul style="list-style-type: none"> ● Includes the citation for the article in a Wikipedia-approved format (APA, MLA, or Harvard). ● Content is summarized in a logical format. Your summary may be divided to sections that reflect content in the introduction and specific subsections. ● All content is your own work. You have both paraphrased and cited the information. ● Includes citations for the article(s) you found using the original paper. 	<p>/30 points</p>

Rubric for Biophysics Wikipedia Proposal

	Summarizes the abstract(s) of the cited articles in 2-3 sentences.	
Components	Description of required material	Instructor Comments
<i>Wikipedia Proposal</i> Depth of Content	The proposal provides accurate and complete explanations of key concepts and theories in biophysics, drawing on relevant literature.	/40 points
Biophysics Relevance	Content relates to molecular and/or cellular biophysics. Description of mechanisms or techniques include physical parameters (e.g., pressure, rigidity, geometry, diffusion, etc.).	
Language	Sentences are complete and grammatical. They flow easily. Words are well chosen; they express the intended meaning precisely.	
Neutral Point of View	Content is free from bias. Tone is neutral and appropriate for Wikipedia.	
Format	Submitted as .pdf of sandbox page. Uses Wikipedia syntax and appropriate links.	
References	All facts are cited from reputable sources that are accessible and up to date. Includes a direct link to each source.	
<i>Description of your proposal</i>	<p>1-2 paragraph description of your proposal, which may include:</p> <ul style="list-style-type: none"> ● A description of the changes to content, citations, and language in the existing Wikipedia page, ● An explanation of the how the material relates to concepts covered in class. ● An explanation of what motivated you to choose a particular scientist or biophysics topic. 	/10 points

Rubric for Biophysics Wikipedia Proposal

3 of 3

BIOL410 B | Spring 2022

<p>Bonus – <i>Submit your changes to Wikipedia</i></p>	<p>AFTER GRADING, submit your proposal to Wikipedia (with any necessary changes), using your Wikipedia account. Email me (hspears@uw.edu) by 11:59pm on June 2nd for credit.</p>	<p>/3 points</p>
---	--	------------------